

PDF hosted at the Radboud Repository of the Radboud University Nijmegen

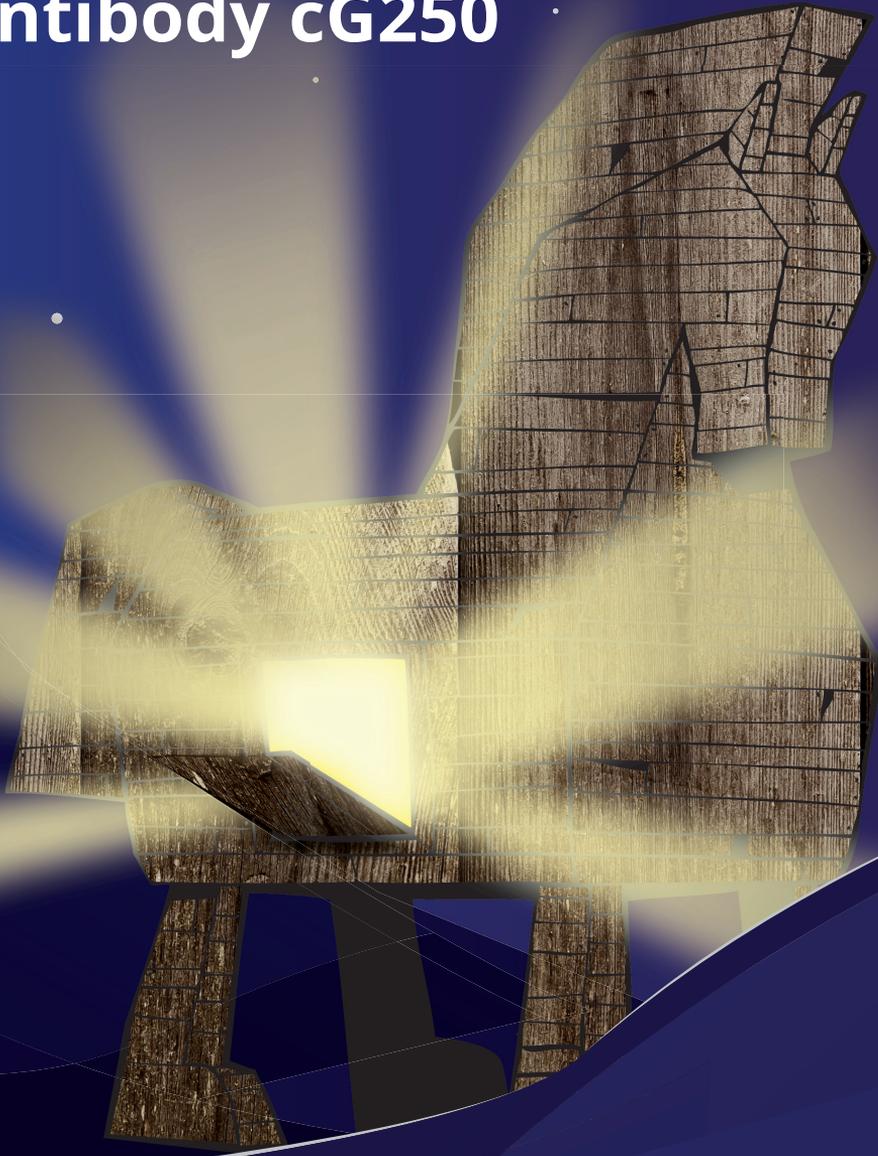
The following full text is a publisher's version.

For additional information about this publication click this link.

<http://hdl.handle.net/2066/124045>

Please be advised that this information was generated on 2018-07-07 and may be subject to change.

Radioimmunodiagnosis and -therapy of renal cell carcinoma using the monoclonal antibody cG250



Alexander Stillebroer

**Radioimmunodiagnosis and -therapy of renal cell carcinoma
using the monoclonal antibody cG250**

Radioimmunodiagnosis and -therapy of renal cell carcinoma using the monoclonal antibody cG250



Colofon

The work presented in this thesis has been performed at the departments of Urology (head: Prof. Dr. P.F.A. Mulders) and Nuclear Medicine (Head: Prof. Dr. W.J.G. Oyen), Radboud University Nijmegen Medical Center, Nijmegen, The Netherlands

The studies presented in this thesis were financially supported by the Dutch Cancer Society, KWF grant KUN 2005-3339.

The publication of this thesis was financially supported by (in alphabetical order): Amgen, Astellas Pharma BV, Bayer Healthcare, GlaxoSmithKline, Pfizer BV, Pohl Boskamp, Willex AG

ISBN: 978-90-9028052-3

About the cover. Although flawed in essence, as it relates to the popular misconception that radioactivity can be seen as visible light, the image conveys a message. Its relation to the subject of research may, however, need some clarification. The Trojan horse can be regarded as the antibody cG250, where Troy is the tumor cell. As the tumor cell 'recognizes' and internalizes the antibody (Trojan horse taken into the city), the antibody is 'opened' and the radioactivity is released within. This is represented by the light coming from within the horse. The radioactivity stays in the tumor cell to deliver its deadly burden and kill the tumor cell. Hence the comparison with the Trojan horse which ultimately led to the demise of Troy.

© Alexander Stillebroer, The Netherlands

All rights reserved. No part of this publication may be reproduced or transmitted in any form or by any means, electronic or mechanical, including photocopy, recording or otherwise, without the written permission of the author.

Cover en lay-out: Linda Grootscholten, 16hoog
Printed by: Platform P, Rotterdam, The Netherlands

Radioimmunodiagnosis and -therapy of renal cell carcinoma using the monoclonal antibody cG250

PROEFSCHRIFT

ter verkrijging van de graad van doctor
aan de Radboud Universiteit Nijmegen
op gezag van de rector magnificus prof. mr. S.C.J.J. Kortmann,
volgens besluit van het college van decanen
in het openbaar te verdedigen op vrijdag 7 februari
om 16.30 uur precies

door

Alexander Boudewijn Stillebroer
geboren op 15 augustus 1982
te Terheijden

PROMOTIECOMMISSIE

Promotoren:

Prof. dr. O.C. Boerman
Prof. dr. P.F.A. Mulders
Prof. dr. W.J.G. Oyen

Copromotor:

Dr. E. Oosterwijk

Manuscriptcommissie:

Prof. dr. J.H.A.M. Kaanders (voorzitter)
Prof. dr. W. Gerritsen
Dr. A.H. Brouwers (UMCG)

TABLE OF CONTENT

1	Introduction and thesis outline	11
	Adapted from published article: "Radiolabeled antibodies in renal cell carcinoma", Stillebroer AB, Oosterwijk E, Oyen WJG, Mulders PFA, Boerman OC; Cancer Imaging, 2007 Nov 19;7:179-88"	
2	Carbonic Anhydrase IX in Renal Cell Carcinoma Implications for Prognosis, Diagnosis and Therapy -	33
	Stillebroer AB, Mulders PF, Boerman OC, Oyen WJ, Oosterwijk E. Published: European Urology 2010 Jul;58(1):75-83	
3	Phase I Radioimmunotherapy Study With ¹⁷⁷Lu-Labeled Anti-Carbonic Anhydrase 9 Monoclonal Antibody Girentuximab In Patients With Advanced Renal Cell Carcinoma -	53
	Stillebroer AB, Boerman OC, Desar IM, Boers-Sonderen MJ, van Herpen CM, Langenhuisen JF, Smith-Jones PM, Oosterwijk E, Oyen WJ, Mulders PF. Published European Urology 2013 Sep;64(3):478-85	
4	Dosimetric analysis of ¹⁷⁷Lu-cG250 radioimmunotherapy in renal cell carcinoma patients: Correlation with myelotoxicity and pre-therapeutic absorbed dose predictions based on ¹¹¹In-cG250 imaging -	69
	Stillebroer AB, Zegers CM, Boerman OC, Oosterwijk E, Mulders PF, O'Donoghue JA, Visser EP, Oyen WJ. Published: Journal of Nuclear Medicine 2012 Jan;53(1):82-9	
5	¹¹¹In-bevacizumab imaging of renal cell cancer and evaluation of neoadjuvant treatment with the vascular endothelial growth factor receptor inhibitor sorafenib -	89
	Desar IM, Stillebroer AB, Oosterwijk E, Leenders WP, van Herpen CM, van der Graaf WT, Boerman OC, Mulders PF, Oyen WJ. Published: Journal of Nuclear Medicine 2010 Nov;51(11):1707-15 (shared first author)	
6	ImmunoPET imaging of renal cell carcinoma with ¹²⁴I- and ⁸⁹Zr-labeled anti-CAIX monoclonal antibody cG250 in mice -	109
	Stillebroer AB, Franssen GM, Mulders PF, Oyen WJ, van Dongen GA, Laverman P, Oosterwijk E, Boerman OC. Published: Cancer Biotherapy Radiopharmaceuticals 2013 Sep;28(7):510-5	
7	Optical imaging of Renal Cell Carcinoma using the anti-CAIX monoclonal antibody girentuximab -	125
	Alexander B. Stillebroer, Constantijn H.J. Muselaers, Mark Rijpkema, Gerben M. Franssen, Egbert Oosterwijk, Peter F.A. Mulders, Wim J.G. Oyen, Otto C. Boerman. Submitted for publication	
	Summary	150
	General discussion and future perspectives	148
	List of publications	153
	Curriculum Vitae	154
	Dankwoord	157

CHAPTER 1

Introduction and thesis outline

Adapted from: Radiolabeled antibodies in renal cell carcinoma,
A.B. Stillebroer¹ MD, P.F.A. Mulders¹ MD PhD, O.C. Boerman² PhD,
W.J.G. Oyen² MD PhD, E. Oosterwijk¹ PhD

Departments of Urology¹ and Nuclear Medicine², Radboud University
Nijmegen Medical Centre, Nijmegen, The Netherlands

Published Cancer Imaging, 2007 Nov 19;7:179-88



Renal Cell Carcinoma (RCC) is the most common malignancy arising in the kidney. In the US alone, each year 39,000 people are diagnosed with RCC and 13,000 people die from the disease ¹. The classic triad (flank pain, hematuria and a palpable abdominal mass) is only seen in approximately 9% of newly diagnosed patients ². This considerably complicates the diagnosis, since the disease can present with a broad array of (paraneoplastic) symptoms ^{3,4}. As a consequence, 30% of patients will present with metastatic disease, whereas of the other 70% treated by nephrectomy, 30-40% will eventually relapse ¹. The 5-year survival rate for small (less than 7 cm) tumors limited to the kidney (pT1 tumor) is more than 90%⁵, but prognosis for metastatic disease is bleak, with a median survival of only 10 months when untreated⁶. RCC is known as a chemotherapy and radiation resistant tumor^{7,8}. Therefore, therapeutic strategies focus on immunotherapy, neoangiogenesis inhibitors and other targeted approaches.

Monoclonal antibodies

Since the first description of Ehrlich to specifically guide cytotoxic agents to cancer tissue ⁹, the feasibility of this approach has been debated. Development of the hybridoma technique ¹⁰ allowed isolation of large quantities of antibodies with predefined specificity. With the identification of the tumor-associated target antigens, real progress was made on developing treatment and/or diagnostic strategies using mAbs.

Tumor-associated antigens (TAA) have been identified for a series of human tumor types ¹¹⁻¹⁵. These are either differentiation antigens, (transiently) expressed during organogenesis, aberrantly expressed antigens, or (transiently) expressed elsewhere in nonrelated normal tissue(s). Expression of antigens on the primary tumor or metastases is generally heterogeneous. For tumor targeting with mAbs this is a suboptimal feature, since not all cells can be targeted by the mAb. Heterogeneous expression between different tumor sites, varying degrees of expression in tumor cells of the same tumor and temporal modulation of TAA-expression are considered major limitations of effective targeting of tumors with mAbs.

In addition to intratumoral heterogeneity of antigen expression, other parameters have been defined that may affect tumor targeting with mAbs. These are size of the tumor mass, antigen density, the fate of antigen-antibody immune complex, presence of circulating antigen, mAb format, mAb dose, route of administration and mAb circulatory half-life ¹⁶. These parameters can differ from one tumor type to another. Also, tumor physiology is an important factor in antigen targeting by mAbs. MAb targeting of tumors is complicated by large tumor blood vessels as well as impaired blood flow in the tumor, elevated interstitial fluid pressure (IFP) and large transport distances in the tumor ¹⁷.

High vascular density is not equivalent to high perfusion rates in the tumor, which are required for optimal mAb delivery. RCC has always been considered a highly vascularized tumor by morphologic standards. However, in comparison with normal kidney tissue RCC is poorly perfused ¹⁷, thereby impeding adequate mAb delivery to the tumor cells. These limitations of delivering the mAb to tumor tissue have to be overcome in order to develop a suitable mAb-based treatment strategy.

Several mechanisms to eradicate tumor cells by mAbs are available: either via effector cells or complement dependent cytotoxicity or through conjugation of the mAb to toxins, drugs or radionuclides. Since antigen expression within tumors is heterogeneous, antigen-negative tumor cells may evade tumor cell lysis by effector cell- or complement-mediated cytotoxicity, which may eventually lead to tumor recurrence. The same applies to mAbs conjugated to toxins or drugs, since internalization of a mAb conjugated to a toxin or drug is required to mediate cell killing ¹⁶.

Radiolabeling of antibodies was pioneered in 1950, when Eisen observed that proteins could be labeled with ¹³¹I without altering their immunological specificity ¹⁸. Besides ¹³¹I, other radionuclides (⁹⁰Y, ¹⁷⁷Lu, ¹⁸⁶Re, ¹⁸⁸Re and ⁶⁷Cu) have since been investigated to induce tumor cell death (**Table 1**). The advantage of the use of radiolabeled antibodies is that the mAb does not have to bind to every tumor cell to induce cytotoxicity, since these radionuclides emit β -particles, which can be effective to up to 50 or more cell diameters. This so-called crossfire effect can thus overcome heterogeneity of antigen

Radio-nuclide	Half-life	β -average (keV)	γ (keV)	Maximum range β -particles in tissue (mm)	Advantages	Disadvantages
¹³¹ I	8.0 days	192	362	3.0	Easy labeling Inexpensive	High radiation burden to personnel/relatives Hospital admittance required
¹⁸⁶ Re	90.7 hr	362	137	5.1	Out-patient treatment possible Ideal gamma for imaging	Laborious labeling
⁹⁰ Y	64 hr	935	none	12	High-energy beta-emission Prolonged tumor retention Out-patient treatment possible	No imaging possible
¹⁷⁷ Lu	6.7 days	149	208	2.5	Prolonged tumor retention	

Table 1. Radionuclides used in radioimmunotherapy of clear cell renal cell carcinoma.

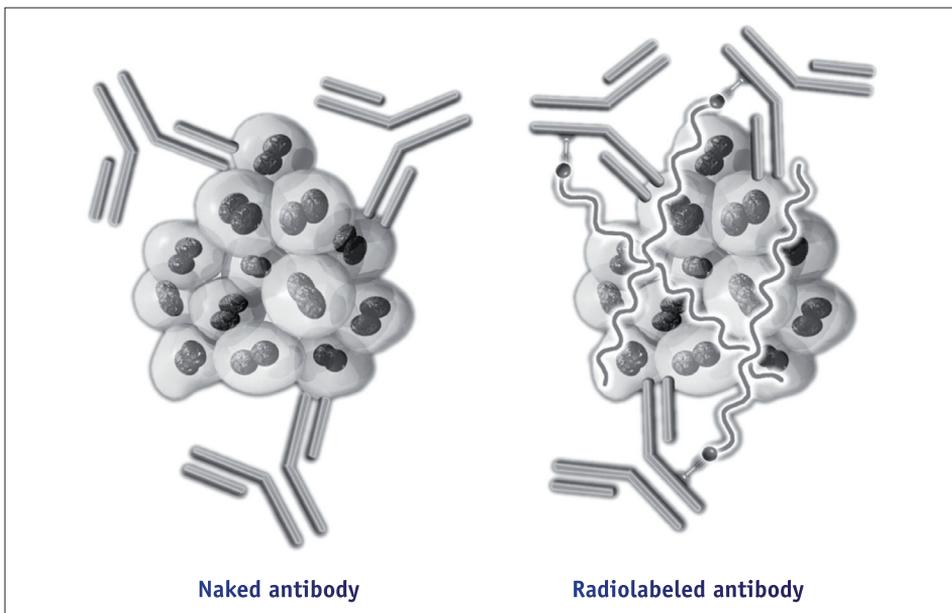


Figure 1. Cross-fire effect of radioimmunotherapy: Not all tumor cells are targeted by the IgG mAb, but the radiation delivered by the mAb kills all tumor cells in the vicinity of the targeted cell (adapted from Fink-Bennett et. Al, J Nucl Med Technol 2003).

Reference	Radiopharmaceutical	Target antigen	MAb type	No. of patients	Responses	Special features
Divgi et al. ⁴⁶	¹³¹ I-G250	G250	Murine G250	33	17 SD	
Steffens et al. ⁵⁷	¹³¹ I-G250	G250	Chimeric G250	12	1 PR; 1 SD	
Divgi et al. ⁵⁹	¹³¹ I-cG250	G250	Chimeric G250	15	7 SD	Fractionated RIT
Brouwers et al. ⁶¹	¹³¹ I-cG250	G250	Chimeric G250	27	5 SD	2 high-dose treatment

Table 2. Phase I/II radioimmunotherapy trials in clear cell renal cell carcinoma.

expression, as the radiation destroys the antigen-negative cells as well (**Figure 1**). Limitation of this approach is the sensitivity of normal organs to radiation, particularly the bone marrow. The dose limiting toxicity of delivering high dose radioimmunotherapy (RIT), using radiolabeled antibodies, is therefore generally hematological.

Using the previously mentioned hybridoma technique a wide array of mAbs against TAAs has been produced, e.g. mAbs against carcinoembryonic antigen (CEA) (mainly expressed in colorectal and medullary thyroid cancer), MUC-1 (ovarian, breast cancer, a.o.), TAG72 (ovarian cancer, colorectal cancer, a.o.), CD20 (Non-Hodgkin's Lymphoma (NHL)) and carbonic anhydrase IX (CAIX) in RCC. In various clinical trials safety and efficacy of these newly developed mAbs labeled with various radionuclides have been investigated ¹¹. RIT with mAbs targeting NHL have shown exciting results. These tumors are relatively radiosensitive and mAbs have good access to the tumor. The effector cell, complement and apoptosis inducing cytotoxicity of the mAb give high intrinsic anti-tumor activity as well. Extensive research has resulted in the first registered treatment with radiolabeled mAbs directed against the surface antigen CD20 expressed on B-cell NHL (⁹⁰Y-labeled anti-CD20 mAb Ibritumomab Tiuxetan (Zevalin[®]) and ¹³¹I-labeled anti-CD20 mAb tositumomab (Bexxar[®]).

In patients with solid tumors therapeutic strategies with radiolabeled mAbs have been less successful than in patients with hematological malignancies. This is partly due to the lower radiation sensitivity of solid tumors. However, as mentioned previously, tumor-related factors also play an important role. The most common types of solid malignancies targeted in clinical trials with RIT have been epithelial cancers, e.g. colorectal cancer, ovarian cancer, medullary thyroid cancer, breast cancer, prostate cancer and RCC. Results of these trials did not result in registration of radiolabeled mAb preparations for regular treatment of these cancer types. However, patients entered in these trials often had bulky metastatic disease and had been heavily pretreated with chemotherapy and/or radiotherapy in most cases. Complete responses to RIT have incidentally been reported. Partial responses and stabilizations of previously progressive disease have been seen in few patients in most of these trials ¹⁹.

Monoclonal antibodies in renal cell carcinoma

In RCC, several mAbs have been defined that are reactive with RCC-associated antigens ²⁰⁻²⁹. Most of these recognize kidney differentiation antigens expressed by subsets of RCC. Cross-reactivity with non-kidney tissue was seen in some of these mAbs, whereas others were only expressed in the kidney.

One of the mAbs, that showed relative high tumor-to-blood ratios in mice with RCC xenografts is mAb A6H ^{30, 31}. This mAb recognizes an antigen common to RCC, some lung and colon carcinomas, the proximal renal tubules but no other normal tissues *in vivo* ³². In a clinical study, the imaging and RIT potential of this mAb was examined ³¹. Positive images were obtained in only 5 of 15 patients. This low sensitivity was attributed to soluble antigen binding by the mAb and the localization of the antibody in normal tis-

sue, thereby not allowing the mAb to bind to tumor tissue. This clinical finding of localization of the antibody in normal tissue was not in line with the previous findings on antigen expression. After modification of the dosing regimen, the detection rate of metastatic lesions increased, but the number of detected lesions remained unsatisfactory. As a result, the use of mAb A6H for diagnosis and treatment of RCC was discontinued.

Discovery and use of G250; from mG250 to cG250

G250, a mAb against a RCC-associated antigen has been investigated extensively, because the antigen that this mAb recognizes showed remarkable tissue distribution and expression. The mAb G250 was obtained after fusion of spleen cells from a mouse immunized with fresh RCC homogenates. The antigen that mAb G250 targets has been designated in literature as MN, CAIX and G250. The term CAIX will be used in this chapter. Of the 47 primary RCC specimen initially analyzed, 42 (89%) showed homogeneous CAIX expression, whereas 4 tumors showed heterogeneous expression and 1 tumor was CAIX-negative. Of the 8 metastases examined, CAIX expression was homogeneous in 5 (62%), heterogeneous in 2, while 1 did not express the CAIX²⁵. Expression in normal tissues has been evaluated extensively and it has shown to be restricted to the (upper) gastrointestinal mucosa (stomach, ileum, proximal and middle colon) and gastrointestinal related structures (intra- and extrahepatic biliary system, pancreas), with much lower expression levels than in RCC^{25, 33, 34}.

Later studies showed an almost ubiquitous expression (>90%) of CAIX in clear cell RCC (ccRCC), being the most prominent form of RCC (80% of cases)³⁵. CAIX expression in the different histological subtypes of RCC was determined by RT-PCR and immunohistochemistry. All the clear cell tumors displayed CAIX mRNA, but expression of CAIX by oncocytomas, chromophobe or papillary RCC was low or absent³⁵⁻³⁷. Various animal and ex vivo experiments have shown the potential of the G250 mAb as a targeting modality of RCC³⁸⁻⁴³. Since CAIX is high and homogeneously expressed in RCC tissue, is expressed in only a few normal tissues, mAb G250 seemed a suitable candidate for further investigation in clinical studies.

Two clinical studies with radiolabeled murine G250 (mG250) have been completed. Imaging and biodistribution were studied in 16 patients receiving 370 MBq ¹³¹I-labeled mG250 at escalating protein dose levels one week prior to nephrectomy. After 3 to 4 days clear delineation of tumors was seen in 12 patients, imaged with a gamma camera. Ten of these tumors proved to be G250-positive, whereas the other two showed less than 5% CAIX expression. The four tumors that were not visualized were non-clear cell RCC. After nephrectomy, tumor samples were shown to have high and focal uptake of

G250, up to 0.21 % injected dose/gram (%ID/g). Tumor targeting was not the result of blood pooling, as the blood volume marker ^{99m}Tc-labeled human serum albumin showed significantly lower tumor uptake than ¹³¹I-mG250 that had been administered earlier. Therefore, this was indicative of true antibody targeting of the tumor by mG250 ⁴⁴. As good targeting of ccRCC by mG250 was seen in this study, a phase I/II radioimmunotherapy (RIT) dose escalation study was performed by Divgi et al. Patients in this study were treated with one high-activity-dose injection of ¹³¹I-mG250. After reaching the maximum tolerated dose (MTD), another fifteen patients were enrolled and treated at the MTD to monitor any possible therapeutic effects. In the phase I dose-escalation study, MTD was defined at 3330 MBq/m², with hematological toxicity being dose limiting. Transient hepatic toxicity occurred at dose levels of 1665 MBq/m² and higher, but was not dose limiting. Fourteen patients had grade 3 hepatic toxicity, that did not last for more than 2 weeks. A total of 33 patients was treated, 18 in the dose-escalating part of the study and another 15 patients at the MTD (3330 MBq/m²), to evaluate therapeutic efficacy. Of these 33 patients, 17 stabilized for three months, after which patients received other treatments, preventing further follow-up. Three patients showed regression of some of their lesions, but no partial or complete responses were noted ⁴⁵.

The formation of human anti-mouse antibodies (HAMA) in all patients receiving mG250 prohibited retreatment. Formation of immune complexes with rapid clearance of the radiolabeled mAb to liver and spleen would have occurred in the case of repeated administration, thereby limiting targeting of the mAb to the tumor ⁴⁵. This, in combination with the high potential of G250 as a targeting agent in the treatment of metastasized RCC, led to the development of a chimeric form of G250 (cG250) ⁴⁶. This mAb is composed of murine antigen-binding variable domains, that recognize the TAA and human constant domains of heavy and light chains derived from the human IgG1 isotype ^{47, 48}. Rationale behind this construction was the decrease in immunogenicity of the antibody, potentially allowing multiple administrations.

Use of unlabeled antibody cG250

Unlabeled G250 antibody facilitates antibody-dependent cellular cytotoxicity (ADCC) of CAIX expressing cells, which leads to induction of lysis of these cells ⁴⁷. This finding led to a study where 36 patients with metastatic ccRCC received 50 mg cG250 weekly for 12 weeks. No drug-related grade 3-4 toxicity occurred during this trial ⁴⁹. Development of human anti-chimeric antibody (HACA) was low and not clinically significant. Before treatment, 80% of patients were progressive. After treatment, 11 patients had stable

disease and during follow-up one complete and one partial response were seen. The median survival of 15 months suggested that G250 may be able to immunomodulate the natural course of metastatic RCC ⁵⁰. Based on these results, an adjuvant phase III trial has been completed in high-risk ccRCC patients who were nephrectomised and had no known metastases, using this treatment regimen. Results of this trial are awaited.

Since the 1990's, high-dose bolus interleukin-2 (IL-2) has been used as a first-line therapy for metastatic RCC, although in the present era of targeted agents it is not commonly used. IL-2 is a T-cell growth factor that is thought to play a critical role in T-cell dependent immune responses. High-dose bolus IL-2 as therapy in metastatic RCC has had varying success, with responses in up to 15% of patients ⁵¹. It was hypothesized that the immunological specificity of lymphokine-activated killer cells of patients receiving IL-2 therapy may be enhanced through the co-administration of cG250 ⁴⁷. Vice versa, co-administration of IL-2 can enhance the therapeutic efficacy by stimulating G250-mediated ADCC ⁵²⁻⁵⁴.

In a phase II trial 35 patients with progressive ccRCC received weekly i.v. infusions of 50 mg G250 and daily sc low-dose IL-2, for 11 weeks. When patients responded or disease stabilized, therapy was continued for another 6 weeks. Treatment was safe and well tolerated. After 16 weeks, 1 partial response was noted and 11 patients had stabilized. These 12 patients continued treatment. This resulted in 1 partial response and 7 patients retained stable disease. Mean survival was 24 months in this trial, compared to 16.3 months median survival with high-dose IL-2 therapy ⁵¹, while side effects were mild. The authors considered it unlikely that the increased survival was due to the low-dose IL-2, using a 6-fold decrease of normal IL-2 dose used to induce clinical efficacy. They considered it rather a synergic effect of G250 and IL-2 ⁵⁵.

Studies with radiolabeled cG250

After cG250 became available, the pharmacokinetics, biodistribution, imaging characteristics and dosimetry of this new radiolabeled targeting vehicle was studied in a protein dose escalation study as was done with murine G250. Sixteen presurgical RCC patients were entered, receiving increasing doses of cG250 between 2 and 50 mg labeled with ¹³¹I, given i.v. a week before patients underwent nephrectomy. Highest tumor uptake was observed in particular in the patients that received 5 and 10 mg ¹³¹I-mG250, with focal tumor uptake as high as 0.52% ID/g. At higher protein doses, focal tumor uptake did not exceed 0.017% ID/g. This suggested that antigen-saturation could have occurred at protein doses exceeding 10 mg. Excellent images of CAIX positive tumors were obtained, with visualization of tumor lesions and metastases, seen earlier on CT or X-ray. No previously unknown lesions were visualized. Dosimetric analysis showed a high

radiation-absorbed dose to primary tumors as well as metastases (up to 1.9 cGy/MBq to the primary tumor). Up to 20 weeks post injection, Human anti-chimeric antibody (HACA) responses were seen in 2 patients, but titers were considered low and clinically irrelevant⁵⁶. Reducing the immunogenic properties of the antibody opened the possibility to multiple treatments. These results justified further investigation on the use of cG250 as a radioimmunotherapeutic agent.

The MTD of ¹³¹I-cG250 in metastatic RCC was determined in a phase I radioactivity dose escalation trial in patients with progressive metastatic RCC at study entry. Twelve patients received 5 mg cG250 labeled with 185 MBq ¹³¹I (scout dose). When accumulation of antibody was seen in any tumor site, patients received escalating radioactivity doses of ¹³¹I-cG250 one week later. In contrast to the trials performed with murine G250, no hepatic toxicity was seen. This was believed to be the result of saturation of the hepatic compartment by the diagnostic scout dose ¹³¹I-cG250. Besides mild nausea without vomiting and transient fatigue (both grade 1 CTC) no other non-hematological side effects occurred. The MTD was observed to be 2220 MBq/m², with hematological toxicity as the dose-limiting factor. Of the 8 patients receiving treatment, one patient showed stable disease and one had a partial response⁵⁷.

In subsequent studies two strategies were tested to optimize targeting of metastatic ccRCC with RIT. These were fractionation of the dose and two sequential high-dose treatments.

Fractionation of the dose was done in a phase I study by Divgi et al⁵⁸. In this study, patients received 1110 MBq ¹³¹I-cG250 and whole-body activity was measured after 2-3 days. Then, another administration of ¹³¹I-cG250 was given to again 'top up' the radioactivity in the body to 1110 MBq. This was continued until a whole-body absorbed dose of 0.50 Gy was reached. Patients without disease progression were retreated after recovery from hematological toxicity. In subsequent cohorts, the whole-body absorbed dose was increased by 0.25 Gy. A total of 15 Patients were included in the trial. HACA development was measured in 2 patients, altering pharmacokinetics and excluding them from further treatment. Dose-limiting toxicity was again hematologic, with the MTD at 0.75 Gy as whole-body absorbed dose. Four patients received multiple fractionated doses. Seven patients stabilized, but no major clinical responses were seen. This trial therefore provided no evidence on a potential benefit of fractionation of RIT doses in treating ccRCC.

The MTD found in the activity dose-escalation study by Steffens et al.

(2220 MBq/m²), combined with the properties of cG250 allowing multiple administrations led to a study where two sequential high doses of ¹³¹I-cG250 treatment were given. Patients had progressive metastatic ccRCC at study entry. Patients received 2220 MBq/m² ¹³¹I-cG250. Three months later, rapid clearance of the mAb by HACA development was excluded by imaging of a scout dose of 185 MBq ¹³¹I-cG250. When tumor targeting was

seen again, the second high-dose injection ^{131}I -cG250 was given. MTD of the 2nd RIT proved to be again due to hematological toxicity and was set at 1665 MBq/m², being 75% of the MTD of the first infusion. Subsequently, 15 patients were treated at this dose level to evaluate tumor response. In total, 29 patients entered the study, 11 were excluded due to grade 4 hematological toxicity after the first RIT (n=3), palliative treatment (n=2), rapid progressive disease (n=2) or HACA development (n=4). Of the 18 patients evaluated (3 did not receive the 2nd RIT at MTD), 5 patients had stabilization of their disease, lasting 3-12 months. No partial or complete responses were seen. There proved to be an inverse correlation between the size of metastases and radiation absorbed dose. Therapeutic radiation doses (more than 50 Gy)⁵⁹ were only guided to the lesions smaller than 5 grams. The authors concluded that RIT in RCC patients could best be given in the setting of small volume disease or as adjuvant therapy⁶⁰.

Various radionuclides in targeting ccRCC with cG250 have been under investigation. First, the targeting capabilities of ^{111}In -cG250 have been compared to those of ^{131}I -cG250. In nude mice with human tumor xenografts, superior targeting of ^{111}In -cG250 over ^{131}I -cG250 was shown^{61, 62}. As part of the cG250 antibody-antigen complex is internalized, intracellular ^{131}I -cG250 is metabolized and rapidly excreted by the tumor cell. Metallic radionuclides, such as ^{111}In , ^{90}Y and ^{177}Lu , are trapped in the lysosomes and residualize intracellularly after internalization of the mAb-antigen complex by the target cells⁶³⁻⁶⁶. To investigate whether this phenomenon may also occur in humans, 5 patients with metastatic RCC were i.v. injected with 185 MBq ^{111}In -DTPA-cG250 on day 0 and 185 MBq ^{131}I -cG250 on day 4. Gamma images were made directly and on day 4 after both injections and compared. ^{111}In -DTPA-cG250 images (**Fig. 2**) revealed more lesions than ^{131}I -cG250 (47 vs. 30) and quantitative analysis showed higher accumulation of ^{111}In -DTPA-cG250 in 20 of 25 lesions measured in terms of %ID/g³⁴.

The therapeutic properties of cG250 labeled with 4 radionuclides were tested in nude mice with human RCC xenografts. The 4 radionuclides under investigation were ^{90}Y and ^{177}Lu (both residualizing), and ^{131}I and ^{186}Re (both non-residualizing). After determining the MTD for each radionuclide conjugated to cG250 in mice, a RIT experiment was done comparing tumor growth and survival after treatment with each radiolabeled cG250 preparation. Tumor growth was delayed most effectively by ^{177}Lu , followed by ^{90}Y and ^{186}Re and least by ^{131}I (185, 125, 90 and 25 days, respectively). The best median survival was observed for ^{177}Lu (300 days), with the control group having a median survival of less than 150 days. The residualizing radionuclides ^{177}Lu and ^{90}Y administered higher radiation doses to the tumor. These radionuclides should be considered better candidates for RIT with cG250 than ^{131}I ⁶⁷.

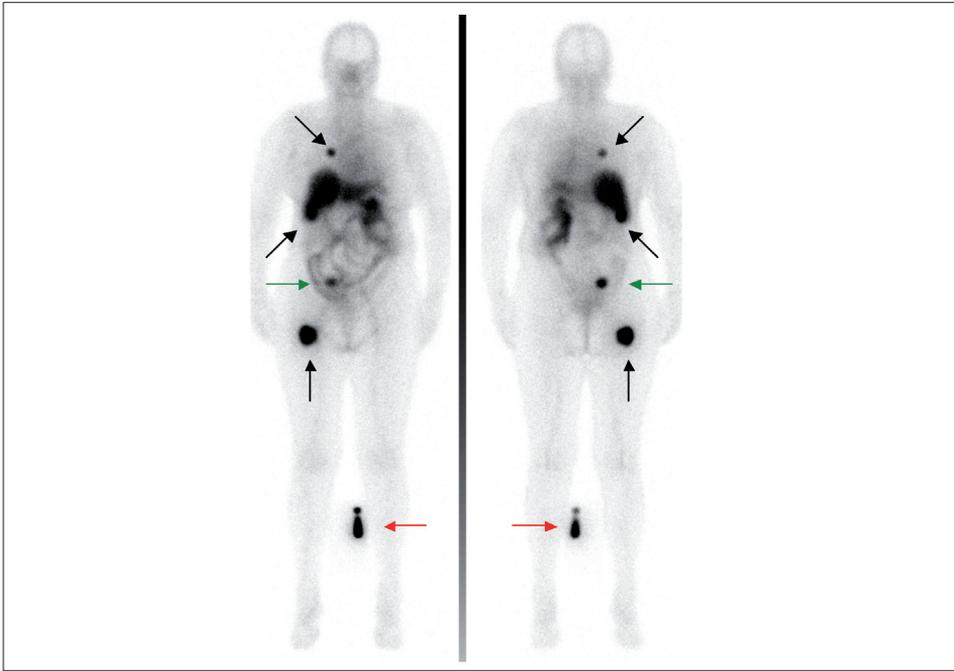


Figure 2a. ^{111}In -cG250 immunoscintigram of a patient with metastatic ccRCC, acquired 6 days after injection of 185 MBq ^{111}In -cG250. Black arrows mark the RCC lesions. Green arrows mark a lesion not seen on the FDG-PET-CT images shown in **Figure 2b**. Red arrows indicate the injection standard. The anterior image is shown in the left panel, the posterior image is shown in the right panel.

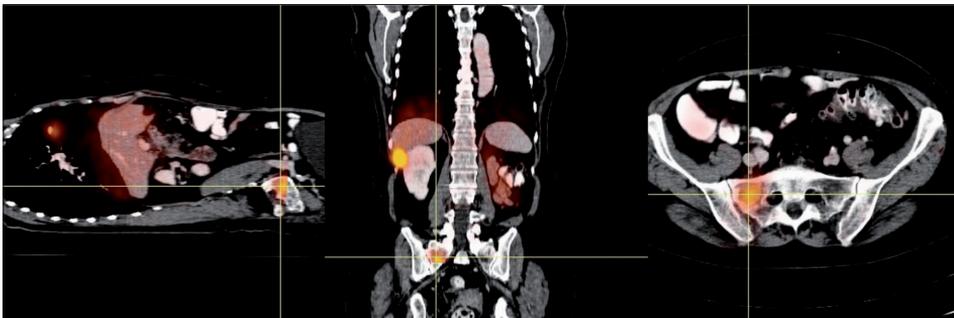


Figure 2b. PET-CT scan of the same patient acquired after injection of 250 MBq ^{18}F -FDG.

Positron emission tomography

18F-Fluorodeoxyglucose Positron Emission Tomography (FDG-PET) has been widely investigated and is now an established molecular imaging modality for various malignancies. In RCC, the diagnostic accuracy depends on the tumor grade, the FDG uptake being higher in dedifferentiated tumors which is also observed in other tumor types. One of the major drawbacks for detection renal cell carcinoma with FDG-PET is the excretion of FDG via the kidneys, resulting in relatively high background activity. This can only partly be reduced by hyperhydration or administration of diuretics. Another disadvantage of imaging renal masses with FDG-PET is the reported false-positive signal in patients with angiomyolipoma, pericytoma, and pheochromocytoma⁶⁸. Wang et al. recently performed a meta-analysis of 14 articles on the role of FDG-PET and FDG-PET/CT in both primary renal tumors as extra-renal lesions⁶⁹. For primary renal tumors the pooled sensitivity and specificity of FDG-PET was 62% and 88%, respectively. The use of FDG-PET/CT improved the accuracy of detecting metastases, as the pooled sensitivity and specificity increased to 91% and 88%, respectively. The authors conclude that combining FDG-PET and CT is mainly helpful for detecting extra-renal metastasis rather than renal lesions. However, the total number of studies assessing the role of FDG-PET/CT evaluated in this meta-analysis is limited and further studies are warranted.

A few investigations have studied the capabilities of cG250-based immunoPET, i.e. combining the favorable characteristics of PET (high spatial resolution, three-dimensional (3D) imaging and accurate quantification of tumour uptake) with the high and specific targeting of cG250 to CAIX-expressing cells⁷⁰⁻⁷². The relatively slow pharmacokinetics of i.v. injected radiolabeled mAbs (optimal tumour uptake after several days) prevents the use of the most commonly used positron emitters (¹¹C and ¹⁸F) because their half-life is too short to be used in immunoPET. The half-lives of the positron emitters ⁸⁹Zr and ¹²⁴I (78 and 100 h, respectively) do match the relatively slow kinetics of antibodies. In a prospective study by Divgi et. al. 25 patients with suspect renal lesions scheduled for nephrectomy were studied with ¹²⁴I-cG250. Of sixteen patients with pathologically confirmed ccRCC after surgery, 15 had a positive scan (tumour-to-normal kidney ratio \geq 3:1). The failure in one patient was attributed to technical problems with the labeled material. The study showed that ¹²⁴I-cG250 could aid in the preoperative characterization of suspect renal masses and might guide crucial aspects of surgical RCC management⁷⁰. A large multicenter trial comparing conventional diagnostic CT to ¹²⁴I-cG250 immunoPET/CT for the detection of ccRCC in 226 patients scheduled for nephrectomy showed a significantly higher rate of ccRCC detection with ¹²⁴I-cG250 immunoPET/CT over conventional CT ($p=0.016$)⁷³.

Current treatment of metastatic RCC

Immunotherapy was the standard systemic treatment of metastatic RCC in the 1980s and 1990s, when it was the only treatment that offered a chance of achieving a durable complete response (IL-2 approximately 5% and interferon- α (IFN- α) approximately 2.5%). However, the development of tyrosine kinase inhibitors (TKI) targeting neo-angiogenesis pathways such as sunitinib, pazopanib and temsirolimus has resulted in significant clinical benefit for patients with metastatic RCC ⁷⁴. Response rates to treatment with these substances are relatively high (70-80% disease control). These agents mainly cause disease stabilisations, while side-effects are common and may be severe in nature ^{75, 76}. In a randomized phase 3 study comparing sunitinib with IFN- α in previously untreated mRCC patients, the progression free survival (PFS) was significantly longer in the sunitinib group compared to the IFN- α group (11 vs. 5 months). In this study, the high-response rate was confirmed with 37% of the patients achieving a partial response by RECIST criteria versus 9% for IFN. ⁷⁵ Pazopanib, another multiple tyrosine kinase inhibitor showed prolonged PFS compared to placebo (9.2 vs. 4.2 months) in treatment-naïve or cytokine-pretreated metastatic RCC patients. ⁷⁷ Bevacizumab in combination with IFN- α was compared to IFN- α with placebo in a phase 3 trial. This study reported a significantly improved PFS for bevacizumab with IFN- α (PFS 10.2 vs. 5.4 months). Overall survival (OS) was also higher for bevacizumab with IFN- α (OS 23.3 vs. 21.3 months), but this was not statistically significant. ^{78, 79} Temsirolimus, targeting the mammalian target of rapamycin (mTOR) in the neo-angiogenesis pathway, also showed a treatment benefit over IFN- α (PFS 5.5 vs. 3.1 months, OS 10.9 vs. 7.3

RCC type	MSKCC risk group	1st-line therapy	2nd-line therapy	3rd-line therapy
Clear cell	Good or intermediate	- Sunitinib - Bevacizumab + IFN- α - Pazopanib - <i>In selected patients (good prognosis, only pulmonary metastases):</i> - Interleukin-2 - IFN- α	<i>Prior TKI:</i> - Axitinib - Sorafenib - Everolimus <i>Prior cytokines:</i> - Sorafenib - Axitinib - Pazopanib	<i>Prior TKI:</i> - Everolimus Poor Temsirrolimus
		Poor	Temsirrolimus	
Non-clear cell	Good, intermediate or poor	Patients should be treated in the framework of clinical trials, however temsirolimus appears to offer a modest clinical benefit in overall survival		

Table 3. Current treatment strategy for metastatic RCC patients. Adapted from the EAU guidelines on renal cell carcinoma – version March 2013 http://www.uroweb.org/gls/pdf/10_Renal_Cell_Carcinoma_LRV2.pdf

months) in a phase 3 trial⁸⁰. There are several other substances in development such as erlotinib, tivozanib, dovitinib, axitinib and everolimus. In **table 3** an overview of the current treatment strategies in metastatic RCC patients is given. However, the fast pace of development of TKI treatment will probably change this treatment paradigm in the near future.

TKI and tumor vascularisation

Sorafenib, approved for the second-line treatment of metastatic RCC, inhibits the tyrosine kinase activity of the vascular endothelial growth factor receptors (VEGFR) and platelet derived growth factor receptors (PDGFR)⁸¹. VEGF plays a pivotal role in tumor angiogenesis. In ccRCC, VEGF is overexpressed^{82,83} due to activation of the hypoxia inducible factor pathways⁸⁴. Bevacizumab is a monoclonal antibody recognizing VEGF-A, and is known to inhibit angiogenesis by preventing VEGF-VEGFR interaction. In colorectal cancer patients administration of high-dose bevacizumab may lead to a short normalization of the tumor microvasculature along with a reduced interstitial fluid pressure⁸⁵. This normalization of the tumor vasculature may temporarily improve tumor perfusion⁸⁶ and enhance the delivery of therapeutic agents, which would explain the synergistic effect of chemotherapy when combined with bevacizumab in colorectal cancer patients⁸⁷. In addition, several studies have shown enhanced mAb accumulation after anti-angiogenic treatment in experimental tumor models^{88,89}. Therefore, co-administration of RIT during angiogenesis treatment in mRCC patients might also work synergistically, due to the enhanced uptake of the radiolabeled mAb in the tumor.

Thesis outline

The aim of this thesis was to investigate new strategies for imaging and treatment of ccRCC lesions based on the use of the anti-CAIX monoclonal antibody cG250. Preclinical and clinical studies are presented in this thesis.

In chapter 2, the mechanism of CAIX expression in ccRCC through the mutational loss of Von-Hippel Lindau protein is described. We examined the literature on prognostic accuracy of CAIX expression patterns and reviewed the current diagnostic and therapeutic applications of CAIX and mAb cG250 in ccRCC.

In chapter 3, the phase I study to determine the maximum tolerated dose of ^{177}Lu -cG250 radioimmunotherapy in patients with metastasized RCC is described. The side effects, immunological response patterns and the preliminary therapeutic efficacy of escalating activity doses of ^{177}Lu -cG250 are described.

Chapter 4 describes the dosimetric analyses of the ^{111}In -cG250 and ^{177}Lu -cG250 scans acquired in the phase I radioimmunotherapy study. This analysis provided insight in the radiation absorbed doses of normal organs, red bone marrow and metastases during radioimmunotherapy with ^{177}Lu -cG250. Simulations of ^{177}Lu -cG250 and ^{90}Y -cG250 radioimmunotherapy radiation doses were performed based on the ^{111}In -cG250 data. These data were compared to the actual ^{177}Lu -cG250 absorbed doses to validate the dosimetric analyses. The correlation between the estimated radiation doses to the red marrow and hematological toxicity was determined.

The effects of neo-adjuvant treatment with sorafenib on the uptake of intravenously administered ^{111}In -labeled bevacizumab were studied in chapter 5. Changes in tumor vascularity, expression patterns of VEGF and subsequent tumor uptake of the radiolabeled antibody as seen after tyrosine kinase inhibitor treatment were determined.

In chapter 6, a study is described examining the tumor targeting characteristics of ^{124}I -cG250 and ^{89}Zr -cG250 in mice with human RCC xenografts and investigated which PET radionuclide was optimal for cG250-based immunoPET imaging of RCC.

A novel diagnostic modality, optical imaging, was used in chapter 7 to detect and depict RCC xenografts in nude mice. Studies were performed to establish antigen-specific binding of the cG250-fluorophore conjugate, cG250-IRDye800CW to RCC tumors. We explored this new technique, which may herald a new diagnostic era in intra-operative detection of positive surgical margins and tumor-affected lymph nodes.

REFERENCE LIST

- (1) Jemal A, Siegel R, Ward E et al. Cancer statistics, 2006. *CA Cancer J Clin* 2006 March;56(2):106-30.
- (2) DeKernion JB. *Real numbers*. Campbell's Urology. ed. Philadelphia 1986.: WB Saunders; 1986.
- (3) Skinner DG, Colvin RB, Vermillion CD, Pfister RC, Leadbetter WF. Diagnosis and management of renal cell carcinoma. A clinical and pathologic study of 309 cases. *Cancer* 1971 November;28(5):1165-77.
- (4) Gold PJ, Fefer A, Thompson JA. Paraneoplastic manifestations of renal cell carcinoma. *Semin Urol Oncol* 1996 November;14(4):216-22.
- (5) Pantuck AJ, Zisman A, Beldegrun AS. The changing natural history of renal cell carcinoma. *J Urol* 2001 November;166(5):1611-23.
- (6) Zisman A, Pantuck AJ, Wieder J et al. Risk group assessment and clinical outcome algorithm to predict the natural history of patients with surgically resected renal cell carcinoma. *J Clin Oncol* 2002 December 1;20(23):4559-66.
- (7) Motzer RJ, Russo P. Systemic therapy for renal cell carcinoma. *J Urol* 2000 February;163(2):408-17.
- (8) Yagoda A, Petrylak D, Thompson S. Cytotoxic chemotherapy for advanced renal cell carcinoma. *Urol Clin North Am* 1993 May;20(2):303-21.
- (9) Ehrlich P. *Collected studies on immunology*. New York: John Wiley; 1906.
- (10) Kohler G, Milstein C. Continuous cultures of fused cells secreting antibody of predefined specificity. *Nature* 1975 August 7;256(5517):495-7.
- (11) Larson SM. Lymphoma, melanoma, colon cancer: diagnosis and treatment with radiolabeled monoclonal antibodies. The 1986 Eugene P. Pendergrass New Horizons Lecture. *Radiology* 1987 November;165(2):297-304.
- (12) Larson SM, Divgi CR, Scott AM. Overview of clinical radioimmunodetection of human tumors. *Cancer* 1994 February 1;73(3 Suppl):832-5.
- (13) Mach JP, Pelegri A, Buchegger F. Imaging and therapy with monoclonal antibodies in non-hematopoietic tumors. *Curr Opin Immunol* 1991 October;3(5):685-93.
- (14) Goldenberg DM. Current status of cancer imaging with radiolabeled antibodies. *J Cancer Res Clin Oncol* 1987;113(3):203-8.
- (15) Goldenberg DM, Larson SM, Reisfeld RA, Schlom J. Targeting cancer with radiolabeled antibodies. *Immunol Today* 1995 June;16(6):261-4.
- (16) Oosterwijk E, Divgi CR, Brouwers A et al. Monoclonal antibody-based therapy for renal cell carcinoma. *Urol Clin North Am* 2003 August;30(3):623-31.
- (17) Jain RK. Delivery of molecular medicine to solid tumors: lessons from in vivo imaging of gene expression and function. *J Control Release* 2001 July 6;74(1-3):7-25.
- (18) Eisen NH, Keston AS. The immunologic reactivity of bovine serum albumin labeled with trace-amounts of radioactive iodine (I-131). *J Immunology* 63, 71-80. 1950.
- (19) Koppe MJ, Postema EJ, Aarts F, Oyen WJ, Bleichrodt RP, Boerman OC. Antibody-guided radiation therapy of cancer. *Cancer Metastasis Rev* 2005 December;24(4):539-67.
- (20) Bander NH, Cordon-Cardo C, Finstad CL et al. Immunohistologic dissection of the human kidney using monoclonal antibodies. *J Urol* 1985 March;133(3):502-5.
- (21) Bander NH, Finstad CL, Cordon-Cardo C et al. Analysis of a mouse monoclonal antibody that reacts with a specific region of the human proximal tubule and subsets renal cell carcinomas. *Cancer Res* 1989 December 1;49(23):6774-80.
- (22) Finstad CL, Cordon-Cardo C, Bander NH, Whitmore WF, Melamed MR, Old LJ. Specificity analysis of mouse monoclonal antibodies defining cell surface antigens of human renal cancer. *Proc Natl Acad Sci U S A* 1985 May;82(9):2955-9.
- (23) Fischer P, Storkel S, Haase W, Scherberich JE. Differential diagnosis of histogenetically distinct human epithelial renal tumours with a monoclonal antibody against gamma-glutamyltransferase. *Cancer Immunol Immunother* 1991;33(6):382-8.

- (24) Kinouchi T, Nakayama E, Ueda R et al. Characterization of a kidney antigen defined by a mouse monoclonal antibody K2.7. *J Urol* 1987 January;137(1):151-4.
- (25) Oosterwijk E, Ruiters DJ, Hoedemaeker PJ et al. Monoclonal antibody G 250 recognizes a determinant present in renal-cell carcinoma and absent from normal kidney. *Int J Cancer* 1986 October 15;38(4):489-94.
- (26) Oosterwijk E, Ruiters DJ, Wakka JC et al. Immunohistochemical analysis of monoclonal antibodies to renal antigens. Application in the diagnosis of renal cell carcinoma. *Am J Pathol* 1986 May;123(2):301-9.
- (27) Tokuyama H, Tokuyama Y. Mouse monoclonal antibodies with restricted specificity for human renal cell carcinoma and ability to modulate the tumor cell growth in vitro. *Hybridoma* 1988 April;7(2):155-65.
- (28) Vessella RL, Lange PH, Palme DF, Chiou RK, Elson MK, Wessels BW. Radioiodinated monoclonal antibodies in the imaging and treatment of human renal cell carcinoma xenografts in nude mice. *Targeted Diagn Ther* 1988;1:245-82.
- (29) Yoshida SO, Imam A. Monoclonal antibody to a proximal nephrogenic renal antigen: immunohistochemical analysis of formalin-fixed, paraffin-embedded human renal cell carcinomas. *Cancer Res* 1989 April 1;49(7):1802-9.
- (30) Chiou RK, Vessella RL, Elson MK et al. Localization of human renal cell carcinoma xenografts with a tumor-preferential monoclonal antibody. *Cancer Res* 1985 December;45(12 Pt 1):6140-6.
- (31) Vessella RL, Chiou RK, Grund FM. Renal Cell Carcinoma (RCC) phase I-II trials with 131-I labeled monoclonal antibody A6H: imaging and pharmacokinetic studies. [Abstr 1525]. 1987. Proc. Am. Ass. Can. Res. 28:480. Ref Type: Generic
- (32) Vessella RL, Moon TD, Chiou RK et al. Monoclonal antibodies to human renal cell carcinoma: recognition of shared and restricted tissue antigens. *Cancer Res* 1985 December;45(12 Pt 1):6131-9.
- (33) Pastorekova S, Parkkila S, Parkkila AK et al. Carbonic anhydrase IX, MN/CA IX: analysis of stomach complementary DNA sequence and expression in human and rat alimentary tracts. *Gastroenterology* 1997 February;112(2):398-408.
- (34) Brouwers AH, Buijs WC, Oosterwijk E et al. Targeting of metastatic renal cell carcinoma with the chimeric monoclonal antibody G250 labeled with (¹³¹I)I or (¹¹¹In)In: an inpatient comparison. *Clin Cancer Res* 2003 September 1;9(10 Pt 2):3953S-60S.
- (35) Bismar TA, Bianco FJ, Zhang H et al. Quantification of G250 mRNA expression in renal epithelial neoplasms by real-time reverse transcription-PCR of dissected tissue from paraffin sections. *Pathology* 2003 December;35(6):513-7.
- (36) Chen YT, Tu JJ, Kao J, Zhou XK, Mazumdar M. Messenger RNA expression ratios among four genes predict subtypes of renal cell carcinoma and distinguish oncocytoma from carcinoma. *Clin Cancer Res* 2005 September 15;11(18):6558-66.
- (37) Uemura H, Nakagawa Y, Yoshida K et al. MN/CA IX/G250 as a potential target for immunotherapy of renal cell carcinomas. *Br J Cancer* 1999 October;81(4):741-6.
- (38) Kranenborg MH, Boerman OC, de Weijert MC, Oosterwijk-Wakka JC, Corstens FH, Oosterwijk E. The effect of antibody protein dose of anti-renal cell carcinoma monoclonal antibodies in nude mice with renal cell carcinoma xenografts. *Cancer* 1997 December 15;80(12 Suppl):2390-7.
- (39) Steffens MG, Kranenborg MH, Boerman OC et al. Tumor retention of 186Re-MAG3, ¹¹¹In-DTPA and 125I labeled monoclonal antibody G250 in nude mice with renal cell carcinoma xenografts. *Cancer Biother Radiopharm* 1998 April;13(2):133-9.
- (40) Steffens MG, Oosterwijk-Wakka JC, Zegwaard-Hagemeyer NE et al. Immunohistochemical analysis of tumor antigen saturation following injection of monoclonal antibody G250. *Anticancer Res* 1999 March;19(2A):1197-200.
- (41) van Dijk J., Oosterwijk E, van Kroonenburgh MJ et al. Perfusion of tumor-bearing kidneys as a model for scintigraphic screening of monoclonal antibodies. *J Nucl Med* 1988 June;29(6):1078-82.
- (42) van Dijk J., Uemura H, Beniers AJ et al. Therapeutic effects of monoclonal antibody G250, interferons and tumor necrosis factor, in mice with renal-cell carcinoma xenografts. *Int J Cancer* 1994 January

15;56(2):262-8.

- (43) van Dijk J., Zegveld ST, Fleuren GJ, Warnaar SO. Localization of monoclonal antibody G250 and bispecific monoclonal antibody CD3/G250 in human renal-cell carcinoma xenografts: relative effects of size and affinity. *Int J Cancer* 1991 July 9;48(5):738-43.
- (44) Oosterwijk E, Bander NH, Divgi CR et al. Antibody localization in human renal cell carcinoma: a phase I study of monoclonal antibody G250. *J Clin Oncol* 1993 April;11(4):738-50.
- (45) Divgi CR, Bander NH, Scott AM et al. Phase I/II radioimmunotherapy trial with iodine-131-labeled monoclonal antibody G250 in metastatic renal cell carcinoma. *Clin Cancer Res* 1998 November;4(11):2729-39.
- (46) Oosterwijk E, Debruyne FM, Schalken JA. The use of monoclonal antibody G250 in the therapy of renal-cell carcinoma. *Semin Oncol* 1995 February;22(1):34-41.
- (47) Surfus JE, Hank JA, Oosterwijk E et al. Anti-renal-cell carcinoma chimeric antibody G250 facilitates antibody-dependent cellular cytotoxicity with in vitro and in vivo interleukin-2-activated effectors. *J Immunother Emphasis Tumor Immunol* 1996 May;19(3):184-91.
- (48) Morrison SL, Johnson MJ, Herzenberg LA, Oi VT. Chimeric human antibody molecules: mouse antigen-binding domains with human constant region domains. *Proc Natl Acad Sci U S A* 1984 November;81(21):6851-5.
- (49) Trotti A, Colevas AD, Setser A et al. CTCAE v3.0: development of a comprehensive grading system for the adverse effects of cancer treatment. *Semin Radiat Oncol* 2003 July;13(3):176-81.
- (50) Bleumer I, Knuth A, Oosterwijk E et al. A phase II trial of chimeric monoclonal antibody G250 for advanced renal cell carcinoma patients. *Br J Cancer* 2004 March 8;90(5):985-90.
- (51) Fyfe G, Fisher RI, Rosenberg SA, Szoln M, Parkinson DR, Louie AC. Results of treatment of 255 patients with metastatic renal cell carcinoma who received high-dose recombinant interleukin-2 therapy. *J Clin Oncol* 1995 March;13(3):688-96.
- (52) Atkins M, Regan M, McDermott D et al. Carbonic anhydrase IX expression predicts outcome of interleukin 2 therapy for renal cancer. *Clin Cancer Res* 2005 May 15;11(10):3714-21.
- (53) Brouwers AH, Boerman OC, Oyen WJ. In vivo molecular prediction of carbonic anhydrase IX-G250MN expression on immunotherapy outcome in renal cancer. *Clin Cancer Res* 2005 December 15;11(24 Pt 1):8886.
- (54) Liu Z, Smyth FE, Renner C, Lee FT, Oosterwijk E, Scott AM. Anti-renal cell carcinoma chimeric antibody G250: cytokine enhancement of in vitro antibody-dependent cellular cytotoxicity. *Cancer Immunol Immunother* 2002 May;51(3):171-7.
- (55) Bleumer I, Oosterwijk E, Oosterwijk-Wakka JC et al. A clinical trial with chimeric monoclonal antibody WX-G250 and low dose interleukin-2 pulsing scheme for advanced renal cell carcinoma. *J Urol* 2006 January;175(1):57-62.
- (56) Steffens MG, Boerman OC, Oosterwijk-Wakka JC et al. Targeting of renal cell carcinoma with iodine-131-labeled chimeric monoclonal antibody G250. *J Clin Oncol* 1997 April;15(4):1529-37.
- (57) Steffens MG, Boerman OC, de Mulder PH et al. Phase I radioimmunotherapy of metastatic renal cell carcinoma with ¹³¹I-labeled chimeric monoclonal antibody G250. *Clin Cancer Res* 1999 October;5(10 Suppl):3268s-74s.
- (58) Divgi CR, O'Donoghue JA, Welt S et al. Phase I clinical trial with fractionated radioimmunotherapy using ¹³¹I-labeled chimeric G250 in metastatic renal cancer. *J Nucl Med* 2004 August;45(8):1412-21.
- (59) Goldenberg DM. Targeted therapy of cancer with radiolabeled antibodies. *J Nucl Med* 2002 May;43(5):693-713.
- (60) Brouwers AH, Mulders PF, de Mulder PH et al. Lack of efficacy of two consecutive treatments of radioimmunotherapy with ¹³¹I-cG250 in patients with metastasized clear cell renal cell carcinoma. *J Clin Oncol* 2005 September 20;23(27):6540-8.
- (61) Carrasquillo JA, Mulshine JL, Bunn PA, Jr. et al. Indium-111 T101 monoclonal antibody is superior to iodine-131 T101 in imaging of cutaneous T-cell lymphoma. *J Nucl Med* 1987 March;28(3):281-7.
- (62) Yokoyama K, Carrasquillo JA, Chang AE et al. Differences in biodistribution of indium-111-and iodine-131-labeled B72.3 monoclonal antibodies in patients with colorectal cancer. *J Nucl Med* 1989 March;30(3):320-7.
- (63) Shih LB, Thorpe SR, Griffiths GL et al. The processing and fate of antibodies and their radiolabels bound to the surface of tumor cells in vitro: a comparison of nine radiolabels. *J Nucl Med* 1994 May;35(5):899-908.

- (64) Geissler F, Anderson SK, Venkatesan P, Press O. Intracellular catabolism of radiolabeled anti-mu antibodies by malignant B-cells. *Cancer Res* 1992 May 15;52(10):2907-15.
- (65) Press OW, Shan D, Howell-Clark J et al. Comparative metabolism and retention of iodine-125, yttrium-90, and indium-111 radioimmunoconjugates by cancer cells. *Cancer Res* 1996 May 1;56(9):2123-9.
- (66) Sharkey RM, Behr TM, Mattes MJ et al. Advantage of residualizing radiolabels for an internalizing antibody against the B-cell lymphoma antigen, CD22. *Cancer Immunol Immunother* 1997 May;44(3):179-88.
- (67) Brouwers AH, van Eerd JE, Frielink C et al. Optimization of radioimmunotherapy of renal cell carcinoma: labeling of monoclonal antibody cG250 with ¹³¹I, ⁹⁰Y, ¹⁷⁷Lu, or ¹⁸⁶Re. *J Nucl Med* 2004 February;45(2):327-37.
- (68) Bachor R, Kotzerke J, Gottfried HW, Brandle E, Reske SN, Hautmann R: [Positron emission tomography in diagnosis of renal cell carcinoma]. *Urologe A* 35(2), 146-150 (1996).
- (69) Wang HY, Ding HJ, Chen JH et al.: Meta-analysis of the diagnostic performance of [18F]FDG-PET and PET/CT in renal cell carcinoma. *Cancer imaging : the official publication of the International Cancer Imaging Society* 12, 464-474 (2012).
- (70) Divgi CR, Pandit-Taskar N, Jungbluth AA et al. Preoperative characterisation of clear-cell renal carcinoma using iodine-124-labelled antibody chimeric G250 (¹²⁴I-cG250) and PET in patients with renal masses: a phase I trial. *Lancet Oncol* 2007 April;8(4):304-10.
- (71) Brouwers A, Verel I, Van EJ et al. PET radioimmunoscintigraphy of renal cell cancer using Zr-labeled cG250 monoclonal antibody in nude rats. *Cancer Biother Radiopharm* 2004 April;19(2):155-63.
- (72) Lawrentschuk N, Lee FT, Jones G et al. Investigation of hypoxia and carbonic anhydrase IX expression in a renal cell carcinoma xenograft model with oxygen tension measurements and (¹²⁴I)-cG250 PET/CT. *Urol Oncol* 2009 June 11.
- (73) Divgi CR, Uzzo RG, Gatsonis C, Bartz R, Treutner S, Yu JQ, Chen D, Carrasquillo JA, Larson S, Bevan P, Russo P. Positron emission tomography/computed tomography identification of clear cell renal cell carcinoma: results from the REDECT trial. *J Clin Oncol*. 2013 Jan 10; 31(2).
- (74) Reeves DJ, Liu CY. Treatment of metastatic renal cell carcinoma. *Cancer Chemother Pharmacol* 2009 June;64(1):11-25.
- (75) Escudier B, Eisen T, Stadler WM et al. Sorafenib in advanced clear-cell renal-cell carcinoma. *N Engl J Med* 2007 January 11;356(2):125-34.
- (76) Motzer RJ, Hutson TE, Tomczak P et al. Sunitinib versus interferon alfa in metastatic renal-cell carcinoma. *N Engl J Med* 2007 January 11;356(2):115-24.
- (77) Sternberg CN, Davis ID, Mardiak J, et al. Pazopanib in locally advanced or metastatic renal cell carcinoma: results of a randomized phase III trial. *J Clin Oncol* 2010;28(6):1061-8
- (78) Escudier B, Pluzanska A, Koralewski P, et al. Bevacizumab plus interferon alfa-2a for the treatment of metastatic renal cell carcinoma: a randomised, double-blind phase III trial. *Lancet* 2007;370(9605): 2103-11.
- (79) Escudier B, Bellmunt J, Negrier S, et al. Phase III trial of bevacizumab plus interferon alfa-2a in patients with metastatic renal cell carcinoma (AVOREN): final analysis of overall survival. *J Clin Oncol* 2010;28(13):2144-50.
- (80) Hudes G, Carducci M, Tomczak P, et al. Temsirolimus, interferon alfa, or both for advanced renal-cell carcinoma. *N Engl J Med* 2007;356(22):2271-81.
- (81) Ahmad T, Eisen T. Kinase inhibition with BAY 43-9006 in renal cell carcinoma. *Clin Cancer Res* 2004 September 15;10(18 Pt 2):6388S-92S.
- (82) Takahashi A, Sasaki H, Kim SJ et al. Markedly increased amounts of messenger RNAs for vascular endothelial growth factor and placenta growth factor in renal cell carcinoma associated with angiogenesis. *Cancer Res* 1994 August 1;54(15):4233-7.
- (83) Turner KJ, Moore JW, Jones A et al. Expression of hypoxia-inducible factors in human renal cancer: relationship to angiogenesis and to the von Hippel-Lindau gene mutation. *Cancer Res* 2002 May 15;62(10):2957-61.
- (84) Bratslavsky G, Sudarshan S, Neckers L, Linehan WM. Pseudohypoxic pathways in renal cell carcinoma. *Clin Cancer Res* 2007 August 15;13(16):4667-71.

- (85) Willett CG, Boucher Y, di TE et al. Direct evidence that the VEGF-specific antibody bevacizumab has antivas-
cular effects in human rectal cancer. *Nat Med* 2004 February;10(2):145-7.
- (86) Jain RK. Normalization of tumor vasculature: an emerging concept in antiangiogenic therapy. *Science* 2005
January 7;307(5706):58-62.
- (87) Giantonio BJ, Catalano PJ, Meropol NJ et al. Bevacizumab in combination with oxaliplatin, fluorouracil, and
leucovorin (FOLFOX4) for previously treated metastatic colorectal cancer: results from the Eastern Coope-
rative Oncology Group Study E3200. *J Clin Oncol* 2007 April 20;25(12):1539-44.
- (88) Baranowska-Kortylewicz J, Abe M, Pietras K et al. Effect of platelet-derived growth factor receptor-beta
inhibition with STI571 on radioimmunotherapy. *Cancer Res* 2005 September 1;65(17):7824-31.
- (89) Tong RT, Boucher Y, Kozin SV, Winkler F, Hicklin DJ, Jain RK. Vascular normalization by vascular endothelial
growth factor receptor 2 blockade induces a pressure gradient across the vasculature and improves drug
penetration in tumors. *Cancer Res* 2004 June 1;64(11):3731-6.

CHAPTER 2

Carbonic Anhydrase IX in Renal Cell Carcinoma-implications for Prognosis, Diagnosis and Therapy

A.B. Stillebroer¹ MD, P.F.A. Mulders¹ MD PhD, O.C. Boerman² PhD,
W.J.G. Oyen² MD PhD, E. Oosterwijk¹ PhD

Departments of Urology¹ and Nuclear Medicine², Radboud University Nijmegen Medical Centre, Nijmegen, The Netherlands

Published: European Urology 2010 Jul;58(1):75-83



Abstract

Context

The clinical management of patients with renal cell carcinoma (RCC) remains difficult and the development of new diagnostic, prognostic and therapeutic tools is still required.

Objective

To review the current knowledge on the RCC-associated antigen carbonic anhydrase IX (CAIX) and provide evidence how this antigen may aid in the clinical management of RCC.

Evidence acquisition

Clinical papers describing diagnostic, prognostic and/or therapeutic applications of CAIX in RCC were selected from the Pubmed database. The search was manually augmented by reviewing the reference lists of articles.

Evidence synthesis

Expression of CAIX is regulated by the Von Hippel Lindau (VHL) protein. Because of the invariable VHL mutational loss in clear cell RCC (ccRCC) patients, CAIX expression is ubiquitous in ccRCC. Determination of CAIX expression in nephrectomy specimens of RCC patients improves prognostic accuracy; high CAIX expression appears to be correlated with a favorable prognosis and a greater likelihood of response to systemic treatment for metastatic disease. Therefore, CAIX expression might be used to stratify metastatic ccRCC (mRCC) patients for systemic treatment. When incorporated in the RCC nomogram, CAIX expression seems to improve diagnostic accuracy for primary as well as mRCC patients, but further evidence is required. Clinical studies with the CAIX-specific monoclonal antibody (mAb) cG250 have provided unequivocal evidence that ccRCC lesions can be imaged with radiolabeled cG250. Results are awaited of a large randomized trial which aims to establish the value of cG250-imaging for primary RCC. The outcome of another large, placebo-controlled study is awaited to establish the usefulness of CAIX-targeted therapy in the adjuvant setting. Therapeutic trials with high-dose radiolabeled cG250 and CAIX-loaded dendritic cells in mRCC patients are still in phase I or II.

Conclusion

CAIX improves diagnostic accuracy and is an attractive target for imaging and therapy of ccRCC.

1. INTRODUCTION

RCC represents 3% of all malignancies, with 57,760 new cases in the US alone in 2009 ⁽¹⁾. About one fourth of patients presents with synchronous or metachronous metastases and will eventually succumb to the disease. When the tumour is confined to the kidney, tumor nephrectomy is the indicated, intentionally curative treatment. In the case of residual or metastatic disease systemic treatment is warranted. Recently, anti-angiogenic treatments were introduced for the treatment of metastatic RCC (mRCC) which are more effective as compared to the previous immunotherapeutic treatment regimes ^(2;3). Unfortunately, complete responses (CR) to these angiogenesis inhibitors are sporadic, whereas treatment with high-dose interleukin-2 (IL-2) and low-dose IFN- α 2a have demonstrated stable CR rates of around 5% ⁽⁴⁾ and 1% ⁽⁵⁾, respectively. Furthermore, treatment with angiogenesis inhibitors is continuous and side effects are common and often severe in nature ⁽⁶⁾. Therefore, more effective and less toxic treatments need to be developed to ensure effective anti-RCC treatment while maintaining the quality of life of patients.

Treatment with angiogenesis inhibitors appears to be mainly effective in patients with ccRCC metastases ⁽⁷⁾. Therefore, classification of the RCC subtype is crucial to determine which systemic treatment is most suitable. Determination of the histological subtype of RCC is based on its morphological and phenotypical characteristics. One marker, almost invariably present on ccRCC, the CAIX antigen, may be useful in the diagnostic process and could serve as a prognostic factor in patients with ccRCC. Moreover, therapeutic strategies are being explored using CAIX as a target for treatment of RCC. This review will describe the potential use and limitations of the CAIX antigen in the prognosis, diagnosis and therapy of ccRCC.

2. EVIDENCE ACQUISITION

A literature search was conducted using the Pubmed database. The database was searched using the terms: CAIX, G250, prognosis, diagnosis, therapy and/or RCC with the limits English, publication date from 1980/01/01, Humans. We augmented this literature search by manually reviewing the reference lists of included studies to identify additional relevant articles. The antigen has been named MN, G250 and CAIX in literature. The term CAIX will be used in this review.

3. EVIDENCE SYNTHESIS

3.1 CAIX

3.1.1 CAIX function

The distribution of CAIX was first described in 1986 (then named G250-antigen) in an immunohistochemical study describing the specificity analysis and tumor specificity of mAb G250. Based on this analysis it was suggested that the recognized moiety could potentially serve as a target for therapy and/or diagnosis in RCC⁽⁸⁾. Subsequent studies demonstrated that the antigen recognized, (CAIX),⁽⁹⁾ is a cytosolic as well as a transmembraneous glycoprotein belonging to the carbonic anhydrase group of enzymes which catalyze the reaction $\text{CO}_2 + \text{H}_2\text{O} \rightleftharpoons \text{HCO}_3^- + \text{H}^+$. These enzymes are critical in the regulation of proton flux in cells and thus in pH regulation⁽¹⁰⁾. In contrast to most carbonic anhydrases, the catalytic site of CAIX is located extracellularly, where it is involved in creating an acidic microenvironment⁽¹¹⁾.

3.1.2 CAIX expression in tumors and normal tissue

CAIX antigen expression in the different histological subtypes of RCC has been determined by RT-PCR and immunohistochemistry. The majority of clear cell tumors (>95%) showed high and homogeneous levels of CAIX expression, while expression of CAIX in oncocytomas, chromophobe and papillary RCC was considerably lower⁽¹²⁾. Furthermore, alveolar and/or tubular growth patterns demonstrated high (94-99%) CAIX expression. Papillary, solid and cystic growth patterns were characterized by significantly lower (14-60%) CAIX expression⁽¹²⁾. In various other tumors, immunohistochemical analyses revealed high levels of CAIX expression: carcinomas of the uterine cervix, esophagus, lung, breast, brain and vulva also express CAIX, albeit all very heterogeneously⁽¹³⁻²⁰⁾. In an extensive analysis, CAIX expression in normal tissue was observed on gastric mucosa, pancreatobiliary epithelium and small intestine crypt bases, but not on normal kidney. CAIX was also detectable in mesothelial cells, ovarian surface epithelium and fetal rete testis, albeit at a much lower level⁽²¹⁾.

3.1.3 Regulation of CAIX expression

CAIX expression has shown to be governed by the transcription factor hypoxia inducible factor-1 α (HIF-1 α) (for review see⁽²²⁾). Under normoxic conditions HIF-1 α is hydroxylated and ultimately degraded through binding to the Von Hippel Lindau protein (pVHL) and subsequent ubiquitination, prohibiting formation of the active HIF-1 α -HIF-1 β di-

mer. Under hypoxic conditions, binding of pVHL to HIF-1 α is inhibited, leading to accumulation of HIF-1 α and subsequent association with HIF-1 β . The resulting HIF-1 causes the downstream transcription of a number of hypoxia-inducible genes, the CAIX antigen being one of those⁽¹⁶⁾ (**Figure 1**). The almost invariable mutational loss of pVHL in ccRCC mimics hypoxic conditions and thus explains the ubiquitous expression of CAIX antigen⁽²³⁾. CAIX expression in all other tumor types (e.g. cervix, lung) is hypoxia-driven⁽²⁴⁾. Therefore, CAIX is regarded as a potential marker of hypoxia in many malignancies other than ccRCC⁽¹⁴⁾. Expression of CAIX in normal tissues is hypothesized to be regulated by either tissue acidosis⁽²⁵⁾ or glucose deprivation⁽²⁶⁾, but this remains to be clarified. In tumors, high CAIX expression and subsequent acidification is thought to (i) aid in the adaptation of tumors to hypoxic conditions (ii) hamper the uptake in tumor cells of weakly basic chemotherapeutic agents leading to chemoresistance of CAIX expressing tumors⁽²⁷⁾.

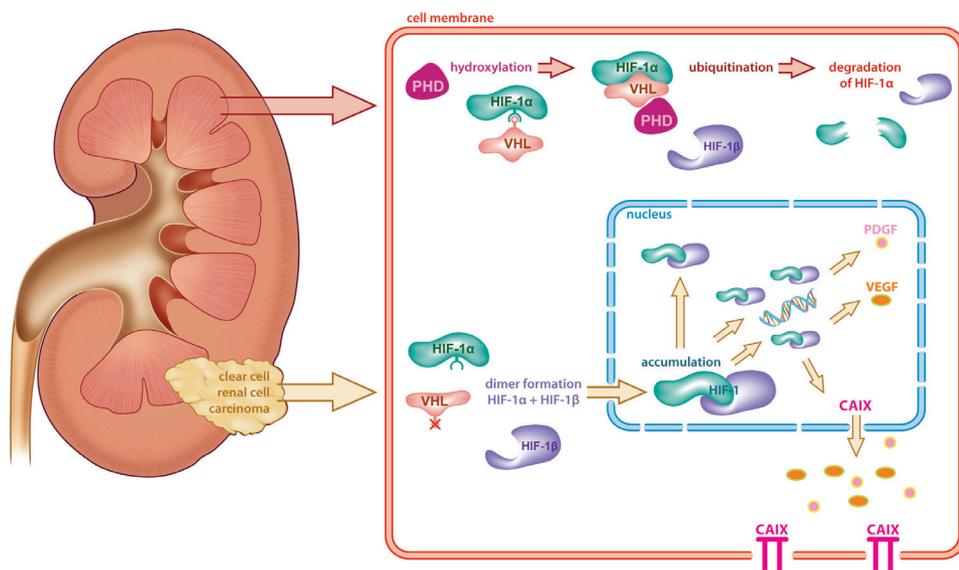


Figure 1. CAIX expression is molecularly linked with pVHL. In normal kidney, HIF-1 α is hydroxylated by prolyl hydroxylase domain proteins (PHDs) and bound by pVHL, catalyzing the polyubiquitylation of prolyl-hydroxylated HIF-1 α for subsequent degradation via the 26S proteasome. In ccRCC the binding of HIF-1 α by pVHL does not occur, thereby escaping degradation and a dimer mimicking hypoxic conditions. HIF-1 α associates with the constitutively stable partner HIF-1 β to form an active heterodimeric HIF-1 transcription factor, which binds to hypoxia-responsive elements located in the promoter/enhancer regions of numerous hypoxia-inducible genes including pro-angiogenic factors (such as VEGF and PDGF) and CAIX, which is ultimately expressed on the tumor cell surface.

3.2 PROGNOSIS

3.2.1 CAIX expression and survival

The prognostic value of CAIX expression in ccRCC has been the subject of several studies. Bui et al. reported that low CAIX expression in primary ccRCC was an adverse predictor of survival in a large series of 321 ccRCC patients. In the multivariate analysis CAIX expression remained an independent prognostic parameter ⁽²⁸⁾. These findings were confirmed in a series of 183 ccRCC cases, which showed that CAIX expression was an independent predictor of survival ⁽²⁹⁾. Patard et al. reported that CAIX was an independent predictor of survival in a series of 100 ccRCC cases ⁽³⁰⁾. However, Leibovich et al. could not confirm these results in a series of 730 ccRCC patients. Although low CAIX expression was associated with death from ccRCC in univariate analysis, this association failed to reach statistical significance in the multivariate analysis, when death from ccRCC and low CAIX expression was corrected for nuclear grade, tumor necrosis and sarcomatoid differentiation. ⁽²¹⁾ The discrepancy to the other results may be explained by a difference in patient population (in this study, only 11% mRCC patients were included, whereas the other studies included 40-60% mRCC patients), or the use of tissue microarray analysis instead of immunohistochemistry to quantify CAIX expression. Recently, CAIX polymorphisms were analyzed in 54 mRCC tissue samples. The single nucleotide polymorphism rs12553173 and CAIX both proved to be independent prognostic factors for OS and were associated with a greater likelihood of response to IL-2 immunotherapy ⁽³¹⁾. Thus, many studies suggest that CAIX is an independent prognostic marker in RCC with a correlation between low CAIX expression and death from ccRCC.

3.2.2 CAIX expression incorporated in RCC nomograms

To predict RCC disease-free survival rates after nephrectomy or predict survival in metastatic patients various clinical and pathological features are taken into account, such as clinical symptoms, age, performance status, TNM stage, nuclear grade and tumor necrosis (for review see ⁽³²⁾). In an effort to improve the nomogram for RCC patients, Kim et al. studied a number of molecular markers, a.o. vimentin, p53, pTEN and CAIX ^(33;34). In the first nomogram the prognostic accuracy of these biomarkers was examined in 318 patients with primary RCC, regardless of the presence of synchronous metastases. Inclusion of the biomarkers improved the prognostic accuracy as compared to the TNM (C=0.79 vs. C=0.73; $p < 0.001$) and UCLA integrated staging system (UISS) (C=0.79 vs. C=0.75; $p = 0.038$) staging systems alone ⁽³⁴⁾. The second nomogram was designed to predict the survival of mRCC patients and incorporated the aforementioned biomarkers, T category and ECOG performance status. This nomogram based on the combination of biomarkers

and clinical parameters proved to be a more accurate prognostic model for mRCC patients as compared to the UISS staging system ($C=0.68$ vs $C=0.62$; $p=0.0033$)⁽³³⁾. Incorporation of CAIX expression in nomograms is complicated due to the lack of commercial availability of the mAb M75, needed for the immunohistochemical detection of CAIX in tissue samples. Commercially available mAb NB100-417 is reported to be a CAIX-specific mAb with similar staining characteristics as M75, recognizing the membrane epitope of CAIX^(35;36), but cross-reactivity at high dilutions with beta-tubulin⁽³⁶⁾ makes specific CAIX detection by mAb NB100-417 impossible. Incorporation of CAIX expression in the RCC nomogram improves prognostic accuracy, but since mAb M75 is not commercially available, widespread use is not yet possible.

3.2.3 CAIX expression and response to systemic treatment

Since the implementation of angiogenesis inhibitors, treatment strategies of mRCC patients have changed significantly. However, immunotherapy still plays a role in the treatment of mRCC since CRs are rarely seen with the use of angiogenesis inhibitors, whereas a significant, though small (5%) percentage of mRCC patients do show CR after IL-2 therapy⁽⁴⁾. When treatment with IL-2 is applicable, CAIX expression could be used to predict the response to treatment. In 2005 Atkins et al. reported that CAIX expression could serve as a predictor of response to IL-2 immunotherapy. Of 66 patients who had received IL-2 immunotherapy, 21 of 27 (78%) responding patients had high CAIX expressing primary tumors compared with 20 of 39 (51%) non-responding patients ($p=0.04$). Moreover, median survival was prolonged in the high CAIX expression group ($p=0.03$) and survival >5 years was only seen in patients with high CAIX expressing tumors⁽³⁷⁾. A prospective, non-randomized trial ('SELECT' trial) is currently investigating in 110 patients whether CAIX expression is a predictor of response to IL-2 therapy⁽³⁸⁾. These, and other⁽³⁹⁾ observations might lead to improved response rates in CAIX-stratified patients treated with IL-2.

Thus far, patient stratification is based on factors determined in the cytokine era, and these may not be entirely applicable to mRCC patients who are receiving targeted therapy. Evidence is mounting that there is a correlation between CAIX expression and response to treatment with angiogenesis inhibitors. In 118 patients the prognostic utility of RCC subtype and CAIX expression in mRCC patients who received sunitinib or sorafenib treatment after nephrectomy was evaluated. A significantly higher treatment response rate, more tumor shrinkage and a longer duration of response was independently associated with ccRCC as compared to other RCC subtypes ($p=0.02$). CAIX expression was not associated with a response to sunitinib treatment, but high CAIX expression could serve

as a predictive biomarker for response to sorafenib treatment ⁽⁴⁰⁾. In a side-study of a randomized phase 2 trial where patients received varying doses of temsirolimus ⁽⁴¹⁾ no correlation between CAIX or HIF-1 α expression and response to temsirolimus treatment was seen ⁽⁴²⁾. However, this was a highly inhomogeneous patient population, with many poor prognosis or non-ccRCC patients. Therefore, more research is warranted to evaluate the predictive value of CAIX expression for the response to targeted agents in the mRCC patient population.

3.3 DIAGNOSIS

CAIX imaging

Approximately 50% of all renal lesions are found incidentally due to improved and increased radiological evaluation. Consequently, new functional and molecular imaging techniques are needed to aid in the differentiation between benign and malignant renal lesions. Positron emission tomography (PET) with [¹⁸F]FDG is a molecular imaging technique widely used in various types of cancer for diagnosis, (re)staging and evaluation of response to treatment ⁽⁴³⁾. Trials with relatively small patient cohorts have shown the high specificity of [¹⁸F]FDG to detect RCC lesions. Sensitivity, however, appears to be relatively low and FDG-PET is now considered unsuited for staging of patients with RCC ^(44;45).

MAb G250 has a high affinity ($K_a = 4.10^9$ M⁻¹) for the CAIX antigen. Although G250 recognizes a different CAIX epitope than mAb M75, no discrepancy between both mAbs has been described. Since the discovery of G250 ⁽⁸⁾, many animal and clinical studies have been performed and confirmed the promising characteristics of this mAb for RCC targeting (**Table 1**). Immunohistochemical analyses have indicated that CAIX is expressed in the vast majority of ccRCC lesions, these studies indicate the possibilities

Author	year	Murine/ chimeric	Imaging agent	# patients	Imaging moment	Diagnostic accuracy	Special features
Oosterwijk et al (74)	1993	Murine	¹³¹ I-mG250	15	Prior to nephrectomy	12/12 primary ccRCC	Protein dose escalation
Steffens et al (47)	1997	Chimeric	¹³¹ I-cG250	16	Prior to nephrectomy	13/13 primary ccRCC	Protein dose escalation
Brouwers et al (48)	2002	Chimeric	¹³¹ I-cG250 vs. [¹⁸ F]-FDG	20	M+RCC patients	¹³¹ I-cG250: 30% [¹⁸ F]-FDG: 69%	Comparative inpatient study
Brouwers et al (49)	2003	Chimeric	¹³¹ I-cG250 vs. ¹¹¹ In-cG250	5	M+RCC patients	¹³¹ I-cG250: 30 lesions ¹¹¹ In-cG250: 47 lesions	Comparative inpatient study
Divgi et al (52)	2007	Chimeric	¹²⁴ I-cG250	26	Prior to nephrectomy	15/16 primary ccRCC	cG250-immunoPET

Table 1. Clinical diagnostic studies with labeled cG250.

Abbreviations: vs.: versus, M+ RCC: metastatic renal cell carcinoma

of clinical ccRCC imaging with mAb cG250. Since administration of murine G250 led to formation of human anti-mouse antibodies (HAMA) in all patients (n=33) ⁽⁴⁶⁾, a chimeric variant of G250 (cG250) was constructed, allowing multiple administrations of the mAb in the same patient ⁽⁴⁷⁾. The pharmacokinetics and biodistribution of the chimerized mAb was determined in presurgical RCC patients and the optimal protein dose was found to be 5-10 mg. Clear visualization of all 13 CAIX-positive tumors as well as metastases was noted. Focal uptake of cG250 in primary RCC lesions was very high (up to 0.52 %ID/g) ⁽⁴⁷⁾. To compare ¹³¹I-cG250 radioimmunoscintigraphy (RIS) with [¹⁸F]FDG-PET, 20 mRCC patients were scanned using both techniques. Of the 112 metastases documented, ¹³¹I-cG250 RIS detected 34 (30%) and [¹⁸F]FDG-PET 77 (69%) lesions ⁽⁴⁸⁾. The low percentage of RCC metastases detected by cG250-RIS in this study contrasts with results of other studies, where excellent visualization of metastases in all sites was noted and often new lesions were diagnosed, which were not seen using conventional imaging techniques ⁽⁴⁹⁻⁵¹⁾.

ImmunoPET, i.e. combining the favorable characteristics of PET (higher spatial resolution, 3D imaging and superior quantitative estimations of uptake) with mAb cG250 seems ideal for imaging (m)RCC lesions. However, the combination of the relatively slow pharmacokinetics of iv injected radiolabeled mAb (optimal tumor uptake after several days) and the most commonly used positron emitters (¹¹C and ¹⁸F) is difficult due to their too short half-life (2 min to 1.8 h). The positron emitters ⁸⁹Zr and ¹²⁴I (half-lives 78 and 100 h, respectively) seem better candidates to match these slow kinetics (**Figure 2**). In a prospective study Divgi et. al. studied 25 patients with suspect renal lesions scheduled for nephrectomy with ¹²⁴I-cG250. The authors hypothesized that ¹²⁴I-cG250 PET imaging might allow visualization of ccRCC in patients with suspect renal masses versus non-ccRCC. Of sixteen patients with histologically confirmed ccRCC after surgery, 15 had a positive (tumor-to-normal kidney ratio \geq 3:1) scan. The failure in one patient was attributed to technical problems with the radiolabeled material. None of the 9 patients with non-ccRCC showed any ¹²⁴I-cG250 uptake. The study showed that immunoPET might be helpful in clinical decision making and might aid in the surgical management of small renal masses scheduled for partial nephrectomy ⁽⁵²⁾. Recently, a large multicenter phase III registration trial comparing conventional diagnostic CT to ¹²⁴I-cG250 immunoPET/CT for the detection of ccRCC in 226 patients scheduled for nephrectomy has been completed ⁽⁵³⁾. This trial will give insight in the sensitivity and specificity of ¹²⁴I-labeled cG250 for PET imaging of ccRCC lesions. If the results confirm the earlier observations, ¹²⁴I-cG250 immunoPET/CT might become a useful, noninvasive tool to prevent unnecessary surgery in patients with undetermined renal masses.

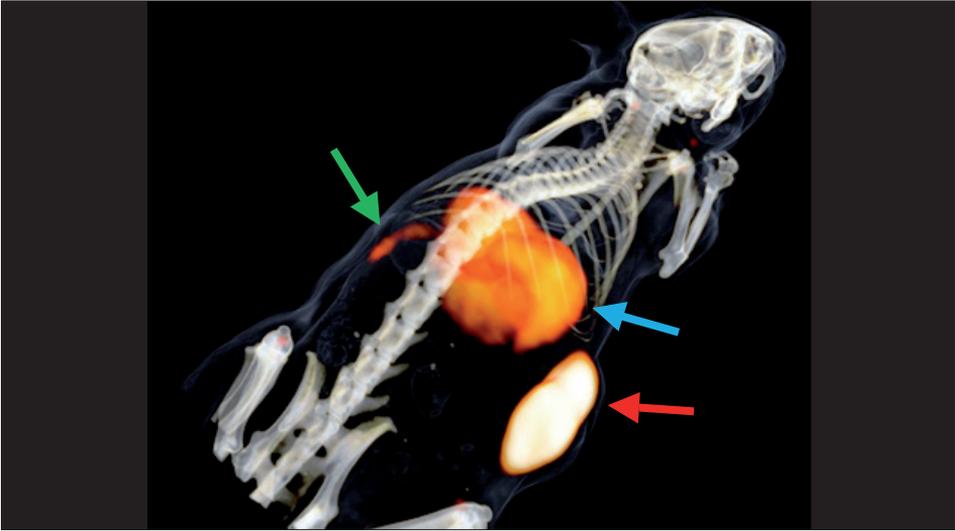


Figure 2. 3D reconstructed PET-CT image of a mouse with a s.c. CAIX expressing ccRCC tumor on the right flank 7 days after injection with ^{89}Zr -cG250. Note the high uptake in the tumor (red arrow) and the low aspecific uptake in the liver (blue arrow) and spleen (green arrow).

3.4 Therapy

3.4.1 CAIX-directed therapy

Antibodies have the capacity to initiate cell lysis through antibody-dependent cellular cytotoxicity (ADCC) or complement directed lysis. After establishing that cG250 could facilitate ADCC and elicit cell lysis of CAIX-positive cells *in vitro* ⁽⁵⁴⁾, a phase I study with escalating doses of 5-50 mg/m² cG250 was initiated, with weekly infusions for 6 weeks. CG250 treatment up to 50 mg/m² was safe and well tolerated. Of the 11 mRCC patients treated, one showed a CR and nine patients had stable disease after one treatment cycle ⁽⁵⁵⁾. In the subsequent phase II study 36 mRCC patients were included, all receiving 50 mg cG250 weekly for 12 weeks. No drug-related grade 3-4 toxicity occurred during this trial. Before treatment, 80% of patients were progressive. After one treatment cycle, 28% of patients had stable disease (SD) and during follow-up one complete (CR) and one partial response (PR) were noted. The median survival of 15 months suggested that cG250 might be able to modulate the natural course of mRCC ⁽⁵⁶⁾. Based on these results, an adjuvant phase III trial is ongoing aiming at reducing the recurrence of disease in nephrectomized RCC patients

who have a high risk of relapse⁽⁵⁷⁾.

IL-2 activated effector cells were more effective in eliciting cG250 ADCC^(54;58). The addition of IL-2 to cG250 therapy was studied in a phase II trial, in which 35 patients with progressive mRCC received weekly i.v. infusions of 50 mg cG250 and daily s.c. low-dose IL-2, for 11 weeks. Treatment was well-tolerated with little toxicity, attributable to IL-2. Clinical benefit was noted in 8 of 35 patients, with 2 PR and 6 long-lasting (>24 weeks) stabilizations of disease. Mean survival was 24 months in this trial. It was considered unlikely that the increased survival was due to the low-dose IL-2, as a 6-fold decrease of the normal IL-2 dose was used. It was hypothesized that the result was due to a synergistic effect of cG250 and IL-2⁽⁵⁹⁾. Larger, randomized trials are warranted to fully determine the effect of the IL-2/cG250 treatment combination on ccRCC.

3.4.2 CAIX radioimmunotherapy

Since accumulation of cG250 in RCC lesions is very high, up to 10 times higher than uptake seen with mAbs in other tumors, several strategies to deliver tumor-sterilizing radiation doses to tumor cells with cG250 as carrier molecule have been examined (**Table 2**). The maximum tolerated dose (MTD) of ¹³¹I-cG250 in progressive mRCC patients was determined in a radioactivity dose escalation trial. In the initial RIT trials hepatic toxicity was observed, most likely due to cG250 accumulation in the liver. In subsequent trials patients first received a ¹³¹I-cG250 scout dose to prevent administration of high ¹³¹I-cG250 to patients with CAIX-negative tumors. Unexpectedly, through the administration of the scout dose liver toxicity was avoided, most likely due to sa-

Author	year	Murine/ chimeric	Therapy	# patients	CR/PR/SD/PD	CR/PR/SD duration	Special features
Davis et al (55)	2007	Chimeric	Cold	13	1 CR; 9 SD; 3 PD	6-66 weeks	Phase I
Bleumer et al (56)	2004	Chimeric	Cold	36	1 CR; 1 PR; 8 SD; 26 PD	1-20+ weeks	Phase II
Davis et al (75)	2007	Chimeric	Cold + l.d. IL-2	9	2 SD; 7 PD	6 & 12 weeks	Phase I
Bleumer et al (59)	2006	Chimeric	Cold + l.d. IL-2	35	2 PR; 6 SD; 27 PD	24+ weeks	Phase II
Divgi et al (46)	1998	Murine	¹³¹ I-mG250	33	17 SD; 16 PD	2-3 months	Phase I/II
Steffens et al (60)	1999	Chimeric	¹³¹ I-cG250	12	1 PR; 1 SD; 10 PD	3 & 9+ months	Phase I
Divgi et al (66)	2004	Chimeric	¹³¹ I-cG250	15	7 SD; 8 PD	2-11 months	Phase I dose fractionation
Brouwers et al (50)	2005	Chimeric	¹³¹ I-cG250	27	5 SD; 22 PD	3-12 months	Two high-dose treatments
Bleumer et al (68)	2007	n.a.	Dendritic cells	6	6 PD	n.a.	CAIX peptide pulsed DC
Uemura et al (69)	2006	n.a.	Peptides	23	3 PR; 6 SD; 14 PD	7-18 months	CAIX derived peptides

Table 2. Clinical therapeutic studies with (un)labeled cG250 or G250 peptide fragments. Abbreviations: cold: unlabeled monoclonal antibody, l.d.: low dose, IL-2: Interleukin-2, n.a.: not applicable, CR: complete responses, PR: partial responses, SD: stable disease, PD: progressive disease, DC: dendritic cells.

turation of the liver compartment. Besides mild nausea without vomiting and transient fatigue (both grade 1 CTC) no other non-hematological side effects occurred. The MTD was 2220 MBq/m², with hematological toxicity as the dose-limiting factor. Of the 8 patients receiving treatment, one patient showed stable disease and one patient had a PR ⁽⁶⁰⁾. A study by Brouwers et al. was designed to evaluate the effect of two sequential high-dose ¹³¹I-cG250 treatments. Similar to the earlier trial, progressive mRCC patients received a scout dose of 185 MBq ¹³¹I-cG250. When tumor targeting was observed, this was followed by 2220 MBq/m² ¹³¹I-cG250. After 3 months, if disease progression had halted and tumor targeting with another scout dose was established, patients received the second high-dose injection ¹³¹I-cG250. MTD of the 2nd RIT was set at 1665 MBq/m² again due to hematological toxicity. In total, 29 patients entered the study, of which 18 patients were evaluable for tumor response. No objective responses were seen, but 5 patients had stabilization of their disease, lasting 3-12 months ⁽⁵⁰⁾. An inverse correlation between the size of metastases and radiation absorbed dose was observed. Therapeutic radiation doses (more than 50 Gy) were only guided to the lesions smaller than 5 grams ⁽⁵¹⁾. It was concluded that RIT in mRCC patients could best be given in the setting of small volume disease or as adjuvant therapy.

When the radiolabeled mAb cG250 has bound to the CAIX antigen expressed on ccRCC cells, part of the antibody-antigen complex is internalized. Intracellular ¹³¹I-cG250 is metabolized and tyrosine-¹³¹I is rapidly excreted by the tumor cell upon internalization. Metallic radionuclides, such as ¹¹¹In, ⁹⁰Y and ¹⁷⁷Lu, are trapped in the lysosomes and residualize after internalization of the mAb-antigen complex by the target cells ⁽⁶¹⁻⁶³⁾. In an inpatient comparison, 5 mRCC patients were injected with ¹³¹I-cG250 and ¹¹¹In-cG250 one week apart. ¹¹¹In-cG250 revealed 47 metastatic lesions where ¹³¹I-cG250 detected only 30 lesions ⁽⁴⁹⁾. The therapeutic properties of cG250 labeled with 4 different radionuclides at MTD have been tested in nude mice with human RCC xenografts. Tumor growth was delayed most effectively by cG250 labeled with ¹⁷⁷Lu, followed by ⁹⁰Y, ¹⁸⁶Re and ¹³¹I (delays of 185, 125, 90 and 25 days, respectively). Therefore, ¹⁷⁷Lu and ⁹⁰Y were considered better candidates for RIT with cG250 than ¹³¹I ⁽⁶⁴⁾. Based on these data, a phase I/II ¹⁷⁷Lu-cG250 dose escalation RIT study in mRCC patients was designed, which is currently ongoing. In this trial in patients with progressive mRCC, adequate targeting of tumors is verified with an imaging dose of ¹¹¹In-cG250. This is followed by up to three cycles of high-dose ¹⁷⁷Lu-cG250 to determine MTD and assess preliminary therapeutic efficacy ⁽⁶⁵⁾. So far, most patients (70%) had stable disease after one treatment cycle and one PR was observed lasting 9 months.

Thiry et al. raised the question whether therapies directed at CAIX might induce fulminant toxicities due to the expression of CAIX in normal tissue, predominantly in the

epithelial structures ⁽¹⁴⁾. Cross-reactivity with non-target tissues is a known feature of many mAbs, but this generally does not lead to toxicity. Therapeutic trials with either labeled or unlabeled cG250 have thus far shown little toxicity in CAIX expressing normal organs ^(50;55;56;60;66), except for the liver toxicity in the first RIT trial, which was not seen in later RIT trials. Whether CAIX-related toxicity will occur when small molecules inhibiting CAIX are administered remains to be determined.

3.4.3 Cellular and humoral immunotherapy with CAIX derived peptides

Exploiting the highly immunogenic characteristics of ccRCC, 6 progressive, cytokine-refractory mRCC patients received vaccinations of mature dendritic cells (DC) loaded with CAIX-derived peptides. These peptides define two different epitopes (HLA-A2.01 and HLA-DR) of the CAIX antigen and are able to induce cytotoxic T-lymphocytes (CTL) responses against CAIX expressing cells *in vitro* ⁽⁶⁷⁾. Although skin biopsies suggested an increased influx of T-helper cells, no evidence was found for induction of CAIX-specific immunity. The treatment was not associated with any toxicity, but clinical responses were absent ⁽⁶⁸⁾. In retrospect, the DCs in this trial were probably not adequately matured. Therefore, a new trial with mature DCs is warranted. Multiple vaccinations with three CAIX-derived peptides defining the HLA-A24 epitope resulted in development of peptide-specific CTLs and peptide-reactive serum immunoglobulin G in 23 progressive, cytokine-refractory mRCC patients ⁽⁶⁹⁾. No major adverse events occurred, 3 patients had a PR and 6 patients had stable disease for >6 months, with a median survival of all patients of 21 months. Because of the higher response rate, the approach of direct vaccination with CAIX-derived peptides, without the use of DCs, seems more promising as an anti-RCC treatment, but larger, prospective trials are needed to establish it as a treatment modality.

Several investigators have examined the potential of fusing the cG250 mAb with immunomodulatory factors, specifically enhancing the immunologic anti-RCC response of mRCC patients. Tso et al. fused cG250 with granulocyte/macrophage-colony stimulating factor (GM-CSF). This fusion protein (FP) could enhance macrophage and granulocyte natural cytotoxicity against CAIX expressing tumor cells *in vitro* ⁽⁷⁰⁾. The gene encoding for this FP (GM-CAIX gene) was then used to transduce DCs with a recombinant adenovirus containing this fusion gene. These DCs were able to induce CAIX-specific cytotoxic lymphocytes *in vitro* and GM-CAIX gene transduced kidney cancer cells were able to *in vivo* produce a GM-CAIX protein that was targeted to the cell membrane ⁽⁷¹⁾. Currently, a clinical trial in mRCC patients is ongoing in which patient-specific DCs are transduced with the adenoviral GM-CAIX construct ⁽⁷²⁾. Bauer et al. constructed a cG250-tumor ne-

cross factor (TNF) FP. TNF is a mediator of hemorrhagic tumor necrosis which causes in vivo regression of xenografted human tumors. Systemic TNF administration leads to profound toxicity, prohibiting its application as systemic cancer therapy in humans. Specific cG250-TNF targeting might alleviate toxicity, while retaining its anti-cancer properties. In nude mice bearing CAIX-positive RCC xenografts specific accumulation and retention of cG250-TNF was observed, which resulted in growth inhibition and improved survival. Co-administration of IFN- γ , known to enhance TNF-mediated RCC rejection, resulted in synergistic tumoricidal activity ⁽⁷³⁾.

4. CONCLUSIONS

The vast majority of primary and metastatic ccRCC lesions have high and homogeneous CAIX expression. CAIX expression on primary ccRCC tumors is a prognostic factor for survival and is a predictor of response to IL-2 immunotherapy in ccRCC patients. Whether high CAIX expression also predicts response to treatment with angiogenesis inhibitors needs further investigation. Imaging ccRCC lesions with mAb cG250, targeting CAIX, is a promising tool for diagnosing and (re)staging of the disease and results of a large prospective trial are upcoming. Given the high expression of CAIX in ccRCC the outcome of a large, placebo-controlled study is awaited to establish the usefulness of CAIX-targeted therapy in the adjuvant setting. Therapeutic trials in mRCC patients are still in the phases I and II.

REFERENCE LIST

- (1) Jemal A, Siegel R, Ward E, Hao Y, Xu J, Thun MJ. Cancer statistics, 2009. *CA Cancer J Clin* 2009 July;59(4):225-49.
- (2) Motzer RJ, Hutson TE, Tomczak P, Michaelson MD, Bukowski RM, Rixe O et al. Sunitinib versus interferon alfa in metastatic renal-cell carcinoma. *N Engl J Med* 2007 January 11;356(2):115-24.
- (3) Motzer RJ, Hutson TE, Tomczak P, Michaelson MD, Bukowski RM, Oudard S et al. Overall survival and updated results for sunitinib compared with interferon alfa in patients with metastatic renal cell carcinoma. *J Clin Oncol* 2009 August 1;27(22):3584-90.
- (4) Fyfe G, Fisher RI, Rosenberg SA, Sznol M, Parkinson DR, Louie AC. Results of treatment of 255 patients with metastatic renal cell carcinoma who received high-dose recombinant interleukin-2 therapy. *J Clin Oncol* 1995 March;13(3):688-96.
- (5) Negrier S, Perol D, Ravaud A, Chevreau C, Bay JO, Delva R et al. Medroxyprogesterone, interferon alfa-2a, interleukin 2, or combination of both cytokines in patients with metastatic renal carcinoma of intermediate prognosis: results of a randomized controlled trial. *Cancer* 2007 December 1;110(11):2468-77.
- (6) Hartmann JT, Haap M, Kopp HG, Lipp HP. Tyrosine kinase inhibitors - a review on pharmacology, metabolism and side effects. *Curr Drug Metab* 2009 August;10(5):470-81.
- (7) Heng DY, Choueiri TK. Non-clear cell renal cancer: features and medical management. *J Natl Compr Canc Netw* 2009 June;7(6):659-65.
- (8) Oosterwijk E, Ruiter DJ, Hoedemaeker PJ, Pauwels EK, Jonas U, Zwartendijk J et al. Monoclonal antibody G 250 recognizes a determinant present in renal-cell carcinoma and absent from normal kidney. *Int J Cancer* 1986 October 15;38(4):489-94.
- (9) Grabmaier K, Vissers JL, De Weijert MC, Oosterwijk-Wakka JC, Van BA, Brakenhoff RH et al. Molecular cloning and immunogenicity of renal cell carcinoma-associated antigen G250. *Int J Cancer* 2000 March 15;85(6):865-70.
- (10) Opavsky R, Pastorekova S, Zelnik V, Gibadulinova A, Stanbridge EJ, Zavada J et al. Human MN/CA9 gene, a novel member of the carbonic anhydrase family: structure and exon to protein domain relationships. *Genomics* 1996 May 1;33(3):480-7.
- (11) Supuran CT. Carbonic anhydrases: catalytic and inhibition mechanisms, distribution and physiological roles. *Carbonic Anhydrase. Its Inhibitors and Activators*. CRC Press; 2004. p. 1-23.
- (12) Bismar TA, Bianco FJ, Zhang H, Li X, Sarkar FH, Sakr WA et al. Quantification of G250 mRNA expression in renal epithelial neoplasms by real-time reverse transcription-PCR of dissected tissue from paraffin sections. *Pathology* 2003 December;35(6):513-7.
- (13) Saarnio J, Parkkila S, Parkkila AK, Pastorekova S, Haukipuro K, Pastorek J et al. Transmembrane carbonic anhydrase, MN/CA IX, is a potential biomarker for biliary tumours. *J Hepatol* 2001 November;35(5):643-9.
- (14) Thiry A, Dogne JM, Masereel B, Supuran CT. Targeting tumor-associated carbonic anhydrase IX in cancer therapy. *Trends Pharmacol Sci* 2006 November;27(11):566-73.
- (15) Bartosova M, Parkkila S, Pohlodek K, Karttunen TJ, Galbavy S, Mucha V et al. Expression of carbonic anhydrase IX in breast is associated with malignant tissues and is related to overexpression of c-erbB2. *J Pathol* 2002 July;197(3):314-21.
- (16) Ivanov S, Liao SY, Ivanova A, nilkovitch-Miagkova A, Tarasova N, Weirich G et al. Expression of hypoxia-inducible cell-surface transmembrane carbonic anhydrases in human cancer. *Am J Pathol* 2001 March;158(3):905-19.
- (17) Hynninen P, Vaskivuo L, Saarnio J, Haapasalo H, Kivela J, Pastorekova S et al. Expression of transmembrane carbonic anhydrases IX and XII in ovarian tumours. *Histopathology* 2006 December;49(6):594-602.
- (18) Kivela A, Parkkila S, Saarnio J, Karttunen TJ, Kivela J, Parkkila AK et al. Expression of a novel transmembrane carbonic anhydrase isozyme XII in normal human gut and colorectal tumors. *Am J Pathol* 2000 February;156(2):577-84.

- (19) Kivela AJ, Parkkila S, Saarnio J, Karttunen TJ, Kivela J, Parkkila AK et al. Expression of transmembrane carbonic anhydrase isoenzymes IX and XII in normal human pancreas and pancreatic tumours. *Histochem Cell Biol* 2000 September;114(3):197-204.
- (20) Saarnio J, Parkkila S, Parkkila AK, Haukipuro K, Pastorekova S, Pastorek J et al. Immunohistochemical study of colorectal tumors for expression of a novel transmembrane carbonic anhydrase, MN/CA IX, with potential value as a marker of cell proliferation. *Am J Pathol* 1998 July;153(1):279-85.
- (21) Leibovich BC, Sheinin Y, Lohse CM, Thompson RH, Chevillie JC, Zavada J et al. Carbonic anhydrase IX is not an independent predictor of outcome for patients with clear cell renal cell carcinoma. *J Clin Oncol* 2007 October 20;25(30):4757-64.
- (22) Kaluz S, Kaluzova M, Liao SY, Lerman M, Stanbridge EJ. Transcriptional control of the tumor- and hypoxia-marker carbonic anhydrase 9: A one transcription factor (HIF-1) show? *Biochim Biophys Acta* 2009 April;1795(2):162-72.
- (23) Grabmaier K, Weijert MC Ad, Verhaegh GW, Schalken JA, Oosterwijk E. Strict regulation of CAIX(G250/MN) by HIF-1alpha in clear cell renal cell carcinoma. *Oncogene* 2004 July 22;23(33):5624-31.
- (24) Shin KH, az-Gonzalez JA, Russell J, Chen Q, Burgman P, Li XF et al. Detecting changes in tumor hypoxia with carbonic anhydrase IX and pimonidazole. *Cancer Biol Ther* 2007 January;6(1):70-5.
- (25) Ihnatko R, Kubes M, Takacova M, Sedlakova O, Sedlak J, Pastorek J et al. Extracellular acidosis elevates carbonic anhydrase IX in human glioblastoma cells via transcriptional modulation that does not depend on hypoxia. *Int J Oncol* 2006 October;29(4):1025-33.
- (26) Rafajova M, Zatovicova M, Kettmann R, Pastorek J, Pastorekova S. Induction by hypoxia combined with low glucose or low bicarbonate and high posttranslational stability upon reoxygenation contribute to carbonic anhydrase IX expression in cancer cells. *Int J Oncol* 2004 April;24(4):995-1004.
- (27) Chiche J, Ilc K, Laferriere J, Trottier E, Dayan F, Mazure NM et al. Hypoxia-inducible carbonic anhydrase IX and XII promote tumor cell growth by counteracting acidosis through the regulation of the intracellular pH. *Cancer Res* 2009 January 1;69(1):358-68.
- (28) Bui MH, Seligson D, Han KR, Pantuck AJ, Dorey FJ, Huang Y et al. Carbonic anhydrase IX is an independent predictor of survival in advanced renal clear cell carcinoma: implications for prognosis and therapy. *Clin Cancer Res* 2003 February;9(2):802-11.
- (29) Sandlund J, Oosterwijk E, Grankvist K, Oosterwijk-Wakka J, Ljungberg B, Rasmuson T. Prognostic impact of carbonic anhydrase IX expression in human renal cell carcinoma. *BJU Int* 2007 September;100(3):556-60.
- (30) Patard JJ, Fergelot P, Karakiewicz PI, Klatter T, Trinh QD, Rioux-Leclercq N et al. Low CAIX expression and absence of VHL gene mutation are associated with tumor aggressiveness and poor survival of clear cell renal cell carcinoma. *Int J Cancer* 2008 July 15;123(2):395-400.
- (31) de Martino M., Klatter T, Seligson DB, LaRochelle J, Shuch B, Caliliw R et al. CA9 gene: single nucleotide polymorphism predicts metastatic renal cell carcinoma prognosis. *J Urol* 2009 August;182(2):728-34.
- (32) Galfano A, Novara G, Iafrate M, Cavalleri S, Martignoni G, Gardiman M et al. Mathematical models for prognostic prediction in patients with renal cell carcinoma. *Urol Int* 2008;80(2):113-23.
- (33) Kim HL, Seligson D, Liu X, Janzen N, Bui MH, Yu H et al. Using tumor markers to predict the survival of patients with metastatic renal cell carcinoma. *J Urol* 2005 May;173(5):1496-501.
- (34) Kim HL, Seligson D, Liu X, Janzen N, Bui MH, Yu H et al. Using protein expressions to predict survival in clear cell renal carcinoma. *Clin Cancer Res* 2004 August 15;10(16):5464-71.
- (35) Al-Ahmadie HA, Alden D, Qin LX, Olgac S, Fine SW, Gopalan A et al. Carbonic anhydrase IX expression in clear cell renal cell carcinoma: an immunohistochemical study comparing 2 antibodies. *Am J Surg Pathol* 2008 March;32(3):377-82.
- (36) Li Y, Wang H, Oosterwijk E, Selman Y, Mira JC, Medrano T et al. Antibody-specific detection of CAIX in breast and prostate cancers. *Biochem Biophys Res Commun* 2009 August 28;386(3):488-92.
- (37) Atkins M, Regan M, McDermott D, Mier J, Stanbridge E, Youmans A et al. Carbonic anhydrase IX expression predicts outcome of interleukin 2 therapy for renal cancer. *Clin Cancer Res* 2005 May 15;11(10):3714-21.
- (38) McDermott D. The High-Dose Aldesleukin (IL-2) "Select" Trial for Patients With Metastatic Renal Cell Carci-

- noma (SELECT). 10-5-2009. Clinicaltrials.gov: NCT 00554515
- (39) Klatte T, Zomorodian N., Kabinavar F.F., Belldegrün A, Pantuck A. Prospective evaluation of carbonic anhydrase IX (CAIX) as a molecular marker in metastatic renal cell carcinoma. *Journal Clinical Oncology* 25[185]. 6-20-2007. Ref Type: Abstract
 - (40) Choueiri T.K., Regan M., Oh W., Clement J., Amato A., McDermott D. et al. Prognostic and predictive values of carbonic anhydrase IX (CAIX) and pathologic features in patients with metastatic clear cell renal cell carcinoma receiving targeted therapy. *Journal Clinical Oncology* 27[15 suppl], 16067. 5-20-0009. Ref Type: Abstract
 - (41) Atkins MB, Hidalgo M, Stadler WM, Logan TF, Dutcher JP, Hudes GR et al. Randomized phase II study of multiple dose levels of CCI-779, a novel mammalian target of rapamycin kinase inhibitor, in patients with advanced refractory renal cell carcinoma. *J Clin Oncol* 2004 March 1;22(5):909-18.
 - (42) Cho D, Signoretti S, Dabora S, Regan M, Seeley A, Mariotti M et al. Potential histologic and molecular predictors of response to temsirolimus in patients with advanced renal cell carcinoma. *Clin Genitourin Cancer* 2007 September;5(6):379-85.
 - (43) Poeppel TD, Krause BJ, Heusner TA, Boy C, Bockisch A, Antoch G. PET/CT for the staging and follow-up of patients with malignancies. *Eur J Radiol* 2009 June;70(3):382-92.
 - (44) Powles T, Murray I, Brock C, Oliver T, Avril N. Molecular positron emission tomography and PET/CT imaging in urological malignancies. *Eur Urol* 2007 June;51(6):1511-20.
 - (45) Ak I, Can C. F-18 FDG PET in detecting renal cell carcinoma. *Acta Radiol* 2005 December;46(8):895-9.
 - (46) Divgi CR, Bander NH, Scott AM, O'Donoghue JA, Sgouros G, Welt S et al. Phase I/II radioimmunotherapy trial with iodine-131-labeled monoclonal antibody G250 in metastatic renal cell carcinoma. *Clin Cancer Res* 1998 November;4(11):2729-39.
 - (47) Steffens MG, Boerman OC, Oosterwijk-Wakka JC, Oosterhof GO, Witjes JA, Koenders EB et al. Targeting of renal cell carcinoma with iodine-131-labeled chimeric monoclonal antibody G250. *J Clin Oncol* 1997 April;15(4):1529-37.
 - (48) Brouwers AH, Dorr U, Lang O, Boerman OC, Oyen WJ, Steffens MG et al. ¹³¹I-cG250 monoclonal antibody immunoscintigraphy versus [18 F]FDG-PET imaging in patients with metastatic renal cell carcinoma: a comparative study. *Nucl Med Commun* 2002 March;23(3):229-36.
 - (49) Brouwers AH, Buijs WC, Oosterwijk E, Boerman OC, Mala C, De Mulder PH et al. Targeting of metastatic renal cell carcinoma with the chimeric monoclonal antibody G250 labeled with (¹³¹I)I or (¹¹¹In)In: an inpatient comparison. *Clin Cancer Res* 2003 September 1;9 (10 Pt 2):3953S-60S.
 - (50) Brouwers AH, Mulders PF, De Mulder PH, van den Broek WJ, Buijs WC, Mala C et al. Lack of efficacy of two consecutive treatments of radioimmunotherapy with ¹³¹I-cG250 in patients with metastasized clear cell renal cell carcinoma. *J Clin Oncol* 2005 September 20;23(27):6540-8.
 - (51) Brouwers AH, Buijs WC, Mulders PF, De Mulder PH, van den Broek WJ, Mala C et al. Radioimmunotherapy with [¹³¹I]cG250 in patients with metastasized renal cell cancer: dosimetric analysis and immunologic response. *Clin Cancer Res* 2005 October 1;11(19 Pt 2):7178s-86s.
 - (52) Divgi CR, Pandit-Taskar N, Jungbluth AA, Reuter VE, Gonen M, Ruan S et al. Preoperative characterization of clear-cell renal carcinoma using iodine-124-labelled antibody chimeric G250 (¹²⁴I-cG250) and PET in patients with renal masses: a phase I trial. *Lancet Oncol* 2007 April;8(4):304-10.
 - (53) Pre-Surgical Detection of Clear Cell Renal Cell Carcinoma Using Radiolabeled G250-Antibody. 2009. Clinicaltrials.gov: NCT 00606632
 - (54) Surfus JE, Hank JA, Oosterwijk E, Welt S, Lindstrom MJ, Albertini MR et al. Anti-renal-cell carcinoma chimeric antibody G250 facilitates antibody-dependent cellular cytotoxicity with in vitro and in vivo interleukin-2-activated effectors. *J Immunother Emphasis Tumor Immunol* 1996 May;19(3):184-91.
 - (55) Davis ID, Wiseman GA, Lee FT, Gansen DN, Hopkins W, Papenfuss AT et al. A phase I multiple dose, dose escalation study of cG250 monoclonal antibody in patients with advanced renal cell carcinoma. *Cancer Immun* 2007;7:13.

- (56) Bleumer I, Knuth A, Oosterwijk E, Hofmann R, Varga Z, Lamers C et al. A phase II trial of chimeric monoclonal antibody G250 for advanced renal cell carcinoma patients. *Br J Cancer* 2004 March 8;90(5):985-90.
- (57) Monoclonal Antibody Therapy (Rencarex®) in Treating Patients Who Have Undergone Surgery for Non-Metastatic Kidney Cancer. 2009. Clinicaltrials.gov: NCT 00087022
- (58) Liu Z, Smyth FE, Renner C, Lee FT, Oosterwijk E, Scott AM. Anti-renal cell carcinoma chimeric antibody G250: cytokine enhancement of in vitro antibody-dependent cellular cytotoxicity. *Cancer Immunol Immunother* 2002 May;51(3):171-7.
- (59) Bleumer I, Oosterwijk E, Oosterwijk-Wakka JC, Voller MC, Melchior S, Warnaar SO et al. A clinical trial with chimeric monoclonal antibody WX-G250 and low dose interleukin-2 pulsing scheme for advanced renal cell carcinoma. *J Urol* 2006 January;175(1):57-62.
- (60) Steffens MG, Boerman OC, De Mulder PH, Oyen WJ, Buijs WC, Witjes JA et al. Phase I radioimmunotherapy of metastatic renal cell carcinoma with ¹³¹I-labeled chimeric monoclonal antibody G250. *Clin Cancer Res* 1999 October;5(10 Suppl):3268s-74s.
- (61) Shih LB, Thorpe SR, Griffiths GL, Diril H, Ong GL, Hansen HJ et al. The processing and fate of antibodies and their radiolabels bound to the surface of tumor cells in vitro: a comparison of nine radiolabels. *J Nucl Med* 1994 May;35(5):899-908.
- (62) Press OW, Shan D, Howell-Clark J, Eary J, Appelbaum FR, Matthews D et al. Comparative metabolism and retention of iodine-125, yttrium-90, and indium-111 radioimmunoconjugates by cancer cells. *Cancer Res* 1996 May
- (63) Sharkey RM, Behr TM, Mattes MJ, Stein R, Griffiths GL, Shih LB et al. Advantage of residualizing radiolabels for an internalizing antibody against the B-cell lymphoma antigen, CD22. *Cancer Immunol Immunother* 1997 May;44(3):179-88.
- (64) Brouwers AH, van Eerd JE, Frielink C, Oosterwijk E, Oyen WJ, Corstens FH et al. Optimization of radioimmunotherapy of renal cell carcinoma: labeling of monoclonal antibody cG250 with ¹³¹I, ⁹⁰Y, ¹⁷⁷Lu, or ¹⁸⁶Re. *J Nucl Med* 2004 February;45(2):327-37.
- (65) Study of Lutetium-177 Labeled cG250 in Patients With Advanced Renal Cancer. 2009. Clinicaltrials.gov: NCT 00142415
- (66) Divgi CR, O'Donoghue JA, Welt S, O'Neil J, Finn R, Motzer RJ et al. Phase I clinical trial with fractionated radioimmunotherapy using ¹³¹I-labeled chimeric G250 in metastatic renal cancer. *J Nucl Med* 2004 August;45(8):1412-21.
- (67) Vissers JL, De V, I, Schreurs MW, Engelen LP, Oosterwijk E, Figdor CG et al. The renal cell carcinoma-associated antigen G250 encodes a human leukocyte antigen (HLA)-A2.1-restricted epitope recognized by cytotoxic T lymphocytes. *Cancer Res* 1999 November 1;59(21):5554-9.
- (68) Bleumer I, Tiemessen DM, Oosterwijk-Wakka JC, Voller MC, De WK, Mulders PF et al. Preliminary analysis of patients with progressive renal cell carcinoma vaccinated with CA9-peptide-pulsed mature dendritic cells. *J Immunother* 2007 January;30(1):116-22.
- (69) Uemura H, Fujimoto K, Tanaka M, Yoshikawa M, Hirao Y, Uejima S et al. A phase I trial of vaccination of CA9-derived peptides for HLA-A24-positive patients with cytokine-refractory metastatic renal cell carcinoma. *Clin Cancer Res* 2006 March 15;12(6):1768-75.
- (70) Tso CL, Zisman A, Pantuck A, Calilli R, Hernandez JM, Paik S et al. Induction of G250-targeted and T-cell-mediated antitumor activity against renal cell carcinoma using a chimeric fusion protein consisting of G250 and granulocyte/monocyte-colony stimulating factor. *Cancer Res* 2001 November 1;61(21):7925-33.
- (71) Hernandez JM, Bui MH, Han KR, Mukouyama H, Freitas DG, Nguyen D et al. Novel kidney cancer immunotherapy based on the granulocyte-macrophage colony-stimulating factor and carbonic anhydrase IX fusion gene. *Clin Cancer Res* 2003 May;9(5):1906-16.
- (72) Avigan D. Vaccination of Patients With Renal Cell Cancer With Dendritic Cell Tumor Fusions and GM-CSF. 9-29-2009. Clinicaltrials.gov: NCT 00458536
- (73) Bauer S, Oosterwijk-Wakka JC, Adrian N, Oosterwijk E, Fischer E, Wuest T et al. Targeted therapy of renal cell carcinoma: synergistic activity of cG250-TNF and IFNγ. *Int J Cancer* 2009 July 1;125(1):115-23.

(74) Oosterwijk E, Bander NH, Divgi CR, Welt S, Wakka JC, Finn RD et al. Antibody localization in human renal cell carcinoma: a phase I study of monoclonal antibody G250. *J Clin Oncol* 1993 April;11(4):738-50.

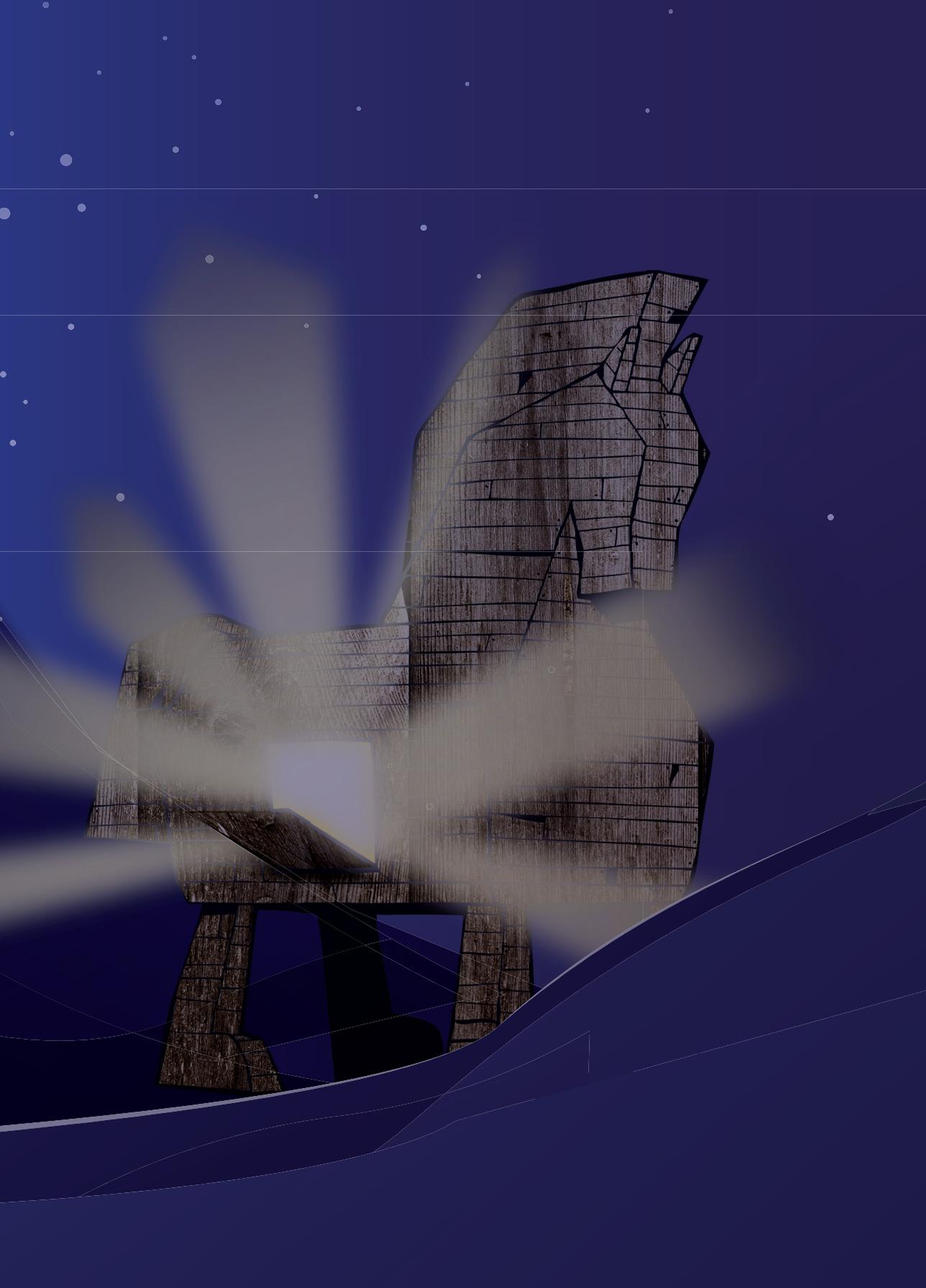
CHAPTER 3

Phase 1 Radioimmunotherapy Study with Lutetium 177-labeled Anti-Carbonic Anhydrase IX Monoclonal Antibody Girentuximab in Patients with Advanced Renal Cell Carcinoma

A. B. Stillebroer^{1,2}, O.C. Boerman², I.M.E. Desar³, M.J. Boers-Sonderen³, C.M.L. van Herpen³, J.F. Langenhuijsen¹, P.M. Smith-Jones⁴, E. Oosterwijk¹, W.J.G. Oyen², P.F.A. Mulders¹

Departments of Urology¹, Nuclear Medicine² and Medical Oncology³, Radboud University Nijmegen Medical Centre, Nijmegen, The Netherlands
Department of Nuclear Medicine⁴, Memorial Sloan Kettering Cancer Center, NY, NY, I

Published European Urology 2013 Sep;64(3):478-85



ABSTRACT

Background

Patients with metastatic clear cell Renal Cell Carcinoma (ccRCC) have a dismal prognosis. Therefore, new and less toxic treatments are needed.

Objective

Here, we determined the maximum tolerated dose (MTD) and potential therapeutic efficacy of multiple infusions of ^{177}Lu -cG250 on various dose levels in a phase I trial in patients with progressive metastasized ccRCC.

Design, setting and participants

In this uncontrolled case series in 23 patients with progressive ccRCC metastases cG250 accumulation was verified by diagnostic ^{111}In -cG250 imaging. Patients then received a high-activity dose of ^{177}Lu -cG250.

Interventions

Groups of three patients received ^{177}Lu -cG250, starting at a dose level of 1110 MBq/m² ^{177}Lu -cG250, with dose increments of 370 MBq/m² per group. In the absence of persistent toxicity, progressive disease and accelerated blood clearance, patients were eligible for re-treatment after 3 months with 75% of the previous activity dose. Patients could receive in total 3 treatment cycles.

Outcome measurements

Determination of the MTD was the primary and therapeutic efficacy the secondary outcome measurement of the study.

Results and limitations

The MTD was 2405 MBq/m², as higher doses resulted in dose-limiting myelotoxicity. Some patients received 2nd (13/23, 56%) and 3rd (4/23, 17%) treatment cycles. Most patients (17/23, 74%) demonstrated stable disease 3 months after the first treatment and one patient showed a partial response, which lasted for 9 months. Mean growth of target tumor lesions was reduced from 40.4% (95%CI \pm 17.0) during the last 3 months before study entry to 5.5% (95%CI \pm 5.3, p <0.001) at 3 months after the 1st treatment cycle. No major non-hematological side effects were observed.

Conclusions

^{177}Lu -cG250 radioimmunotherapy in metastatic ccRCC patients is well-tolerated at an activity dose level as high as 2405 MBq/m² (MTD). Radioimmunotherapy with ^{177}Lu -cG250 may stabilize previously progressive metastatic ccRCC.

INTRODUCTION

Clear cell Renal Cell Carcinoma (ccRCC) is the most common malignancy arising in the kidney.⁽¹⁾ Current first-line treatment for metastasized disease is angiogenesis inhibition with a variety of drugs.⁽²⁾ Response rates to treatment with these agents are relatively high, but mainly restricted to transient disease stabilizations and partial responses while side-effects are common and may be severe in nature.^(3;4) Although progress has been made in the management of advanced ccRCC, there is a great need for effective and less toxic treatment modalities.

Chimeric monoclonal antibody (mAb) cG250 (Girentuximab) is reactive with CAIX,⁽⁵⁻⁷⁾ a heat-sensitive, transmembraneous glycoprotein.⁽⁸⁻¹⁰⁾ Previous studies showed an almost ubiquitous expression (>90%) of CAIX in ccRCC. Expression in normal tissues has been evaluated extensively and is restricted to the gastrointestinal mucosa and gastrointestinal related structures with much lower expression levels than ccRCC.^(11;12)

Various studies have been performed with radiolabeled mAb cG250 in ccRCC patients.^(12;13) In an activity dose-escalation study with ¹³¹I-cG250 in progressive ccRCC patients a maximum tolerated dose (MTD) of 2220 MBq/m² was established.⁽⁶⁾ These findings led to a phase I/II study in which metastatic ccRCC (mRCC) patients were treated with 2220 MBq/m² ¹³¹I-cG250. After three months patients were retreated with ¹³¹I-cG250, the MTD of this 2nd injection was found to be 75% of the first dose. Stabilization of previously progressive disease was noted in 4 of 16 (25%) patients treated at the optimal dose level at six months,⁽¹⁴⁾ clearly indicating that improvements were necessary.

In radioimmunotherapy experiments in nude mice with human RCC xenografts, tumor growth was delayed more effectively with ¹⁷⁷Lutetium(¹⁷⁷Lu)-cG250 than with ¹³¹I-cG250.⁽¹⁵⁾ Moreover, an inpatient comparison revealed higher uptake of cG250 labeled with the residualizing radionuclide ¹¹¹In as compared to ¹³¹I-cG250,⁽¹³⁾ indicating that higher radiation doses could be guided to tumor lesions when cG250 was labeled with a residualizing radionuclide such as ¹⁷⁷Lu. Here, we report the results of a phase 1 study of radioimmunotherapy with ¹⁷⁷Lu-labeled cG250 in mRCC patients.

The primary aim of the study was to determine the MTD and toxicity of ¹⁷⁷Lu-cG250. The secondary aim was to determine the preliminary therapeutic efficacy of a maximum of three doses of ¹⁷⁷Lu-cG250.

PATIENTS AND METHODS

Patient Characteristics

25 progressive mRCC patients were included (21 males and 4 females, mean age 57 years, range 29-74 years) from 2005 until 2010. The inclusion and exclusion criteria are given in **Table 1**. The study (ClinicalTrials NCT00142415) was approved by the regional Medical Ethical Review Committee of the Radboud University Medical Centre and the institutional review board of the Ludwig Institute for Cancer Research. Written informed consent was obtained from all patients.

Study Design

The primary endpoint was to determine the MTD and to evaluate toxicity of increasing activity doses of ^{177}Lu -cG250 in progressive mRCC patients. The secondary endpoint was to evaluate the preliminary therapeutic efficacy of the treatment on the metastases as reflected by tumor response on contrast enhanced CT scans of the chest and abdomen using RECIST v1.0, progression free survival (PFS) and overall survival (OS).

Monoclonal Antibody cG250 and Radiolabeling

Chimeric mAb G250 (Girentuximab) is a high affinity ($K_a = 4 \times 10^9 \text{ M}^{-1}$) IgG1 mAb, reactive with CAIX. Clinical grade cG250 conjugated with 1,4,7,10-tetraazacyclododecane-1,4,7,10-tetraacetic acid (DOTA; Macrocylics, Dallas, Texas, USA) was obtained from the Ludwig Institute for Cancer Research, New York. The conjugation with DOTA was performed as described earlier.⁽¹⁶⁾

Inclusion Criteria	Exclusion Criteria
Proven advanced and progressive clear cell renal cell carcinoma.	Known brain metastases.
Previous tumour nephrectomy.	Untreated hypercalcemia.
At least one measurable metastasis less than 5 cm diameter.	Metastatic disease limited to the bone.
Performance status: Karnofsky score $\geq 70\%$.	Pre-exposure to murine/chimeric antibody therapy
Baseline CT scan of chest and abdomen within 4 weeks before study entry	Chemotherapy, external beam radiation or immunotherapy within 4 weeks prior to study. Limited field external beam radiotherapy to prevent pathological fractures was allowed.
Laboratory values obtained less than 14 days prior to registration: <ul style="list-style-type: none">• White blood cells (WBC) $> 3.5 \times 10^9/\text{l}$• Thrombocyte count $> 100 \times 10^9/\text{l}$• Hemoglobin $> 6 \text{ mmol/l}$• Total bilirubin $< 2 \times$ upper limit of normal (ULN)• ASAT, ALAT $< 3 \times$ ULN ($< 5 \times$ ULN if liver metastases present)• Serum creatinine $< 2 \times$ ULN	Cardiac disease with New York Heart Association classification of III or IV.
Age over 18 years.	Patients who are pregnant or nursing.
Ability to given written informed consent.	Life expectancy shorter than 6 months.

Table 1. In- and Exclusion criteria

Diagnostic injections consisted of 185 MBq ^{111}In -cG250 (protein dose 10 mg). The administered ^{177}Lu activity dose was adjusted on the activity-dose level, the body surface area, calculated with the formula from Mosteller,⁽¹⁷⁾ and treatment cycle, but the cG250 protein dose was 10 mg/injection in all patients.

Study Procedures

Patients received a diagnostic i.v. infusion of 185 MBq /10 mg ^{111}In Indium(^{111}In)-cG250 (total volume 10 ml) followed by acquisition of three whole-body scintigraphic images; directly, 2-4 days and 5-7 days after injection. If targeting of ^{111}In -cG250 to metastatic lesions was observed in the scintigraphic images, patients were eligible for treatment with ^{177}Lu -cG250 a week after the diagnostic infusion. Patients were followed-up weekly and blood laboratory parameters were analyzed. Toxicities were scored according to the U.S. National Cancer Institute Common Toxicity Criteria (CTC version 3.0). Dose-limiting toxicity (DLT) was defined as \geq grade 3 non-hematological toxicity or \geq grade 4 hematological toxicity which lasted for more than 4 weeks or the occurrence of hemoglobin < 4.9 mmol/l or thrombocytes $< 10 \times 10^9/\text{l}$. Three patients were entered at each dose level, starting at 1110 MBq/m², with dose increments of 370 MBq/m² if all three patients did not show a DLT. If one out of three patients had a DLT, another three patients were entered at the same dose level. The MTD was defined as the dose level at which no more than one out of six patients showed a DLT. When MTD was reached, the dose was reduced with 185 MBq/m² to evaluate an intermediate dose level. A CT scan was performed 3 months after the ^{177}Lu -cG250 radioimmunotherapy infusion to evaluate therapeutic efficacy. If this scan showed no progression of disease, the patient was eligible to receive a second radioimmunotherapy infusion, provided that thrombocyte and leucocyte levels had fully recovered. One week before the second treatment a second diagnostic infusion (185 MBq/10 mg ^{111}In -cG250) was administered mainly to rule out the presence of Human Anti Chimeric Antibodies (HACA) that would lead to rapid clearance of the radiolabeled antibody from the blood and enhanced uptake in liver, spleen and bone marrow. In the absence of rapid clearance the patient was retreated at 75% of the ^{177}Lu -cG250 activity dose administered in the first radioimmunotherapy infusion.⁽¹⁴⁾ If the CT scan made 3 months after the second radioimmunotherapy infusion showed no sign of disease progression, a third diagnostic infusion of ^{111}In -cG250 was administered. Again, if there were no signs of rapid clearance of the radiolabeled mAb and myelotoxicity was absent, a third radioimmunotherapy infusion was administered at an activity dose level of 75% of the second infusion. The last CT-scan was made 3 months after the third radioimmunotherapy infusion.

Tumor Responses

Tumor responses were evaluated according to the RECIST criteria. Measurements were performed 3 months prior to baseline, at baseline and 3 months after each radioimmunotherapy infusion.

HACA analysis

Serum samples were analyzed for the presence of human anti-chimeric antibodies (HACA) as described previously.^(5,6)

Statistical Analysis

Statistical analysis of the tumor response was analyzed using a paired t-test. The difference was considered statistically significant when $p \leq 0.05$.

RESULTS

Radioimmunoscintigraphy

Of the 25 patients who received a first scout injection of ^{111}In -cG250, 23 showed visible targeting in at least one of the known metastatic lesions at 5-7 days after injection. Two patients did not show targeting of ^{111}In -cG250 to the tumor lesions, but fast clearance and high liver

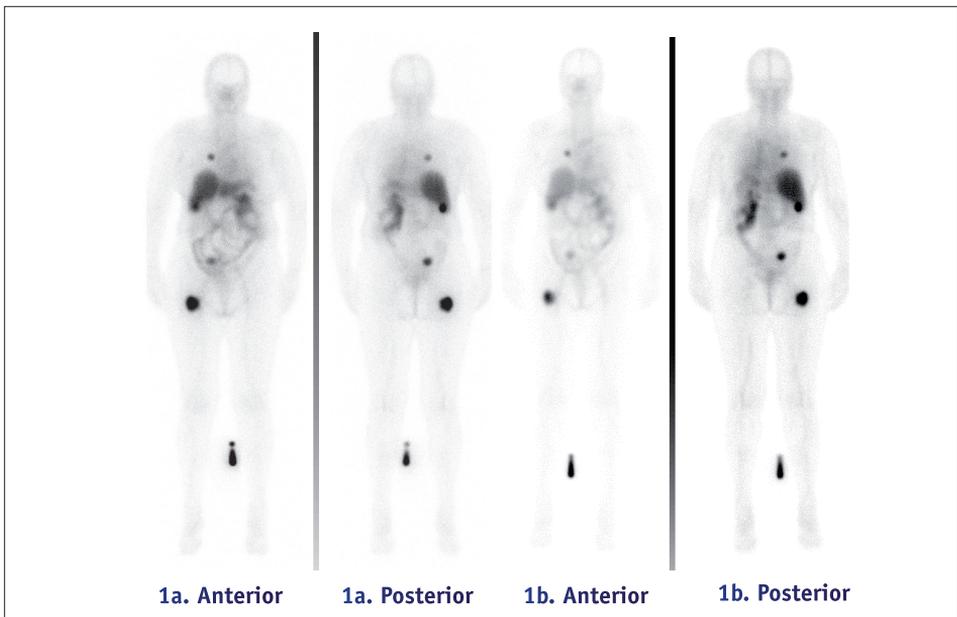


Figure 1a. and 1b. Clear visualization of ccRCC metastases in lung, abdomen and pelvis on immunoscintigraphy **a.** ^{111}In -cG250 immunoscintigram of a patient with metastatic ccRCC, acquired 7 days after injection of 185 MBq ^{111}In -cG250 **b.** ^{177}Lu -cG250 immunoscintigram of the same patient, acquired 6 days after injection of 1887 MBq ^{177}Lu -cG250.

and spleen uptake of the ^{111}In -cG250. Fast protein liquid chromatography analysis of these two cG250 preparations showed signs of aggregation of the radiolabeled mAb. As a result, 23 patients received the first high-dose ^{177}Lu -cG250 injection. Metastases were visualized highly similar at all sites (lymph node regions, bone, abdominal organs, lung) with the scout dose ^{111}In -cG250 and the high dose ^{177}Lu -cG250 (**Figure 1**).

Patient Characteristics, Toxicity and Clinical Observations

Most patients (15/23) had received prior IFN- α immunotherapy, with or without Interleukin-2 and 5-Fluorouracil (**Table 2**). When this study started, angiogenesis inhibitors were not yet standard for the treatment of mRCC. Therefore, 21 of 23 patients had not been treated with these agents before study entry. Radiolabeled antibody injections were well tolerated and no infusion-related or acute allergic reactions were noted after injection of ^{111}In -cG250 or ^{177}Lu -cG250.

Hematological toxicity was the most prominent toxicity and was dose-limiting. At the first two dose levels (1110 and 1480 MBq/m²) no DLT was noted. In these patients the nadir in the thrombocyte counts was observed 4-6 weeks and the nadir in the leucocyte counts 5-7 weeks after injection of ^{177}Lu -cG250 (**Fig. 2**). Patient #8, treated at the next dose level (1850 MBq/m²), experienced a grade 4 thrombocyte and leucocyte toxicity after the first injection of ^{177}Lu -cG250. Due to this DLT, three additional patients were entered at this dose level, and because no DLT was noted in these patients dose escalation was continued. No DLT was observed at the 2220 MBq/m² dose level. At the 2590 MBq/m² dose level, two patients experienced long-lasting grade 4 toxicity of both thrombocytes and leucocytes, requiring hospital admission and multiple thrombocyte infusions. Since both patients experienced a DLT, the dose was reduced to 2405 MBq/m². At this dose level, one of the three patients developed a DLT existing of grade 4 toxicity, and three additional patients were entered who experienced no DLT. Thus, the MTD of ^{177}Lu -cG250 radioimmunotherapy in this study was 2405 MBq/m². Second radioimmunotherapy injections with 75% of the previously administered dose caused higher myelotoxicity than after the first administration in 2 out of 13 patients, which was not clinically significant (\leq grade 2) in both cases. One out of the four patients receiving a 3rd radioimmunotherapy injection experienced higher myelotoxicity as compared to the toxicity after the 2nd radioimmunotherapy dose (grade 2 instead of grade 1 thrombocyte toxicity) (**Table 2**).

Patient #11 died while on study due to the sequelae of an ischemic cerebrovascular accident 8 weeks after the second radioimmunotherapy administration, judged unrelated to the study drug. Most patients (14/23, 61%) complained of mild fatigue or nausea (CTC grade 1 at most) in the first 2-3 weeks after radioimmunotherapy injection, but these symptoms recovered completely.

Patient number	Age at study entry	Age at diagnosis	Sex	Prior Therapy	Prognostic group Motzer (41)	Activity dose level RIT (MBq/m ²)	Activity ¹⁷⁷ Lu-GD250 (MBq)			Toxicity Grade (Common Terminology Criteria Adverse Events v3.0)						Response after each cycle (RECIST)	PFS (mos)	OS (mos)
							RIT 1	RIT 2	RIT 3	L	T	L	T	L	T			
1	50	48	M	IFN-α	Intermediate	1110	2035	-	-	0	0	-	-	-	-	PD ^d	3	15
2	62	61	F	IFN-α	Favorable	1110	1887	1480	-	0	0	0	0	-	-	SD, PD	6	46
3	57	57	F	EBRT	Favorable	1110	1887	1406	1073	1	0	2	1	2	1	SD, SD, SD	70+	70+
4	46	45	M	IFN-α	Intermediate	1480	3515	-	-	0	1	-	-	-	-	PD	0	6
5	66	64	M	Triple	Intermediate	1480	2997	2146	-	0	0	3	3	-	-	SD, PD ^e	6	11
6	70	64	M	IFN-α	Favorable	1480	2775	2072	1554	0	0	2	2	0	2	SD, SD, PD	9	44
7	67	64	M	Triple	Favorable	1850	3589	2664	2035	0	1	0	1	0	2	SD, SD, SD	30	59+
8	67	64	M	Tumor vaccin ^a	Favorable	1850	3996	3034	-	4 ^c	4 ^c	3	4	-	-	PR, PR ^f	9	33
9	74	71	M	-	Favorable	1850	4033	-	-	0	1	-	-	-	-	SD ^g	8	13
10	51	50	M	IFN-α	Intermediate	1850	4477	-	-	1	3	-	-	-	-	PD	0	25
11	68	65	M	Triple, sorafenib sunitinib	Intermediate	1850	3256	2405	-	2	2	0	1	-	-	SD ^h	3	6
12	61	59	F	EBRT, IFN-α	Intermediate	1850	3293	2479	-	0	1	0	2	-	-	SD, SD ⁱ	3	31
13	50	47	M	IFN-α	Intermediate	2220	4366	3515	-	1	1	0	0	-	-	SD, PD	3	16
14	58	58	M	Neo-adjuvant sorafenib ^b	Favorable	2220	4477	-	-	1	1	-	-	-	-	PD	0	31
15	46	44	M	Triple	Favorable	2220	5328	3996	-	1	3	2	3	-	-	SD, SD ^j	15	38+
16	50	41	F	IFN-α	Favorable	2590	5698	-	-	4	4	-	-	-	-	SD ^k	10	11
17	29	26	M	Triple, EBRT	Favorable	2590	5772	-	-	4	4	-	-	-	-	SD ^k	19	31+
18	59	53	M	-	Favorable	2405	5365	-	-	3	4 ^c	-	-	-	-	SD ^k	30+	30+
19	64	61	M	Metastectomy	Favorable	2405	4921	3626	2738	2	3	2	3	1	3	SD, SD, SD	13	24+
20	55	53	M	-	Intermediate	2405	4699	-	-	3	3	-	-	-	-	PD ^l	0	10
21	68	67	M	IFN-α	Favorable	2405	4995	3626	-	3	3	2	3	-	-	SD, PD	3	12
22	57	56	M	-	Favorable	2405	4662	-	-	0	1	-	-	-	-	SD ^g	9	15+
23	42	39	M	IFN-α	Favorable	2405	4736	3663	-	2	3	0	2	-	-	SD, SD ^m	7+	7+

Table 2. Patient Characteristics.

- h. Patient #11 died of an ischemic cerebrovascular accident 8 weeks after the 2nd RIT unrelated to the study drug, before evaluation of the 2nd RIT was possible
- i. Although patient #12 had a stabilization of target lesions and no new lesions after the 2nd cycle, due to rapid progression of non-target lesions she was excluded from the study
- j. Although patient #15 had a stabilization of disease after 2 cycles, due to prolonged myelotoxicity the 3rd RIT dose was not given because of the risk of myelodysplastic syndrome
- k. Patients #16, #17 and #18 showed stabilization of disease after 1 cycle, but due to the grade 4 myelotoxicity patients were excluded from further treatment
- l. Patient #20 had stable disease according to RECIST but had progressive and painful spinal cord metastases for which he received radiotherapy during the first cycle
- m. Patient #23 could not receive the 3rd RIT cycle due to logistical reasons
- n. Patient #23 had an ongoing stabilization of the previously progressive disease and was alive 7 months after the study start (7+)

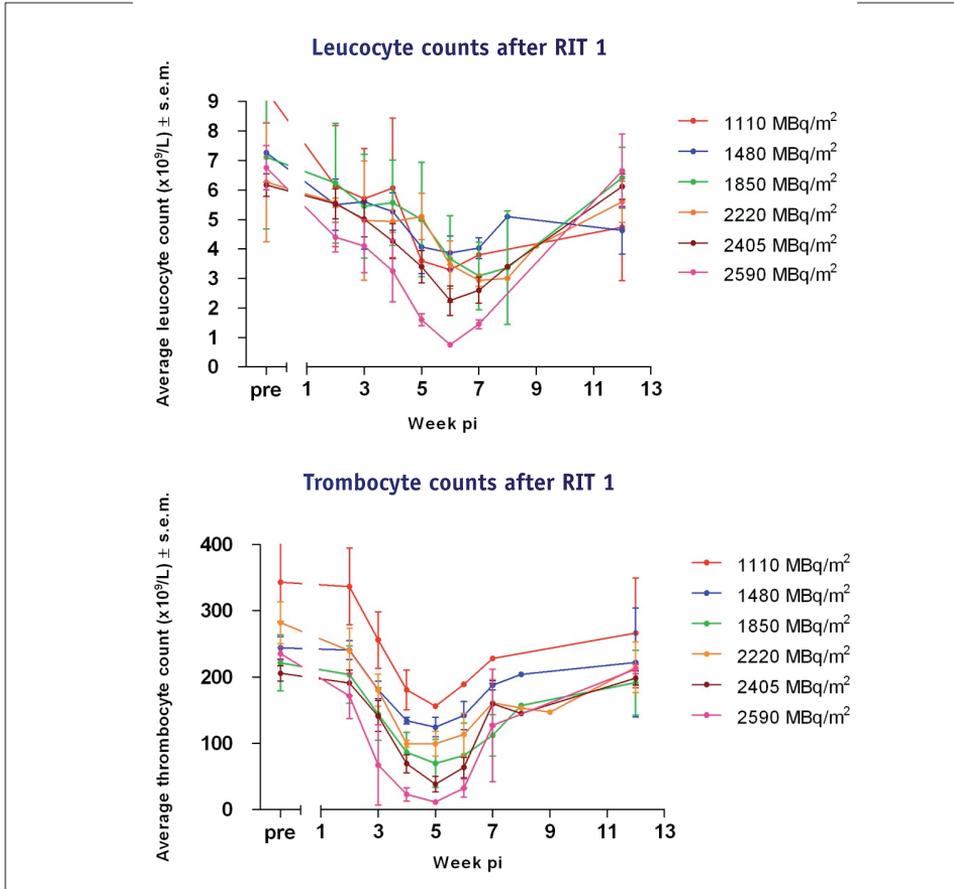


Figure 2. Mean leucocyte and thrombocyte counts \pm SD of all patients after the first radioimmunotherapy ¹⁷⁷Lu-cG250 dose.

Tumor Response

In total, 23 patients were evaluable after the first RIT cycle with ¹⁷⁷Lu-cG250. Patient #8 showed a partial response after two RIT treatments which lasted 9 months. Seventeen patients (74%) had stable disease during the three months after the first RIT dose. Of these, 12 patients were eligible for a second cycle: two patients were suspected for HACA and three patients experienced grade 4 myelotoxicity after the first radioimmunotherapy.

Seven patients had stable disease after the second radioimmunotherapy, of which four patients went on to receive a third treatment cycle. Two patients were excluded from further treatment because of rapid progression of non-target lesions (#12) or prolonged myelotoxicity (#15). Patient #23 did not receive the 3rd administration for logistical reasons.

Of the four patients receiving three radioimmunotherapy cycles, two patients experienced long-

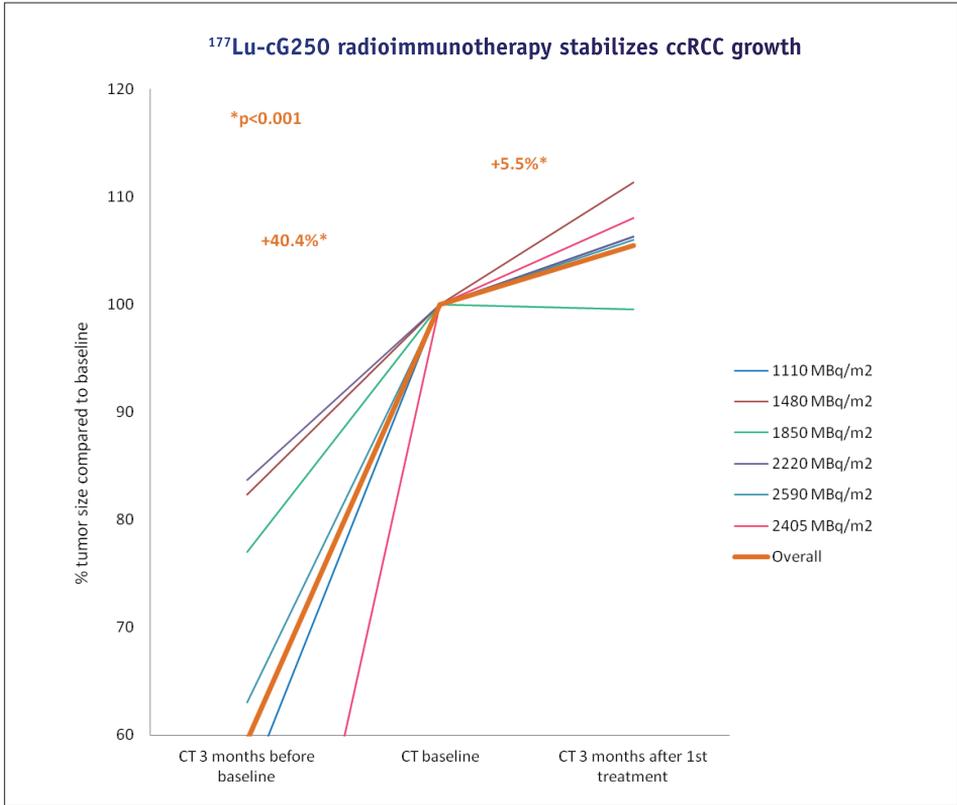


Figure 3. Tumor growth of all target lesions at each dose level. Mean growth of all tumor lesions in 23 study patients is reduced from 40.4% (95%CI \pm 17.0) during the 3 months before treatment to 5.5% (95%CI \pm 5.3) during the 3 months of the first treatment ($p < 0.001$).

lasting stabilizations of disease for two years (#7) and almost six years (#3), respectively. Mean growth of the longest diameter of all target lesions in all 23 study patients was reduced from 40.4% (95%CI \pm 17.0) during the 3 months before treatment to 5.5% (95%CI \pm 5.3) after the 1st treatment cycle ($p < 0.001$) (**Fig. 3**). Mean PFS of all patients, treated at various dose levels, was 11.1 months (95%CI \pm 6.3). At disease progression most patients received angiogenesis inhibitors. Mean OS was 25.3 months (95%CI \pm 7.1).

HACA response

Four patients developed elevated HACA levels during treatment (#3, #5, #8 and #9). HACA levels in patients #5 and #9 precluded administration of a subsequent treatment cycle.

DISCUSSION

The primary aim of the present study was to determine the MTD of radioimmunotherapy with ^{177}Lu -cG250. Besides the hematological toxicity, antibody administrations were well tolerated and besides some mild fatigue and mild nausea no other toxicities were observed. The MTD of radioimmunotherapy with ^{177}Lu -cG250 in mRCC patients was 2405 MBq/m². This is similar to the observations of Vallabhajosula et al.⁽¹⁸⁾, who treated 35 patients with prostate cancer with high activity doses ^{177}Lu -labeled humanized J591 (huJ591), an anti-PSMA mAb with a MTD of 2590 MBq/m² ^{177}Lu -huJ591. Successive injections with 75% of the previous dose were administered 3 months apart and no clinically significant higher toxicity levels were noted in patients after the second and/or third radioimmunotherapy injections. Total activity doses of up to 11,285 MBq ^{177}Lu -cG250 have been given to individual patients without dose-limiting toxicity. However, two patients (#8 and #15) experienced prolonged myelotoxicity after the 2nd radioimmunotherapy injection. The 3rd radioimmunotherapy injection was therefore not administered to avoid bone marrow aplasia. These data indicate that, in some patients, 75% of the previous activity dose may still be too high when given 3 months apart. Blumenthal et al.⁽¹⁹⁻²¹⁾ postulated that normal thrombocyte or leucocyte counts after a myelosuppressive therapy do not accurately reflect the status of the bone marrow. Peripheral blood cell counts may have normalized, while there still is an incomplete myelorecovery reflected by a reduced number of pluripotent stem cells and/or enhanced proliferation of stem cells in the bone marrow. When a second myelosuppressive therapy is given while stem cells are still recovering and actively proliferating, this may enhance toxicity. There is a great need for an improved method to predict myelotoxicity during radioimmunotherapy, since it would allow for optimal dosing in each patient.

High and specific uptake of the radiolabeled anti-CAIX antibody was seen in tumor lesions in almost all patients. Also lung lesions, that were notoriously difficult to visualize with ^{131}I -cG250^(13,14,22), showed high and preferential uptake on the ^{111}In -cG250 and ^{177}Lu -cG250 scintigrams. The full dosimetric analysis of this study has been published elsewhere.⁽²³⁾ The use of ^{124}I -labeled cG250 has been evaluated in positron emission tomography (PET) for pre-operative assessment of patients with suspected renal masses.⁽²⁴⁾ In 15 of 16 patients with ccRCC ^{124}I -cG250 visualized the tumors, whereas scans in patients with non-clear cell renal masses (n=9) were negative. The advantages of PET over conventional scintigraphy are the higher spatial resolution and the ability to accurately determine antibody uptake in tissues quantitatively⁽²⁵⁾. This allows for imaging of smaller lesions and may allow for dose optimization in patients eligible for radioimmunotherapy; PET could therefore be more suitable than conventional scintigraphy.

Our secondary endpoint was to evaluate the therapeutic efficacy of a maximum of three consecutive treatments with ^{177}Lu -cG250. One patient had an objective response which lasted 9 months after receiving two radioimmunotherapy administrations of 3996 MBq and 3034 MBq ^{177}Lu -cG250, respectively. This patient had small volume disease, with only one small (2.4 cm in diameter) lymph node metastasis. This observation is in line with previous studies, where it was noted that radioimmunotherapy in solid malignancies could be best applied in patients with small volume disease, since higher doses would be guided to these lesions.^(26, 27) In this study, at various ^{177}Lu -cG250 dose levels, disease had stabilized or responded in 8/12 (67%) patients evaluable after six months. This is superior over two consecutive ^{131}I -cG250 treatments at MTD, which showed no objective responses and only four of 16 patients (25%) had stable disease after six months.⁽¹⁴⁾ Evaluation of all target tumor lesions prior to and after the first radioimmunotherapy showed that mean growth was significantly reduced suggesting that ^{177}Lu -cG250 had therapeutic efficacy in patients with metastatic RCC. Four patients completed all three radioimmunotherapy administrations, of which two had stabilization of disease lasting for almost two and six years. The results of our present study are encouraging and indicate an overall improvement of therapeutic efficacy of radiolabeled cG250 RIT when using ^{177}Lu as a radionuclide, as compared to ^{131}I .

In conclusion, in this phase I dose escalation study in which patients were treated with a maximum of three consecutive radioimmunotherapy doses, ^{177}Lu -cG250 radioimmunotherapy was well tolerated and safe. MTD was determined at 2405 MBq/m². The clinical observations in this study in patients with progressive metastasized RCC suggest that ^{177}Lu -cG250 RIT may prevent disease progression, albeit the patient population was heterogeneous and not all patients received the same number of treatment cycles. The phase II study has recently been initiated to evaluate the therapeutic efficacy of multiple doses ^{177}Lu -cG250 at MTD.

Acknowledgements

The authors wish to thank Dr. C. Verfaillie and all the CRA staff of the Omnicare Corporation who were involved in the monitoring of this study. This study was funded by a grant from the Dutch Cancer society (KWF grant KUN 2005-3339).

REFERENCES

- (1) Jemal A, Siegel R, Xu J, Ward E. Cancer statistics, 2010. *CA Cancer J Clin* 2010 September;60(5):277-300.
- (2) Reeves DJ, Liu CY. Treatment of metastatic renal cell carcinoma. *Cancer Chemother Pharmacol* 2009 June;64(1):11-25.
- (3) Escudier B, Eisen T, Stadler WM et al. Sorafenib in advanced clear-cell renal-cell carcinoma. *N Engl J Med* 2007 January 11;356(2):125-34.
- (4) Motzer RJ, Hutson TE, Tomczak P et al. Sunitinib versus interferon alfa in metastatic renal-cell carcinoma. *N Engl J Med* 2007 January 11;356(2):115-24.
- (5) Steffens MG, Boerman OC, Oosterwijk-Wakka JC et al. Targeting of renal cell carcinoma with iodine-131-labeled chimeric monoclonal antibody G250. *J Clin Oncol* 1997 April;15(4):1529-37.
- (6) Steffens MG, Boerman OC, de Mulder PH et al. Phase I radioimmunotherapy of metastatic renal cell carcinoma with ¹³¹I-labeled chimeric monoclonal antibody G250. *Clin Cancer Res* 1999 October;5(10 Suppl):3268s-74s.
- (7) Oosterwijk E, Ruiter DJ, Hoedemaeker PJ et al. Monoclonal antibody G 250 recognizes a determinant present in renal-cell carcinoma and absent from normal kidney. *Int J Cancer* 1986 October 15;38(4):489-94.
- (8) Opavsky R, Pastorekova S, Zelnik V et al. Human MN/CA9 gene, a novel member of the carbonic anhydrase family: structure and exon to protein domain relationships. *Genomics* 1996 May 1;33(3):480-7.
- (9) Pastorek J, Pastorekova S, Callebaut I et al. Cloning and characterization of MN, a human tumor-associated protein with a domain homologous to carbonic anhydrase and a putative helix-loop-helix DNA binding segment. *Oncogene* 1994 October;9(10):2877-88.
- (10) Grabmaier K, Vissers JL, De Weijert MC et al. Molecular cloning and immunogenicity of renal cell carcinoma-associated antigen G250. *Int J Cancer* 2000 March 15;85(6):865-70.
- (11) Pastorekova S, Parkkila S, Parkkila AK et al. Carbonic anhydrase IX, MN/CA IX: analysis of stomach complementary DNA sequence and expression in human and rat alimentary tracts. *Gastroenterology* 1997 February;112(2):398-408.
- (12) Steffens MG, Oosterwijk-Wakka JC, Zegwaart-Hagemeier NE et al. Immunohistochemical analysis of tumor antigen saturation following injection of monoclonal antibody G250. *Anticancer Res* 1999 March;19(2A):1197-200.
- (13) Brouwers AH, Buijs WC, Oosterwijk E et al. Targeting of metastatic renal cell carcinoma with the chimeric monoclonal antibody G250 labeled with (¹³¹I) or (¹¹¹In): an inpatient comparison. *Clin Cancer Res* 2003 September 1;9(10 Pt 2):3953S-60S.
- (14) Brouwers AH, Mulders PF, de Mulder PH et al. Lack of efficacy of two consecutive treatments of radioimmunotherapy with ¹³¹I-cG250 in patients with metastasized clear cell renal cell carcinoma. *J Clin Oncol* 2005 September 20;23(27):6540-8.
- (15) Brouwers AH, van Eerd JE, Frielink C et al. Optimization of radioimmunotherapy of renal cell carcinoma: labeling of monoclonal antibody cG250 with ¹³¹I, ⁹⁰Y, ¹⁷⁷Lu, or ¹⁸⁶Re. *J Nucl Med* 2004 February;45(2):327-37.
- (16) Lewis MR, Raubitschek A, Shively JE. A facile, water-soluble method for modification of proteins with DOTA. Use of elevated temperature and optimized pH to achieve high specific activity and high chelate stability in radiolabeled immunoconjugates. *Bioconjug Chem* 1994 November;5(6):565-76.
- (17) Mosteller RD. Simplified calculation of body-surface area. *N Engl J Med* 1987 October 22;317(17):1098.
- (18) Vallabhajosula S, Goldsmith SJ, Kostakoglu L, Milowsky MI, Nanus DM, Bander NH. Radioimmunotherapy of prostate cancer using ⁹⁰Y- and ¹⁷⁷Lu-labeled J591 monoclonal antibodies: effect of multiple treatments on myelotoxicity. *Clin Cancer Res* 2005 October 1;11(19 Pt 2):7195s-200s.
- (19) Blumenthal RD, Lew W, Juweid M, Alisaukas R, Ying Z, Goldenberg DM. Plasma FLT3-L levels predict bone marrow recovery from myelosuppressive therapy. *Cancer* 2000 January 15;88(2):333-43.
- (20) Juweid ME, Zhang CH, Blumenthal RD, Hajjar G, Sharkey RM, Goldenberg DM. Prediction of hematologic

toxicity after radioimmunotherapy with (¹³¹I)-labeled anticarcinoembryonic antigen monoclonal antibodies. *J Nucl Med* 1999 October;40(10):1609-16.

- (21) Siegel JA, Yeldell D, Goldenberg DM et al. Red marrow radiation dose adjustment using plasma FLT3-L cytokine levels: improved correlations between hematologic toxicity and bone marrow dose for radioimmunotherapy patients. *J Nucl Med* 2003 January;44(1):67-76.
- (22) Brouwers AH, Buijs WC, Mulders PF et al. Radioimmunotherapy with [¹³¹I]cG250 in patients with metastasized renal cell cancer: dosimetric analysis and immunologic response. *Clin Cancer Res* 2005 October 1;11(19 Pt 2):7178s-86s.
- (23) Stillebroer AB, Zegers CM, Boerman OC et al. Dosimetric analysis of 177Lu-cG250 radioimmunotherapy in renal cell carcinoma patients: correlation with myelotoxicity and pretherapeutic absorbed dose predictions based on 111In-cG250 imaging. *J Nucl Med*. 2012 Jan;53(1):82-9.
- (24) Divgi CR, Pandit-Taskar N, Jungbluth AA et al. Preoperative characterisation of clear-cell renal carcinoma using iodine-124-labelled antibody chimeric G250 (¹²⁴I-cG250) and PET in patients with renal masses: a phase I trial. *Lancet Oncol* 2007 April;8(4):304-10.
- (25) Juweid ME, Cheson BD. Positron-emission tomography and assessment of cancer therapy. *N Engl J Med* 2006 February 2;354(5):496-507.
- (26) Chatal JF, Saccavini JC, Gestin JF et al. Biodistribution of indium-111-labeled OC 125 monoclonal antibody intraperitoneally injected into patients operated on for ovarian carcinomas. *Cancer Res* 1989 June 1;49(11):3087-94.
- (27) Behr TM, Liersch T, Greiner-Bechert L et al. Radioimmunotherapy of small-volume disease of metastatic colorectal cancer. *Cancer* 2002 February 15;94(4 Suppl):1373-81.
- (28) Wood C, Srivastava P, Bukowski R et al. An adjuvant autologous therapeutic vaccine (HSPPC-96; vitespen) versus observation alone for patients at high risk of recurrence after nephrectomy for renal cell carcinoma: a multicentre, open-label, randomised phase III trial. *Lancet* 2008 July 12;372(9633):145-54.
- (29) Desar IM, Stillebroer AB, Oosterwijk E et al. 111In-Bevacizumab Imaging of Renal Cell Cancer and Evaluation of Neoadjuvant Treatment with the Vascular Endothelial Growth Factor Receptor Inhibitor Sorafenib. *J Nucl Med*. 2010 Nov;51(11):1707-15.

CHAPTER 4

Dosimetric analysis of ^{177}Lu -cG250 radio-immunotherapy in renal cell carcinoma patients: Correlation with myelotoxicity and pre-therapeutic absorbed dose predictions based on ^{111}In -cG250 imaging

Alexander B. Stillebroer^{1,2}, Catharina M.L. Zegers², Otto C. Boerman², Egbert Oosterwijk¹, Peter F.A. Mulders¹, Joseph A. O'Donoghue³, Eric P. Visser², Wim J.G. Oyen²

Departments of Urology¹ and Nuclear Medicine², Radboud University Nijmegen Medical Centre, Nijmegen, The Netherlands.

Department of Medical Physics³, Memorial Sloan-Kettering Cancer Centre, New York, USA

Published: J Nucl Med. 2012 Jan;53(1):82-9



ABSTRACT

Background

This study aimed to estimate the radiation absorbed doses to normal tissues and tumor lesions during radioimmunotherapy with ^{177}Lu -cG250. Serial planar scintigrams after injection of $^{111}\text{In}/^{177}\text{Lu}$ -cG250 in patients with metastasized renal cell carcinoma (mRCC) were analyzed quantitatively. The estimated radiation doses were correlated with observed hematological toxicity. In addition the accuracy of the predicted therapeutic absorbed doses, based on diagnostic ^{111}In -cG250 data, were determined.

Methods

Twenty patients received a diagnostic tracer activity of ^{111}In -cG250 (185 MBq) followed by radioimmunotherapy with ^{177}Lu -cG250. The administered activity of ^{177}Lu -cG250 was escalated by entering three patients at each activity level starting at 1110 MBq/m² with increments of 370 MBq/m². After each diagnostic and therapeutic administration whole body scintigraphic images and pharmacokinetic data were acquired. Hematologic toxicity was graded based on the Common Toxicity Criteria version 3.0. Diagnostic ^{111}In -cG250 data were used to simulate ^{177}Lu - and ^{90}Y -data by correcting for the difference in physical decay. Absorbed doses were calculated for the whole body, red marrow, organs and tumor metastases for the therapeutic ^{177}Lu -cG250, simulated ^{177}Lu -cG250 and simulated ^{90}Y -cG250 data.

Results

Observed hematological toxicity, especially platelet toxicity, correlated significantly with the administered activity ($r = 0.85$), whole body absorbed dose ($r = 0.65$) and red marrow dose ($r = 0.62$ and 0.75). An inverse relationship between the mass and absorbed dose of the tumor lesions was observed. Calculated mean absorbed doses were similar for the simulated and measured ^{177}Lu -cG250 data. Absorbed doses (whole body, red marrow) based on the simulated ^{177}Lu -cG250 data correlated with the observed platelet toxicity ($r = 0.65$ and 0.82). The tumor-to-red marrow dose ratio was higher for radioimmunotherapy with ^{177}Lu -cG250 than for radioimmunotherapy with ^{90}Y -cG250, indicating that ^{177}Lu has a wider therapeutic window for radioimmunotherapy with cG250 as compared to ^{90}Y .

Conclusion

In patients with mRCC, hematological toxicity after treatment with ^{177}Lu -cG250 can be predicted on the basis of administered activity, whole body and red marrow absorbed dose. Diagnostic ^{111}In -cG250 data can be used to accurately predict absorbed doses and myelotoxicity of radioimmunotherapy with ^{177}Lu -cG250. These estimations indicate that in these patients higher radiation doses can be guided to the tumors with ^{177}Lu -cG250 than with ^{90}Y -cG250.

INTRODUCTION

Renal cell carcinoma (RCC) is a disease with ~ 58,000 new patients each year in the USA and accounts for 3% of all malignancies.¹ The only curative option to date for RCC is (partial) nephrectomy. Prognosis of untreated mRCC is poor with a median survival of 12 months. With the advent of targeted agents, this prognosis has increased dramatically, more than doubling overall survival.² However, side effects of these compounds are common and often severe.³ Therefore we aim to develop an effective radioimmunotherapeutic approach for the treatment of RCC using the radiolabeled anti-CAIX antibody, cG250. The main goal in radioimmunotherapy is to maximize the absorbed dose to the tumor, while maintaining the dose to healthy tissues at acceptable levels. The dose-limiting normal tissue in radioimmunotherapy is the red marrow. Thrombocytopenia and leucopenia are generally the initial and most severe manifestations of myelotoxicity after radioimmunotherapy.⁴

In several studies, methods are defined to estimate the red marrow dose based on blood activity data or planar scintigrams.⁵⁻⁸ Previous studies on the relationship between radiation dose estimates and myelotoxicity were variable.^{7, 9-15} Results might have been influenced by the used method to calculate the red marrow dose, the radionuclide used or patient specific factors. Recently, Baechler et al. showed for example that the elapsed time since the last chemotherapy is an important parameter in the prediction of toxicity.¹⁶

The ability to predict the therapeutic dose to tumor lesions and healthy organs could provide tools for treatment planning. For individual dosing each radioimmunotherapy treatment can be preceded by a diagnostic infusion of the same monoclonal antibody (mAb) labeled with a γ -emitter.¹¹ The analysis of the images of an antibody labeled with ¹¹¹In could potentially be used to predict the targeting of the same antibody labeled with the β -emitting radionuclide ⁹⁰Y or ¹⁷⁷Lu. In a study of DeNardo et al. mAb Lym-1 labeled with ¹¹¹In was used to calculate the absorbed doses for ⁹⁰Y-Lym-1 in patients with non-Hodgkin's lymphoma.¹⁷ Vallabhajosula et al. used ¹¹¹In-J591 as a surrogate for ⁹⁰Y-J591.¹⁰ However, because ⁹⁰Y is not suitable for imaging since it is a pure β -emitting radionuclide, the accuracy of these dosimetric predictions could not be proven.

During a phase I study at our institution, patients with progressive clear cell RCC could receive multiple therapeutic doses of ¹⁷⁷Lu-cG250. Before each therapeutic administration patients received a diagnostic infusion with ¹¹¹In-cG250. We used the pharmacokinetic and scintigraphic data to estimate radiation doses of the therapeutic injections to normal tissues and metastases and investigated whether these doses correlated with the observed hematological toxicity. We investigated whether the dosimetric analysis of the diagnostic injections could be used to predict the radiation doses of the therapeutic

injections after the first treatment cycle. Furthermore absorbed dose predictions were made for radioimmunotherapy with ^{90}Y -cG250 to determine the most suitable β -emitter for radioimmunotherapy with the radiolabeled anti-CAIX antibody in these patients.

MATERIALS AND METHODS

Patients

Twenty patients with progressive mRCC (16 males, 4 females) who had all undergone a nephrectomy of the tumorous kidney were included. The mean age of the patients was 58 years (range 29 - 74 yrs). The study (ClinicalTrials NCT00142415) was approved by the regional Medical Ethical Review Committee of the Radboud University Nijmegen Medical Centre and the Institutional Review Board of the Ludwig Institute for Cancer Research. The study was monitored by the Omnicare corporation, commissioned by the Ludwig Institute for Cancer Research. Written informed consent was obtained from all patients before study entry.

MAb cG250 and radiolabeling

cG250 is a high-affinity ($K_a = 4 \times 10^9 \text{ M}^{-1}$) chimeric, IgG1 mAb, reactive with the CAIX antigen, a transmembrane glycoprotein overexpressed on the cell surface of the majority (> 95%) of clear cell RCCs.¹⁸ Vials (10 mg/mL) clinical grade cG250 were obtained from The Ludwig Institute for Cancer Research (New York, NY). Conjugation of cG250 with 1,4,7,10-tetraazacyclododecane-1,4,7,10-tetraacetic acid (DOTA) (Macrocyclics, Dallas, TX) was performed as described previously¹⁹ at Memorial-Sloan Kettering Cancer Centre (New York, NY). The cG250-DOTA conjugate was radiolabeled with ^{111}In (Covidien, Petten, The Netherlands) for tracer injections in a 0.25 M ammonium acetate buffer, pH 5.4 for 30 min at 45 °C. Labeling of cG250-DOTA with ^{177}Lu (IDB Holland, Tilburg, The Netherlands) for therapeutic injections was performed in 0.25 M ammoniumacetate buffer, pH 5.4 for 60 min at 45 °C. All labeling procedures using ^{111}In or ^{177}Lu were performed under strict metal-free conditions. All radiolabeled cG250 preparations were purified by gel filtration on a PD-10 column (GE Healthcare, Woerden, The Netherlands) eluted with phosphate-buffered saline (PBS) supplemented with 5 mM DTPA and 10 mM ascorbic acid. For all preparations, the amount of non-mAb-associated radiolabel was determined by instant thin-layer chromatography (ITLC) with ITLC silica gel strips (Pall Corporation Life Sciences, New York, NY, USA), using 0.1 M citrate buffer, pH 6.0 as the mobile phase ($R_f = 0$ for radiolabeled antibody, and $R_f = 0.8$ – 1 for free and chelated radionuclides).¹⁸ The radiochemical purity was >99% for ^{111}In -DOTA-cG250 and $99.3 \pm 0.9\%$ for ^{177}Lu -DOTA-cG250. The immunoreactive fraction determined as described previously was $90.1 \pm 5.3\%$ and $89.8 \pm 6.8\%$ for the ^{111}In -cG250 and ^{177}Lu -cG250 preparations, respectively.

Study design

In this phase I study the maximum tolerated dose (MTD) of ^{177}Lu -cG250 radioimmunotherapy was determined by entering three patients at each activity level, starting at 1110 MBq /m² with dose increments of 370 MBq/m². The MTD was defined as the administered activity at which no more than 1 out of 6 patients showed dose limiting toxicity (DLT). DLT was defined as \geq grade 3 non-hematological toxicity or \geq grade 4 hematological toxicity (platelets $< 25 \times 10^9$ /l or leucocytes $< 1.0 \times 10^9$ /l) which lasted for more than 4 weeks or the occurrence of hemoglobin < 4.9 mmol/l or thrombocytes $< 10 \times 10^9$ /l at any time point. The administered ^{177}Lu dose was adjusted on the activity level, the body surface area, calculated with the formula from Mosteller.²⁰

Toxicity was monitored weekly, by determining the hematological and blood chemistry laboratory parameters, and was scored according to the U.S. National Cancer Institute Common Toxicity Criteria (CTC version 3.0). Response to treatment was determined by comparing the baseline computed tomography (CT) scan to CT-scans acquired 3 months after each radioimmunotherapy administration.

All radioimmunotherapy administrations were preceded by a diagnostic tracer of ^{111}In -cG250 (185 MBq, 10 mg cG250, total volume 5 ml) to visually assess preferential uptake of the radiolabeled antibody in the tumor lesions and to exclude the presence of human anti-chimeric antibodies (HACA), that would cause accelerated clearance of the radiolabeled antibody from the blood and enhanced uptake in liver, spleen and bone marrow.

Imaging and pharmacokinetics

Following each ^{111}In -cG250 administration three whole-body scintigrams were acquired (directly, 2-4 days and 5-7 days post injection (p.i.)). The images were recorded in conjugate view using a double-headed gamma camera (ECAM, Siemens Inc., Hoffman Estates, IL, USA), equipped with parallel-hole medium-energy collimators. Symmetric energy windows were set at 15% of the ^{111}In photopeaks at 172 and 247 keV. Images consisted of summed counts collected in both windows. The scan speed was 8 cm/min, 6 cm/min and 4 cm/min at day 0, 2-4, and 5-7 p.i., respectively. The matrix size was 256 x 1024, with a pixel size of 2.4 x 2.4 mm². Images obtained after infusion of ^{177}Lu -cG250 were recorded using a symmetric 15% energy window of 208 keV at the same time points and with the same scan speeds as after the ^{111}In -cG250 infusion.

Blood samples were drawn directly, 30, 60, 120 minutes, 2-4 days and 5-7 days after the ^{111}In -cG250 and ^{177}Lu -cG250 infusions. The activity concentration in the serum from these samples was counted in a shielded 3-inch well-type gamma counter (Wizard, LKB/Wallac, Perkin-Elmer, Boston, MA). To correct for radioactive decay, reference samples containing a known fraction of the administered activity were measured simultaneously.

The activity concentrations in the serum samples were corrected for the hematocrit content in the patient's blood to obtain blood activity concentrations.

Dosimetry

The radiation absorbed dose to the whole body, liver, red marrow, lungs, heart, testes, normal kidney and metastases delivered by therapeutic $^{177}\text{Lu-cG250}$ injections were calculated according to the Medical Internal Radiation Dose (MIRD) scheme.²¹

Metastatic lesions measurable on CT and visualized in at least one of the scintigraphic images were analyzed. The volume and background correction factor of the metastatic lesions were derived from CT imaging. Tumor volumes were converted to mass assuming that the tumor density equals 1 g/cm^3 .

The residence times of the source organs and metastases were calculated using SPRIND, a software package for integrated data processing for internal dose assessment.⁶ Regions of interest (ROI) for source organs and tumors were drawn on both anterior and posterior scintigraphic images. The counts within the ROI were corrected for attenuation and background contribution as described by Visser et al.⁶ The geometric mean was calculated and the data were integrated over time using the trapezoid method. After the last scan, SPRIND assumes only physical decay of the radionuclide in the source organs. To calculate the absorbed doses, residence times were imported into the software package OLINDA/EXM.²² Radiation absorbed doses to the whole body and organs of interest were calculated using the adult male and the adult female phantom. The spheres model was used to determine the radiation absorbed doses of the metastases.²²

The red marrow absorbed dose was calculated using two methods. First, the absorbed dose to the red marrow was calculated using the scintigraphic images. In SPRIND, ROIs were drawn over the left and right part of the cranium. The residence times of the left and right cranium were summed and divided by the fraction of the red marrow mass in the cranium to the total red marrow mass in the body, for which the default value of 0.119 was taken from ICRP23's Reference Man.²³ The second method was the blood-based method as described by Shen et al.⁵ This method was also implemented in SPRIND, for more information we refer to Visser et al.⁶

In the blood-based method the dose to the red marrow is composed of the dose from the red marrow to the red marrow ($\text{rm} \leftarrow \text{rm}$) and the dose from the whole body to the red marrow ($\text{rm} \leftarrow \text{wb}$). The electron contribution ($\text{rm} \leftarrow \text{rm}$) of the red marrow absorbed dose can be calculated in the absence of whole body planar scintigrams with the following equation.⁵

$$\frac{D_{rm}}{A_{adm}} = \Delta_{el} \phi_{el}(rm \leftarrow rm) \left\{ R_{rm,bl} \frac{\tau_{bl}}{m_{bl}} \right\}$$

Dr_{rm} = red marrow absorbed dose due to electron-radiation [Gy]

A_{adm} = administered activity [Bq]

Δ_{el} = mean electron energy emitted per nuclear transition [J]

Φ_{el} (rm ← rm) = absorbed fraction of electron radiation from red marrow to red marrow [-]

R_{rm,bl} = red marrow to blood concentration ratio [-]

τ_{bl} = residence time of the blood [s]

m_{bl} = total blood mass [kg]

The fraction of the red marrow dose due to electron contribution was calculated for each patient to determine if an estimation of the red marrow dose can be made in the absence of scintigraphic images. An estimation of the red marrow dose, based on blood samples alone will have the advantage that whole body scintigrams can be cancelled.

Predictive dosimetry

Data obtained after the diagnostic ¹¹¹In-cG250 infusion were used to estimate therapeutic doses from ¹⁷⁷Lu-cG250, assuming identical biodistribution and biological clearance of ¹¹¹In-cG250 and ¹⁷⁷Lu-cG250. Simulated ¹⁷⁷Lu scans were generated by correcting the ¹¹¹In whole body scintigrams for the difference in physical decay of ¹¹¹In and ¹⁷⁷Lu. Each ¹¹¹In-cG250 scintigram (anterior and posterior images) was pixel-wise multiplied by $e^{t(\lambda_{In} - \lambda_{Lu})}$ (t = time p.i.) to obtain simulated whole body scintigrams for ¹⁷⁷Lu. The resulting simulated ¹⁷⁷Lu scintigrams were used to calculate residence times with SPRIND and the simulated absorbed doses with OLINDA for the organs of interest and metastases.

The blood-based red marrow absorbed dose for ¹⁷⁷Lu was also simulated. To simulate the blood residence time of ¹⁷⁷Lu, ¹¹¹In-cG250 blood data and reference samples were used to determine the biological clearance of activity from the blood, physical clearance was incorporated by multiplication with $e^{-\lambda_{Lu} t}$.

To provide insight in the absorbed doses for radioimmunotherapy with ⁹⁰Y-cG250, the same methods were used to simulate ⁹⁰Y data.

Statistical analysis

The Pearson correlation coefficient was determined to evaluate the relationship between (i) the image and blood-based method to calculate the red marrow dose (ii) the tumor mass and tumor absorbed dose and (iii) the calculated absorbed doses for ¹⁷⁷Lu-cG250 and the simulated data. Hematological toxicity was correlated with administered acti-

vity, whole body dose, red marrow dose and the electron contribution of the red marrow dose. In addition the relationship between hematological toxicity and the simulated whole body and red marrow dose was determined. Because the red marrow is the dose limiting organ, tumor-to-red marrow dose ratios were determined to compare (simulated) $^{177}\text{Lu-cG250}$ data with simulated $^{90}\text{Y-cG250}$ data.

RESULTS

Patients

All 20 patients completed at least one cycle of $^{111}\text{In}/^{177}\text{Lu-cG250}$ radioimmunotherapy. In each patient only data from the first treatment cycle were used for dosimetric analysis. DLT was noted in one patient at the 1850 MBq/m² activity level. The other five patients that received this activity showed no DLT, so the administered activity was further incremented. On the 2590 MBq/m² activity level, DLT was seen in all 3 patients, therefore the administered activity was reduced to 2405 MBq/m². This activity level proved to be safe in 6 patients (only 1 out of 6 patients had DLT) and by definition the latter dose was designated as the MTD.

Data

The first treatment cycle was used to determine the absorbed dose in the organs of interest and metastases after administration with $^{177}\text{Lu-cG250}$. The diagnostic $^{111}\text{In-cG250}$ data of the first cycle were also used to evaluate the predictive value of the simulated $^{177}\text{Lu-cG250}$ data and to calculate absorbed doses for radioimmunotherapy with $^{90}\text{Y-cG250}$.

The $^{177}\text{Lu-cG250}$ data of two patients had to be excluded from the analysis due to incomplete or inconsistent scintigraphic data. Another patient (patient 17) showed an unexpected high uptake in the liver and red marrow after injection of $^{177}\text{Lu-cG250}$ due to the presence of HACA or due to the presence of aggregates in the radiolabeled antibody preparation. The dosimetric results of this patient were therefore excluded from the analysis.

For the $^{177}\text{Lu-cG250}$ and $^{111}\text{In-cG250}$ data a total of respectively 40 and 48 metastases were used for tumor absorbed dose calculations. The weight of these tumors, determined on the CT images, ranged from 0.6 to 319 gram.

A complete set of blood activity data was acquired from 15 ($^{177}\text{Lu-cG250}$) and 16 ($^{111}\text{In-cG250}$) patients. These pharmacokinetic data were used to calculate the blood-based red marrow absorbed dose in these patients.

Organs	¹⁷⁷ Lu-cG250 radioimmunotherapy			simulated ¹⁷⁷ Lu-cG250 radioimmunotherapy			simulated ⁹⁰ Y-cG250 radioimmunotherapy		
	Mean +/- SD	Min	Max	Mean +/- SD	Min	Max	Mean +/- SD	Min	Max
Whole body	0.24 ± 0.04	0.19	0.36	0.25 ± 0.03	0.21	0.33	0.64 ± 0.08	0.57	0.82
Liver	1.26 ± 0.25	0.93	1.75	1.22 ± 0.23	0.93	1.75	3.03 ± 0.63	2.27	4.49
Heart wall	0.76 ± 0.16	0.47	1.12	0.68 ± 0.13	0.47	0.93	2.05 ± 0.38	1.41	2.69
Red marrow									
<i>Image-based</i>	0.44 ± 0.07	0.32	0.62	0.41 ± 0.06	0.35	0.57	0.90 ± 0.11	0.78	1.11
<i>Blood-based</i>	0.35 ± 0.07	0.24	0.46	0.31 ± 0.07	0.21	0.46	0.81 ± 0.21	0.47	1.23
Kidney	1.30 ± 0.35	0.78	1.92	1.43 ± 0.49	0.76	2.57	3.77 ± 1.26	2.00	6.24
Lungs	0.49 ± 0.13	0.34	0.74	0.48 ± 0.10	0.37	0.65	1.45 ± 0.35	1.06	2.08
Testes	1.90 ± 0.45	1.20	2.70	1.64 ± 0.36	1.11	2.36	4.32 ± 0.99	2.84	6.26
Metastases	5.72 ± 4.52	0.47	17.29	4.86 ± 4.69	0.52	19.92	9.76 ± 8.88	1.31	37.52

Table 1. Radiation absorbed dose in whole body, organs and metastases for ¹⁷⁷Lu-cG250, simulated ¹⁷⁷Lu-cG250 and simulated ⁹⁰Y-cG250 (mGy/MBq). is significant at the 0.05 level).

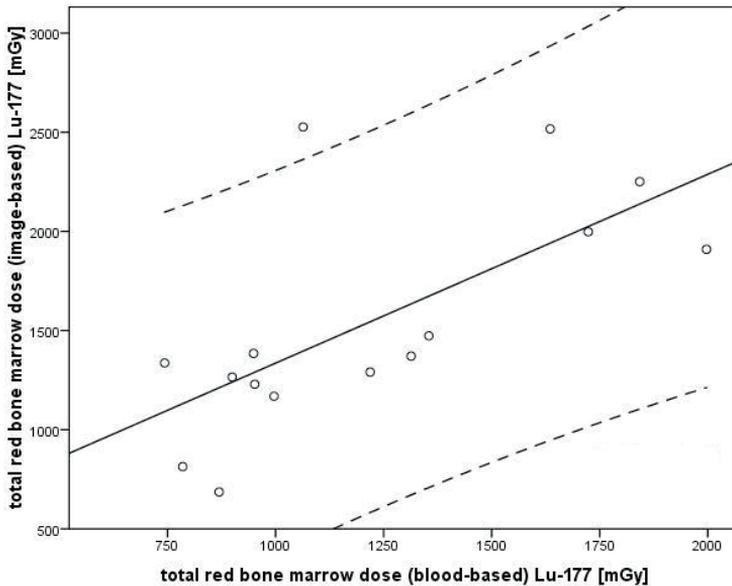


Figure 1. Total red bone marrow dose based on the image-based method plotted against the total red bone marrow dose based on the blood-based method ($r = 0.68$, $P = 0.005$). The striped-line is the 95% confidence interval.

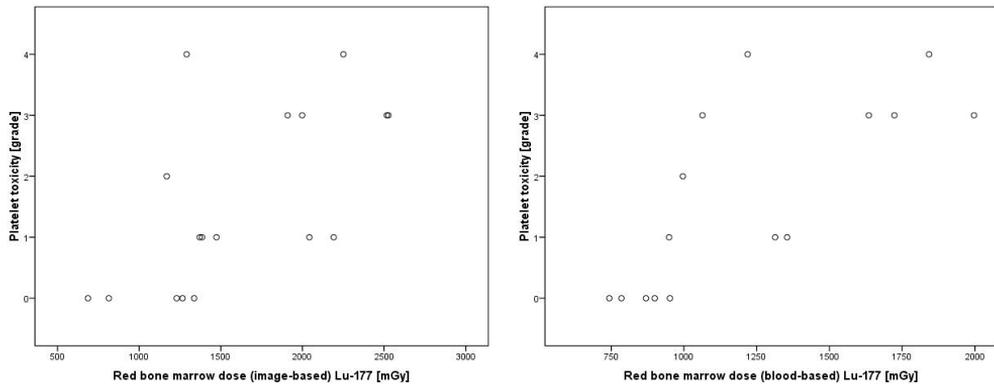


Figure 2. Platelet toxicity (grade according to CTC version 3.0) plotted against the red marrow dose based on the image-based method ($r = 0.62$, $p = 0.07$) and the blood-based method ($r = 0.75$, $p = 0.01$).

¹⁷⁷Lu-cG250 radiation doses

The estimated mean radiation absorbed doses after ¹⁷⁷Lu-cG250 radioimmunotherapy were 0.24 ± 0.04 mGy/MBq for the whole body, 0.49 to 1.90 mGy/MBq for the healthy organs, 0.44 ± 0.07 mGy/MBq (image-based) and 0.35 ± 0.07 mGy/MBq (blood-based) for the red marrow (**Table 1**).

The results of the image- and blood-based method to calculate the red marrow absorbed dose, correlated significantly ($r = 0.68$, $P = 0.005$, **Fig.1**). Observed thrombocyte toxicity correlated significantly with the administered activity ($r = 0.85$), whole body dose ($r = 0.65$) and image- and blood-derived red marrow dose ($r = 0.62$ and 0.75 , respectively, **Fig. 2**). Leukocyte toxicity correlated significantly with the administered activity ($r = 0.66$) and the blood-based red marrow dose ($r = 0.53$). However, there was no significant relationship between the leukocyte toxicity and the whole body dose or the image-based red marrow dose. The electron contribution was 61.6 – 77.3% ($N = 15$, $\bar{x} = 71.3\%$) of the blood-based red marrow dose. This part of the red marrow absorbed dose correlated significantly with the thrombocyte ($r = 0.76$) and leukocyte toxicity ($r = 0.56$). The correlations are summarized in **Table 2**.

Absorbed doses to the tumor lesions varied widely from 0.47 to 17.29 mGy/MBq. The mean tumor-to-red marrow dose ratio for ¹⁷⁷Lu-cG250 was 13.0 and 16.3 for respectively the image- and blood-based method. The total tumor dose during the first treatment cycle varied from 1.9 to 92.0 Gy. The radiation dose to the tumor lesions correlated inversely with the mass of the tumor lesions ($r = -0.44$, $P < 0.005$, **Fig. 3**).

¹¹⁷Lu-cG250

		Administered Activity [MBq]	Total whole body dose	Total RM dose (image-based)	Total RM dose (blood-based)	Electron contribution RM dose
Thrombocyte toxicity	Pearson Correlation	0.85 [*]	0.65 [*]	0.62 [*]	0.75 [*]	0.76 [*]
	Sig. (2-tailed)	<0.001	0.005	0.007	0.001	0.001
	N	20	17	17	15	15
Leukocyte toxicity	Pearson Correlation	0.66 [*]	0.32	0.27	0.53 [†]	0.56 [†]
	Sig. (2-tailed)	0.001	0.214	0.287	0.043	0.029
	N	20	17	17	15	15

Simulated ¹¹⁷Lu-cG250

		Total whole body dose	Total RM dose (image-based)	Total RM dose (blood-based)
Thrombocyte toxicity	Pearson Correlation	0.82 [*]	0.81 [*]	0.65 [*]
	Sig. (2-tailed)	<0.001	<0.001	0.007
	N	19	19	16
Leukocyte toxicity	Pearson Correlation	0.61 [*]	0.55 [†]	0.49
	Sig. (2-tailed)	0.006	0.015	0.054
	N	19	19	16

Table 2. Pearson correlation coefficients (and its two-tailed significance) between the toxicity grade and administered activity or absorbed dose calculations for ¹¹⁷Lu-cG250 and simulated ¹¹⁷Lu-cG250 (mGy). (RM = Red marrow, * correlation is significant at the 0.01 level, † correlation is significant at the 0.05 level).

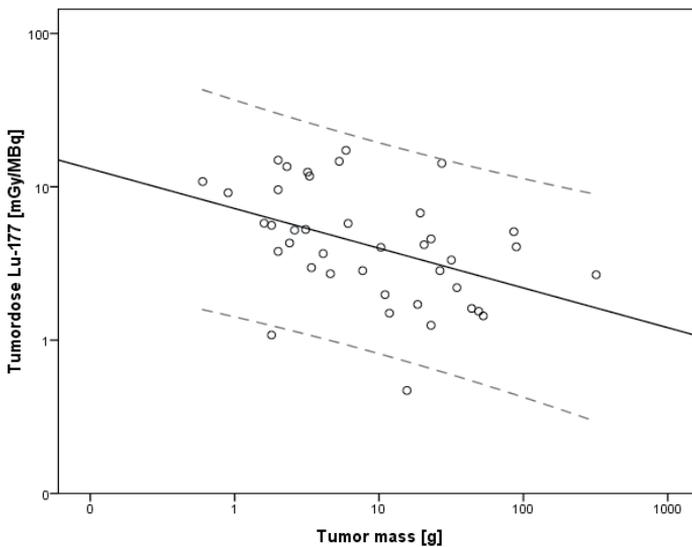


Figure 3. Absorbed dose in the metastases for ¹¹⁷Lu-cG250 radioimmunotherapy plotted against the weight of metastatic lesions on logarithmic scales ($r = -0.44$, $P < 0.005$). The striped-line is the 95% confidence interval.

Simulated ^{177}Lu -cG250 radiation doses

The simulated ^{177}Lu -cG250 absorbed doses for the whole body, organs and metastases, based on the diagnostic ^{111}In -cG250 data are presented in Table 1. The calculated doses were similar to the doses as derived from the ^{177}Lu -cG250 images (**Figure 4**). However, for the individual patient slight differences were found. For example, the largest differences in calculated red marrow dose were -20.0% and 14.9% for the image-based method and -25.5% and 7.7% for the blood-based method. There is a significant correlation between the ^{177}Lu -cG250 and simulated absorbed dose calculations for the whole body, liver, heart wall, red marrow, lungs, testes and metastases ($r = 0.82$ - 0.98 , $P < 0.001$). In contrast, the calculated kidney absorbed dose of the simulated data in comparison to the ^{177}Lu -cG250 data did not show any correlation ($r = -0.28$).

Thrombocyte and leukocyte toxicity correlated significantly with the simulated whole body and red marrow (image-based) dose ($r = 0.55$ - 0.82 , $P < 0.05$). In addition, thrombocyte toxicity correlated significantly with the blood-based red marrow dose ($r = 0.65$, $P < 0.01$). These correlations are summarized in Table 2. For the simulated ^{177}Lu -cG250 data the tumor-to-red marrow dose ratio was 11.9 (image-based) and 15.7 (blood-based).

Simulated ^{90}Y -cG250 radiation doses

Simulated mean radiation absorbed doses for radioimmunotherapy with ^{90}Y -cG250 were 0.64 mGy/MBq for the whole body, 1.45 to 4.32 mGy/MBq for the normal organs, 0.90 mGy/MBq (image-based) and 0.81 mGy/MBq (blood-based) for the red marrow (**Table 1**). Radioimmunotherapy with ^{90}Y -cG250 resulted in a theoretical mean absorbed dose of 9.76 mGy/MBq to the metastases. The tumor-to-red marrow dose ratio for this simulated ^{90}Y -cG250 data was 10.8 and 12.0 for the image and blood-based method respectively. Mean absorbed doses to the bone marrow (mGy/MBq) were approximately 2-3 times as high as compared to the (simulated) ^{177}Lu -cG250 data (**Figure 4**).

DISCUSSION

This study was designed to estimate the radiation absorbed doses to normal tissues and tumor lesions during radioimmunotherapy with ^{177}Lu -cG250 in patients with ccRCC. Radiation-induced myelotoxicity was dose limiting in these patients. An accurate estimation of the red marrow dose is essential for reliable predictions of the maximum activity that can be administered safely. The radiation dose to the red marrow dose can be estimated based on the activity levels in the blood ⁵ as long as the radiolabeled antibody does not bind specifically to the cells in the bone marrow. However, various other imaging methods to estimate the red marrow dose have been described.⁶⁻⁸ DeNardo et al. showed for example that an image-based method, unlike the blood-based method, was able to predict thrombocytopenia and leucopenia.⁷ In the present study both the blood-based method and an image-based method were used to estimate the red marrow dose. The calculated mean absorbed doses for both methods were in the same range, 0.35 versus 0.44 mGy/MBq. In addition, there was a significant correlation between the red marrow dose calculated with both methods ($r = 0.68$, $P = 0.005$). The blood-based red marrow absorbed dose was 0.35 ± 0.07 mGy/MBq for ^{177}Lu -cG250, which is somewhat higher than reported by Vallabhajosula et al.¹⁰ for radioimmunotherapy with ^{177}Lu -J591 (0.32 ± 0.10 mGy/MBq). This slight difference in red marrow dose is in agreement with the difference in MTD: 2405 MBq/m² for ^{177}Lu -cG250 and 2590 MBq/m² for ^{177}Lu -J591.¹⁰ In this patient population the observed hematological toxicity ranged from grade 0 to 4. The relationship between hematological toxicity, the administered activity and the absorbed dose calculations (whole body, red marrow) were analyzed. Myelotoxicity, especially thrombocyte toxicity, correlated significantly with the administered activity, whole body dose and red marrow dose. The correlation between myelotoxicity and the blood-based red marrow dose was higher in comparison to the image-based method. Therefore, in these patients, the blood-based method was a better predictor of myelotoxicity. In a series of previous radioimmunotherapy studies no correlations were found between radiation absorbed doses and myelotoxicity.^{7, 9, 12, 13} On the other hand, Divgi et al.¹⁴, showed a significant correlation between the whole-body absorbed dose and the hematological toxicity after radioimmunotherapy with ^{131}I -cG250. Juweid et al.¹⁵ described a significant correlation between the calculated red marrow dose and hematologic toxicity for radioimmunotherapy with a ^{131}I -labeled anti-CEA antibody. Furthermore, Vallabhajosula et al.¹⁰ showed that myelotoxicity correlated with the administered activity and red marrow absorbed dose for radioimmunotherapy with ^{177}Lu -J591. Moreover, Vallabhajosula et al.¹⁰ showed that the blood-based red marrow dose correlated best with the fractional decrease of thrombocytes. Similarly, in our study the blood-based red marrow

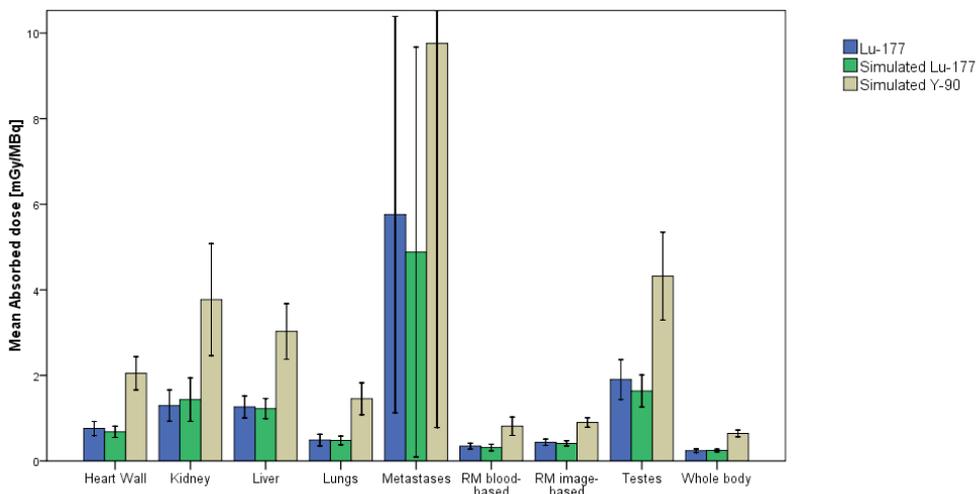


Figure 4. Mean absorbed dose (± 1 SD) in the organs of interest, whole body and metastases for the ^{177}Lu -cG250, simulated ^{177}Lu - and ^{90}Y -cG250 data (RM = red marrow).

dose correlated best with the thrombocyte toxicity grade ($r = 0.75$).

The red marrow absorbed dose during radioimmunotherapy consists of a dose due to emitted electrons and a dose due to emitted photons. For ^{177}Lu -labeled cG250 the electron contribution accounted for approximately 71% of the red marrow dose. An estimation of the red marrow dose can be made by calculating the electron contribution based on the blood data and subsequently add 29% for the photon contribution. In addition there was a significant correlation between the red marrow absorbed dose due to electron radiation and thrombocyte ($r = 0.76$) and leukocyte toxicity ($r = 0.56$). This indicates that in the absence of scintigraphic data, blood samples alone can be used to estimate the red marrow dose and predict myelotoxicity.

Normal organs receiving the highest absorbed doses were the liver, kidney and testes, with a mean dose of respectively 1.26, 1.30 and 1.90 mGy/MBq. This was 5.8 Gy, 6.0 Gy and 8.8 Gy at MTD, for a mean body surface area of 1.79 m^2 ²⁴. The liver and kidney doses were well below the threshold for deterministic effects, which are respectively 30 Gy and 23 Gy.^{25, 26} Based on experiments using external beam radiation therapy it was suggested that a fractionated dose ≥ 2 Gy to the testes could cause permanent infertility.²⁷ This dose was exceeded for radioimmunotherapy with ^{177}Lu -cG250, but fertility status of men in this study was not investigated.

To accurately estimate the tumor absorbed dose, the tumor specific volume and background correction factor were determined by CT. The total tumor dose varied widely

from 0.47 to 17.3 mGy/MBq, mainly due to differences in uptake of the radiolabeled antibody in the lesions. In 17 of the 40 tumors ^{177}Lu -cG250 activity was highest at the last scintigraphic acquisition, which means that there is a slow accumulation of radiolabeled cG250 during 5-7 days. Because there were no scintigraphic data available after 5-7 days p.i., the tumor absorbed dose might be slightly underestimated if only physical decay is taken into account. Conversely, an overestimation of the tumor dose could have occurred due to biological clearance of the radiolabel after the last imaging time point. As described in several other studies^{9, 11, 28}, an inverse relationship between tumor dose and tumor mass was observed in this study. Tumor doses exceeding 50 Gy are considered to be required to achieve a therapeutic response in these patients.²⁹ In this study only 2 out of 40 tumor lesions received a tumor dose of > 50 Gy during the first treatment cycle. Twelve out of 40 tumors received a tumor dose > 25 Gy during the first cycle, suggesting that for these tumors a tumor sterilizing dose can be reached during subsequent treatment cycles.

Diagnostic ^{111}In -cG250 data were used to predict therapeutic absorbed doses by correcting scintigrams and blood activity data for the physical decay difference between the radionuclides. The simulated absorbed doses were compared with the standard acquired absorbed doses for ^{177}Lu -cG250. There was no significant difference between the mean absorbed doses for the simulated and measured ^{177}Lu -cG250 data. In addition, the simulated absorbed dose correlated significantly with the absorbed dose after radioimmunotherapy for the whole body, liver, heart wall, red marrow, lungs, testes and tumor lesions ($r = 0.818-0.982$, $P < 0.001$). Unfortunately, the calculated kidney absorbed dose for ^{177}Lu -cG250 in comparison to the simulated data based on the ^{111}In -cG250 data did not correlate. For an accurate simulation, the biodistribution of ^{111}In -cG250 should be identical to the biodistribution of ^{177}Lu -cG250 at all time points. Activity in the colon, overlapping the kidney region, limits the accuracy of the kidney absorbed dose measurements. The distribution of activity in the colon is time dependent. However, not all scans were acquired at exactly the same time points, which resulted in a variation in calculated kidney doses for simulated and ^{177}Lu -cG250 scintigrams. In this study it was shown that simulations, based on diagnostic data, can be used to predict the absorbed doses, but also to predict myelotoxicity, since the simulated whole body and red marrow absorbed dose correlated significantly with thrombocyte and leukocyte toxicity. These results provide tools for treatment planning, because a toxicity risk assessment can be made prior to radioimmunotherapy.

Another suitable radionuclide for radioimmunotherapy with cG250 is ^{90}Y .³⁰ An advantage of ^{90}Y is the long range of the β -emissions which could overcome the intratumoral heterogeneity of the antibody uptake. A disadvantage is the inability to reliably image the

^{90}Y activity distribution, due to the absence of β^- -emissions. We showed that the ^{111}In -cG250 scintigrams and pharmacokinetic data could be used to accurately estimate the radiation doses after radioimmunotherapy with ^{177}Lu -cG250. Therefore, it was assumed that ^{90}Y -cG250 absorbed doses can also be predicted based on the ^{111}In -cG250 data. The calculated absorbed doses (mGy/MBq) for ^{90}Y -cG250 were approximately 2-3 times higher than for ^{177}Lu -cG250. This is in the same range as described by Vallabhajosula et al.¹⁰ who reported a 3 times higher bone marrow dose for radioimmunotherapy with ^{90}Y -J591 compared to ^{177}Lu -J591. Considering the ratio of blood-based red marrow dose between ^{177}Lu and simulated ^{90}Y found in the present study and assuming this is the main determinant of MTD, the anticipated MTD of ^{90}Y -cG250 radioimmunotherapy would be around 25-28 MBq/kg, which is substantially lower than that of ^{177}Lu -cG250. A more relevant parameter to compare tumor doses of ^{90}Y and ^{177}Lu -cG250 is the ratio between the tumor and red marrow dose, rather than the absolute doses to the tumor and the red marrow. The tumor-to-red marrow dose ratio was higher for (simulated) ^{177}Lu -cG250 in comparison to ^{90}Y -cG250. The tumor absorbed dose depends on the accumulation of radioactive cG250. Due to the slow accumulation of cG250 in the metastases and a longer half-life of ^{177}Lu , as compared to that of ^{90}Y , the radiation dose that can be guided to the tumor lesions is anticipated to be higher for radioimmunotherapy with ^{177}Lu -cG250.

CONCLUSION

In patients with RCC, hematological toxicity, especially thrombocyte toxicity, after radioimmunotherapy with ^{177}Lu -cG250 can be predicted on the basis of administered activity, whole body and red marrow dose. In the absence of whole body scintigrams, blood activity data alone can be used to estimate the red marrow dose and predict hematological toxicity. Diagnostic ^{111}In -cG250 data can be used to predict absorbed doses for radioimmunotherapy with ^{177}Lu -cG250 and ^{90}Y -cG250. In these patients treatment with ^{177}Lu -cG250 provides a higher tumor-to-red marrow dose ratio in comparison to treatment with ^{90}Y -cG250.

REFERENCES

- (1) Jemal A, Siegel R, Ward E, Hao Y, Xu J, Thun MJ. Cancer statistics, 2009. *CA Cancer J Clin* 2009 July;59(4):225-49.
- (2) Motzer RJ, Hutson TE, Tomczak P et al. Sunitinib versus interferon alfa in metastatic renal-cell carcinoma. *N Engl J Med* 2007 January 11;356(2):115-24.
- (3) Hartmann JT, Haap M, Kopp HG, Lipp HP. Tyrosine kinase inhibitors - a review on pharmacology, metabolism and side effects. *Curr Drug Metab* 2009 August;10(5):470-81.
- (4) DeNardo GL, Siantar CL, DeNardo SJ. Radiation dosimetry for radionuclide therapy in a nonmyeloablative strategy. *Cancer Biother Radiopharm* 2002 February;17(1):107-18.
- (5) Shen S, DeNardo GL, Sgouros G, O'Donnell RT, DeNardo SJ. Practical determination of patient-specific marrow dose using radioactivity concentration in blood and body. *J Nucl Med* 1999 December;40(12):2102-6.
- (6) Visser E, Postema E, Boerman O, Visschers J, Oyen W, Corstens F. Software package for integrated data processing for internal dose assessment in nuclear medicine (SPRIND). *Eur J Nucl Med Mol Imaging* 2007 March;34(3):413-21.
- (7) DeNardo DA, DeNardo GL, O'Donnell RT et al. Imaging for improved prediction of myelotoxicity after radioimmunotherapy. *Cancer* 1997 December 15;80(12 Suppl):2558-66.
- (8) Siegel JA, Lee RE, Pawlyk DA, Horowitz JA, Sharkey RM, Goldenberg DM. Sacral scintigraphy for bone marrow dosimetry in radioimmunotherapy. *Int J Rad Appl Instrum B* 1989;16(6):553-9.
- (9) Behr TM, Sharkey RM, Juweid ME et al. Phase I/II clinical radioimmunotherapy with an iodine-131-labeled anti-carcinoembryonic antigen murine monoclonal antibody IgG. *J Nucl Med* 1997 June;38(6):858-70.
- (10) Vallabhajosula S, Goldsmith SJ, Hamacher KA et al. Prediction of myelotoxicity based on bone marrow radiation-absorbed dose: radioimmunotherapy studies using ⁹⁰Y- and ¹⁷⁷Lu-labeled J591 antibodies specific for prostate-specific membrane antigen. *J Nucl Med* 2005 May;46(5):850-8.
- (11) Brouwers AH, Buijs WC, Mulders PF et al. Radioimmunotherapy with [¹³¹I]cG250 in patients with metastasized renal cell cancer: dosimetric analysis and immunologic response. *Clin Cancer Res* 2005 October 1;11(19 Pt 2):7178s-86s.
- (12) Wiseman GA, White CA, Sparks RB et al. Biodistribution and dosimetry results from a phase III prospectively randomized controlled trial of Zevalin radioimmunotherapy for low-grade, follicular, or transformed B-cell non-Hodgkin's lymphoma. *Crit Rev Oncol Hematol* 2001 July;39(1-2):181-94.
- (13) Wiseman GA, White CA, Stabin M et al. Phase I/II ⁹⁰Y-Zevalin (yttrium-90 ibritumomab tiuxetan, IDEC-Y2B8) radioimmunotherapy dosimetry results in relapsed or refractory non-Hodgkin's lymphoma. *Eur J Nucl Med* 2000 July;27(7):766-77.
- (14) Divgi CR, Bander NH, Scott AM et al. Phase I/II radioimmunotherapy trial with iodine-131-labeled monoclonal antibody G250 in metastatic renal cell carcinoma. *Clin Cancer Res* 1998 November;4(11):2729-39.
- (15) Juweid ME, Zhang CH, Blumenthal RD, Hajjar G, Sharkey RM, Goldenberg DM. Prediction of hematologic toxicity after radioimmunotherapy with (¹³¹I)-labeled anticarcinoembryonic antigen monoclonal antibodies. *J Nucl Med* 1999 October;40(10):1609-16.
- (16) Baechler S, Hobbs RF, Jacene HA, Bochud FO, Wahl RL, Sgouros G. Predicting hematologic toxicity in patients undergoing radioimmunotherapy with ⁹⁰Y-ibritumomab tiuxetan or ¹³¹I-tositumomab. *J Nucl Med* 2010 December;51(12):1878-84.
- (17) DeNardo GL, O'Donnell RT, Shen S et al. Radiation dosimetry for ⁹⁰Y-2IT-BAD-Lym-1 extrapolated from pharmacokinetics using ¹¹¹In-2IT-BAD-Lym-1 in patients with non-Hodgkin's lymphoma. *J Nucl Med* 2000 May;41(5):952-8.
- (18) Steffens MG, Boerman OC, Oosterwijk-Wakka JC et al. Targeting of renal cell carcinoma with iodine-131-labeled chimeric monoclonal antibody G250. *J Clin Oncol* 1997 April;15(4):1529-37.
- (19) Lewis MR, Kao JY, Anderson AL, Shively JE, Raubitschek A. An improved method for conjugating monoclo-

- nal antibodies with N-hydroxysulfosuccinimidyl DOTA. *Bioconjug Chem* 2001 March;12(2):320-4.
- (20) Mosteller RD. Simplified calculation of body-surface area. *N Engl J Med* 1987 October 22;317(17):1098.
 - (21) Loevinger R., Budinger TF, Watson EE. MIRD primer for absorbed dose calculations. *The Society of Nuclear medicine*; 1988.
 - (22) Stabin MG, Sparks RB, Crowe E. OLINDA/EXM: the second-generation personal computer software for internal dose assessment in nuclear medicine. *J Nucl Med* 2005 June;46(6):1023-7.
 - (23) International Commission on Radiological Protection. Report of the task group on reference man, ICRP publication 23. 1975. Ref Type: Personal Communication
 - (24) Sacco JJ, Botten J, Macbeth F, Bagust A, Clark P. The average body surface area of adult cancer patients in the UK: a multicentre retrospective study. *PLoS One* 2010;5(1):e8933.
 - (25) Koral KF, Huberty JP, Frame B et al. Hepatic absorbed radiation dosimetry during I-131 metaiodobenzylguanidine (MIBG) therapy for refractory neuroblastoma. *Eur J Nucl Med Mol Imaging* 2008 November;35(11):2105-12.
 - (26) Konijnenberg M, Melis M, Valkema R, Krenning E, de JM. Radiation dose distribution in human kidneys by octreotides in peptide receptor radionuclide therapy. *J Nucl Med* 2007 January;48(1):134-42.
 - (27) Howell S, Shalet S. Gonadal damage from chemotherapy and radiotherapy. *Endocrinol Metab Clin North Am* 1998 December;27(4):927-43.
 - (28) Chatal JF, Saccavini JC, Gestin JF et al. Biodistribution of indium-111-labeled OC 125 monoclonal antibody intraperitoneally injected into patients operated on for ovarian carcinomas. *Cancer Res* 1989 June 1;49(11):3087-94.
 - (29) Goldenberg DM. Targeted therapy of cancer with radiolabeled antibodies. *J Nucl Med* 2002 May;43(5):693-713.
 - (30) Brouwers AH, Buijs WC, Oosterwijk E et al. Targeting of metastatic renal cell carcinoma with the chimeric monoclonal antibody G250 labeled with (¹³¹I) or (¹¹¹In): an inpatient comparison. *Clin Cancer Res* 2003 September 1;9(10 Pt 2):3953S-60S.

CHAPTER 5

¹¹¹In-bevacizumab imaging of renal cell cancer and evaluation of neoadjuvant treatment with the vascular endothelial growth factor receptor inhibitor sorafenib

Ingrid M.E. Desar^{1*}, Alexander B. Stillebroer^{2,3*}, Egbert Oosterwijk²,
William P.J. Leenders⁴, Carla M.L. van Herpen¹, Winette T.A. van der Graaf¹, Otto
C. Boerman³, Peter F.A. Mulders², Wim J.G. Oyen³

Department of Medical Oncology¹, Urology², Nuclear Medicine³ and Pathology⁴, Radboud University Nijmegen Medical Centre, Nijmegen, The Netherlands

*IMED and ABS contributed equally to this manuscript

Published: J Nucl Med 2010 Nov;51(11):1707-15



ABSTRACT

Background

Clear cell renal cell cancer (ccRCC) prominently expresses vascular endothelial growth factor-A (VEGF-A), and new treatment strategies for RCC aim at inhibition of VEGF-VEGFR signaling. This study explores the ability of ¹¹¹In-bevacizumab scintigraphy to depict RCC and to evaluate treatment response of neoadjuvant treatment with sorafenib, a VEGFR inhibitor.

Methods

The ability to depict RCC with ¹¹¹In-bevacizumab scintigraphy was tested in fourteen patients scheduled to undergo a tumor nephrectomy, of these nine RCC patients were treated in a neoadjuvant setting with sorafenib 400 mg bid orally. In the latter group baseline and post treatment ¹¹¹In-bevacizumab scans were compared. The intratumoral distribution of ¹¹¹In-bevacizumab was determined scintigraphically ex vivo in a 1-cm lamella of the resected tumorous kidney. Expression of VEGF-A, GLUT-1, CAIX, alpha smooth muscle actin and Ki67 was determined by immunohistochemistry and compared to the local concentration of ¹¹¹In-bevacizumab. Additionally, the VEGF-A content in tumor samples was determined quantitatively by ELISA.

Results

In all five non-neoadjuvant treated patients, preferential accumulation of ¹¹¹In-bevacizumab was observed in the tumors. All ccRCC with enhanced ¹¹¹In-bevacizumab targeting expressed high levels of VEGF-A. Treatment with sorafenib resulted in a significant decrease of ¹¹¹In-bevacizumab uptake in the tumor in the patients with ccRCC (mean change -60.5%, range +1.5 to -90.1%). The decrease in uptake was due to destruction of the tumor neovasculature, whereas the VEGF-A expression remained intact. In the patient with papillary RCC limited uptake without change after sorafenib was observed.

Conclusions

RCC lesions were clearly delineated with ¹¹¹In-bevacizumab scintigraphy. Neoadjuvant treatment with sorafenib resulted in a significant decrease of ¹¹¹In-bevacizumab uptake in RCC. ¹¹¹In-bevacizumab scintigraphy can be an attractive biomarker for response and needs further study.

INTRODUCTION

Treatment options for patients with metastatic renal cell cancer (mRCC) have improved substantially in the past 5 years. Long mired in therapeutic nihilism because of chemotherapy resistance and modest effects of immunotherapy, recently multiple active agents with marked clinical effects have become available for mRCC. Knowledge of underlying molecular characteristics identified the vascular endothelial growth factor-A (VEGF-A) and the mammalian target of rapamycin (mTOR) pathways as fundamental to the biology of RCC. This biological insight provided a rationale for targeting these growth factor signaling pathways in RCC. Small molecules inhibiting the tyrosine kinase portion of the intracellular receptor for VEGF (VEGFR) have undergone extensive clinical testing. Two of these drugs, sunitinib and sorafenib, are now widely used in clinical practice. These agents inhibit not only VEGFR but also a broad spectrum of related receptor tyrosine kinases.

As the development of angiogenesis inhibitors was not paralleled by appropriate evaluation methods for this kind of drugs, new predictive biomarkers are urgently needed. Currently, CT-scans are mostly used to diagnose RCC and to evaluate treatment effects of TKIs. CT scans are volumetric assessments of tumors, and do not provide functional information. The Response Evaluation Criteria in Solid Tumors (RECIST) guidelines, used to evaluate treatment response, are based on the sum of one-dimensional measurements of the greatest diameter of the tumor and/or metastases.^{(1), (2)} However, treatment with TKIs can result in necrosis and cavitation without a change in size, leading to an underestimation of therapeutic efficacy.⁽³⁾ Molecular imaging may be an alternative method to evaluate the efficacy of these new drugs. In clear cell RCC a loss of function of the Von Hippel-Lindau (VHL) gene product leads to accumulation of the hypoxia inducible factor 1 α (HIF-1 α), with subsequent upregulation of HIF target genes, including vascular endothelial growth factor (VEGF-A).^{(4), (5), (6)} This is independent from hypoxia and results in highly vascularized tumors. Therefore, molecular imaging of VEGF-A in ccRCC might be achieved and might provide functional information about the effects of TKI treatment.^{(4), (5), (6)}

Bevacizumab-based scintigraphy may be an interesting approach to image VEGF-producing tumors. Bevacizumab is a humanized monoclonal antibody (mAb) directed against all VEGF-A isoforms which inhibits angiogenesis by preventing VEGF-A from binding to and activating its receptors. VEGF-A is the best characterized member of the VEGF family and is considered the predominant and most critical regulator of neovascularization in various tumor types.⁽⁷⁾ Alternative splicing results in at least six isoforms of VEGF-A:

VEGF121, VEGF145, VEGF165, VEGF183, VEGF189 and VEGF206. In tumors, VEGF121 and VEGF165, and to a lesser extent VEGF189, are predominant.^{(8), (9)} VEGF165 and VEGF189 are cell- or matrix-associated isoforms and are angiogenic, whereas VEGF121 is freely diffusible and mainly induces vasodilatation and vascular permeability.^{(10), (11), (8)} Accumulation of antibodies like bevacizumab in tumors is the result of multiple factors, such as antigen density, circulating antigen concentration, and tumor physiological parameters such as microvessel density, vessel permeability, blood flow and interstitial fluid pressure. In two animal studies and in one clinical study tumor-specific accumulation of radio-labeled bevacizumab has been described.^{(12), (13), (14)} Remarkably, no correlation between VEGF-A levels in plasma or tumor tissue extracts and bevacizumab uptake was observed in a study in patients with metastatic colorectal cancer.⁽¹⁴⁾ In this study, plasma VEGF-A was determined in a sample obtained just prior to labeled bevacizumab administration. The scintigraphy was performed one week after tracer administration. Tumor VEGF-A was determined directly after surgery, 10 days after tracer injection.

In the present study the potential of ¹¹¹In-bevacizumab to image VEGF-A expressing ccRCC tumors was studied in 14 patients with primary RCC scheduled to undergo tumornephrectomy. Nine of these patients were treated with sorafenib for 4 weeks in a neoadjuvant setting. The effect of sorafenib on ¹¹¹In-bevacizumab uptake in RCC was explored in these patients.

METHODS AND MATERIALS

Study design

Nine patients suspected of primary RCC and with baseline enhanced ¹¹¹In-bevacizumab uptake in the renal tumors were treated with sorafenib for four weeks after which ¹¹¹In-bevacizumab scintigraphy was repeated to observe the effect of sorafenib on ¹¹¹In-bevacizumab uptake. As a control, in five patients suspected of primary RCC and scheduled to undergo tumornephrectomy a ¹¹¹In-bevacizumab scintigraphy was performed prior to surgery.

Exclusion criteria for all patients were prior use of bevacizumab or drugs targeting VEGF or VEGFR, prior anticancer therapy, uncontrolled comorbidity, pregnancy and lactation. For the sorafenib treated group, adequate bone marrow (white blood cells (WBC) $\geq 3.5 \times 10^9/L$, platelets $\geq 100 \times 10^9/L$, Hemoglobin ≥ 6 mmol/L) renal (serum creatinine ≤ 2 x upper limit of normal (ULN) and hepatic function (total bilirubin ≤ 1.5 ULN, AST and ALT

$\leq 2.5 \times \text{ULN}$ ($\leq 5 \times$ in case of liver metastases) were required. The study was approved by the regional internal review board. Written informed consent was obtained from all patients.

Study drug

Sorafenib (Nexavar[®], Bayer, München, Germany) was administered 400 mg bid orally during four weeks prior to nephrectomy. Dose interruptions and dose reductions were allowed in case of Common Toxicity Criteria (CTC) \geq grade 3 adverse events.

For scintigraphic imaging, bevacizumab (Avastin[®], Roche, Basel, Switzerland) was conjugated with isothiocyanatobenzyl diethylenetriaminepentaacetic acid (DTPA) as described previously.⁽¹⁵⁾ Kits containing 1 mg of bevacizumab-DTPA conjugate in 1.0 ml of 0.15 M citrate buffer, pH 5.5, ready for radiolabeling were stored at $-20\text{ }^{\circ}\text{C}$ until use. The dose of 1 mg was selected for imaging because optimal accumulation in VEGF-A expressing tumors are obtained at relatively low antibody protein doses.⁽¹³⁾ Upon referral of a patient, a kit was labeled with 100 MBq ^{111}In (Covidien, Petten, The Netherlands). Radiochemical purity of all preparations used in this study exceeded 95%, as determined by instant thin layer chromatography (ITLC). The immunoreactivity was assessed in an ELISA as described previously.⁽¹⁶⁾

Imaging

In the control group, ten days prior to nephrectomy, patients were intravenously injected with 1 mg DTPA-conjugated bevacizumab labeled with 100 MBq ^{111}In within one hour after preparation. A whole-body scan was acquired directly and 7 days after injection, using a double-headed gamma camera (E-Cam, Siemens Inc., Hoffman Estates, IL, USA), equipped with parallel-hole medium-energy collimators (symmetric 15% window over 172 and 247 keV), scan speed 8 cm/min (day 0) and 4 cm/min (day 7). This seven day interval was based on our previous work in which we observed best tumor-to-background ratios in the scans that were acquired 7 days post injection.^{(17), (18)} To allow quantification of antibody targeting to the tumor, a known aliquot of the injected dose in an Adams' phantom was scanned simultaneously. Targeting of the radiolabeled mAb in tumor tissue was determined by comparing the accumulation of the radiolabeled antibody in the renal cell tumors to that in the contralateral kidney. In addition, the targeting of ^{111}In -bevacizumab was scored semi-quantitatively as described previously.⁽¹⁹⁾ In brief, regions of interest were drawn around tumors and the normal kidney on the planar images. ^{111}In -bevacizumab targeting was expressed as the percentage injected dose/tissue weight (as measured on baseline CT), assuming a tissue density of 1.0 g/ml.

Patients underwent nephrectomy 10 days after ^{111}In -bevacizumab administration. After tumornephrectomy, a 1-cm thick slice containing both normal kidney tissue and tumor tissue was obtained from the surgical specimen and distribution of the radiolabeled antibody in the slice was imaged for 45 minutes on the gamma camera after which the slice was cut into 1 cm³ cubicles. The radioactivity in each of the samples was quantified in a well-type gamma counter and thereafter tissue blocks were processed for immunohistochemical analysis.

In the sorafenib treated group, the same imaging procedures were used. Seven days prior to start of sorafenib treatment and after 21 days of treatment ^{111}In -bevacizumab was administered, each time followed by a scintigraphy after 7 days. The sorafenib treatment was discontinued at the day of the last scan. The tumor nephrectomy was performed three days after stop of sorafenib treatment and the tissue was processed as mentioned above for the control patients (**Figure 1.**). After evaluation of the control group, the ^{111}In -bevacizumab scintigraphy directly after administration of the labeled bevacizumab was no longer performed in the sorafenib treated group, because only the blood biodistribution was visualized at these early scans, providing no additional information but did, however, increase the burden to the patients.

Immunohistochemical analysis

Vessel density and VEGF-A expression was determined immunohistochemically in 4- μm formalin fixed and paraffin-embedded sections by staining with anti-CD31 (monoclonal antibody Jc70A, Dako, Glostrup, Denmark) and anti-VEGF monoclonal antibody G153-694 (Pharmingen, San Diego, USA), respectively. An antibody against α -smooth muscle actin (α -SMA, Sigma, Zwijndrecht, The Netherlands) was used for the detection of pericytes as a measure of vessel maturation. To detect CAIX expression, the samples were stained with the anti-CAIX antibody G250 (Wilex AG, München, Germany). As a marker of proliferation Ki67 was stained (clone SP6, Lab Vision Corporation, Fremont, CA, USA). Expression of VEGF-A, CAIX and CD31 were scored semi-quantitatively on a scale ranging from undetectable (-), low (\pm), moderate (+), high (++) to very high (+++).

VEGF-A levels in tumor extracts

In the control group, 10 μm cryosections of each sample of the kidney slice were pooled in RIPA buffer (150 mM NaCl, 10 mM Tris-HCl, pH 7.4, 1 mM EDTA, 1% NP-40, 0.5% sodiumdeoxycholate) containing a protease inhibitors cocktail (Roche, Basel, Switzerland) and heparin (5 U/ml) to release matrix-bound isoforms of VEGF-A. Sections were

homogenized, incubated on ice for 20 minutes and centrifuged (800 g, 20 min, 4 °C) to prepare a clear lysate. The Bradford method (Biorad, Hercules, CA) was used to determine protein concentration. To measure VEGF-A, a four-antibody sandwich ELISA was used which detects all VEGF-A isoforms. ⁽²⁰⁾ Data were expressed as ng VEGF/mg protein for each sample, therefore providing information about the VEGF-A levels in normal kidney tissue as well as in tumor samples.

VEGF-A levels in plasma

In all patients blood samples were collected to determine circulating VEGF-A concentrations prior to injection of ¹¹¹In-bevacizumab. In the sorafenib treated group, a blood sample was also taken after 21 days of treatment with sorafenib, prior to injection of the labeled bevacizumab. Plasma samples were stored at -80 °C within one hour after venipuncture. Plasma concentrations were measured with the four-antibody sandwich ELISA.⁽²⁰⁾ This ELISA measures the unbound VEGF in plasma, which is relevant for the formation of immune complexes with radiolabeled bevacizumab.

Statistics

In the control group, based on the Kolmogorov-Smirnov test and Shapiro-Wilk test, we used the non-parametric 2-tailed Spearman's rho test to analyze the correlation between VEGF-A values and ¹¹¹In-bevacizumab uptake per sample and in each tumor. In the sorafenib treated group, a non-parametric Wilcoxon signed-ranked test was performed to assess the change in ¹¹¹In-bevacizumab uptake in the tumor before and after sorafenib treatment. A 2-tailed paired t-test on log transformed values was used to determine the change in VEGF plasma levels. A p-value < 0.05 was considered significant.

RESULTS

Patients

In the control group, pathological examination of the surgical specimens of all five patients (mean age 61 years; 3 male and 2 female) revealed ccRCC; in one specimen a sarcomatoid component was observed (patient 4). This patient also had pulmonary metastases at presentation. One patient had a synchronous renal oncocytoma (patient 5). (**Table 1**)

Pt	Age (yrs)	G	Type	Diameter (cm)	Volume (cm ³)	%ID/g PRE	%ID/g POST	Δ%	Meta	Necrosis	Mean (range) (ng/mg protein)	VEGF plasma pre	VEGF plasma post	VEGF IHC	G250	CD31	α-SMA	Ki67	
Control patients																			
1	67	M	ccRCC	11.5	622	0.005	NA	NA	Yes	++	5.03 (0.22-18.6)	1.54	NA	+	+	+/-	ND	ND	
2	68	M	ccRCC	5.3	44	0.005	NA	NA	No	+/-	0.87 (0.12-2.71)	1.00	NA	++	+++	+++	ND	ND	
3	61	F	ccRCC	6.0	98	0.028	NA	NA	No	+/-	1.02 (0.19-6.05)	1.39	NA	++	+++	+	+++	++	
4	65	M	Part ccRCC Part sarcomatoid	10.5	462	0.002	NA	NA	Yes	++	5.03 (0.4-21.10)	1.55	NA	++ -	+++ +++	++ +/-	+	+	
5	44	F	ccRCC	4.0	13	0.016	NA	NA	No	+/-	0.25 (0.08-0.41)	0.78	NA	+++	+++	+++	-	+/-	
Patients treated with sorafenib																			
6	64	M	ccRCC	2.1	3.7	0.057	0.006	-90.1	No	+/-	NA	1.67	3.36	+++	++	+	+	5%	
7	59	M	ccRCC	15.8	1104.9	0.009	0.004	-59.7	No	+++	NA	1.83	2.17	+++	++	++	+	5%	
8	78	M	ccRCC	11.3	657.8	0.006	0.005	-21.4	Yes	+++	NA	1.51	2.56	+/-	+/-	-	-	<5%	
9	61	F	ccRCC meta	6.7 3.4	115.2 26.0	0.015 0.034	0.004 0.002	-74.9 -95.1	Yes	++	NA	1.00	1.16	+++	+++	+++	+	<5%	
10	47	M	ccRCC	10.2	486.8	0.004	0.004	+1.5	Yes	+	NA	2.09	1.75	++	++	+	+/-	5%	
11	59	F	ccRCC	6.0	91.6	0.038	0.029	-23.6	No		NA	1.85	-	ND	ND	ND	ND	ND	
12	45	M	ccRCC	7.6	197.7	0.002	0.001	-46.2	Yes	+++	NA	1.47	1.72	+++	+++	+++	+	+	
13	69	M	ccRCC	17.6	1447.5	0.004	ND	-?	Yes		NA	1.37	1.94	+/-	++	+/-	+/-	5-10%	
14	49	M	Papillary RCC	5.0	56.4	0.003	0.002	-8.3	Yes	+	NA	1.15	1.47	++	-	+/-	+	<1%	

Table 1. Patient Characteristics.

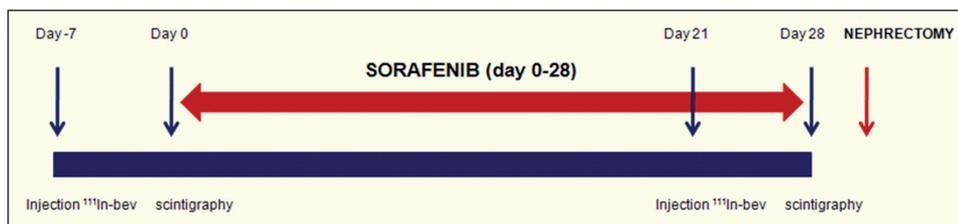


Figure 1. Treatment schedule sorafenib treated group.

Ten patients were included, one of whom was unevaluable as the tumor proved to be not an ccRCC but an oncocytoma. Nine ccRCC patients were treated with sorafenib (2 females, 7 males, median age 61, range 45-78, all ECOG 0-1) after showing enhanced ^{111}In -Bevacizumab accumulation. Pathological examination identified 8 ccRCC and 1 papillary RCC (**Table 1**). Metastases, as assessed on a preoperative CT scan, were found in 6 patients. Neoadjuvant treatment with sorafenib was safe and well tolerated, although 3 patients needed a dose interruption and subsequent dose reduction (200 mg bid), because of grade 3 skin toxicity according to the common toxicity criteria adverse events (CTCAE) 3.0. No additional toxicities were noted after nephrectomy.

Scintigraphic Imaging of RCC with ^{111}In -bevacizumab

Immediately after intravenous injection ^{111}In -bevacizumab distributed in the vascular system and in well perfused organs such as the liver and spleen as judged by ^{111}In -bevacizumab images. The tumors were not visualized on these early images of any of the 14 patients. In all 14 patients, preferential accumulation of ^{111}In -bevacizumab was observed in the tumors 7 days after the injection.

The mean ^{111}In -bevacizumab uptake in ccRCC calculated from the images was 0.015 % injected dose per gram (%ID/g) tumor as quantified at the images (median 0.006 %ID/g, range 0.002-0.028 %ID/g). In patient 4 enhanced accumulation was also observed in the pulmonary metastases (**Table 1**). The scintigraphic images of this patient are shown in **Fig. 2a**. Patient 5, who had a synchronous ccRCC and renal oncocytoma showed only enhanced targeting of the ccRCC. The baseline uptake of ^{111}In -bevacizumab in the papillary RCC was relatively low as compared to the mean baseline uptake in the ccRCC tumors (0.003 vs. 0.019 %ID/g).

In all five control patients, preferential accumulation of ^{111}In -bevacizumab in the tumorous regions was observed, as established by ex vivo scintigraphy of the 1-cm slice taken from the tumorous kidneys. Further quantification of ^{111}In -bevacizumab uptake revealed that the antibody accumulated in areas of viable tumor tissue, while necrotic

Imaging VEGF-A expression in clear cell renal cell carcinoma (ccRCC) with ^{111}In -bevacizumab

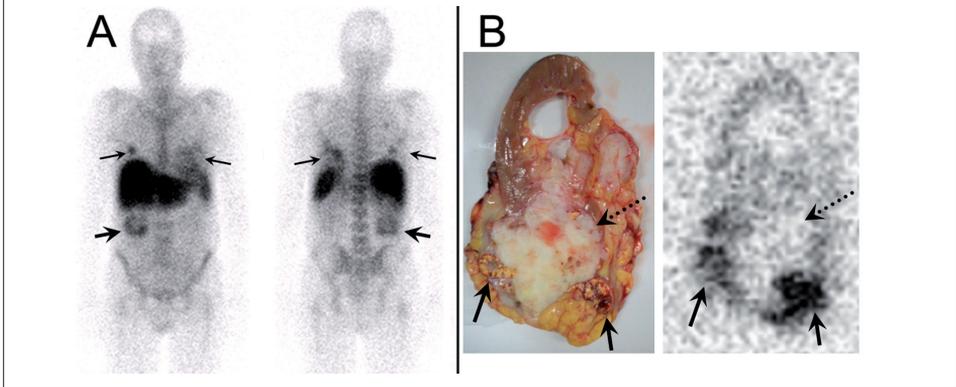


Figure 2a. Anterior and posterior whole body images of patient 4: targeting ccRCC of the right kidney (large arrow) and pulmonary metastases (small arrows); **B.** Macroscopic picture of the slice of patient 4.

Figure 2b. Image of resection specimen showing enhanced VEGF-A targeting of ^{111}In -bevacizumab in the in the ccRCC part of the renal tumor (solid arrows), and decreased uptake in the sarcomatoid part, (dashed arrow) corresponding with the immunohistochemistry results which showed low vessel density in the sarcomatoid part which hampers ^{111}In -bevacizumab delivery.

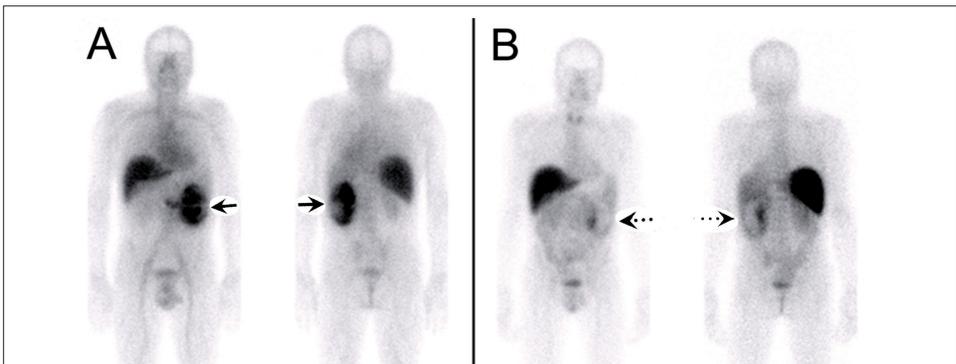


Figure 3. Anterior and posterior ^{111}In -bevacizumab scintigraphy at baseline [A] and after four weeks of treatment with sorafenib [B]. Decrease of ^{111}In -bevacizumab uptake, more enhanced in the central parts of the tumor.

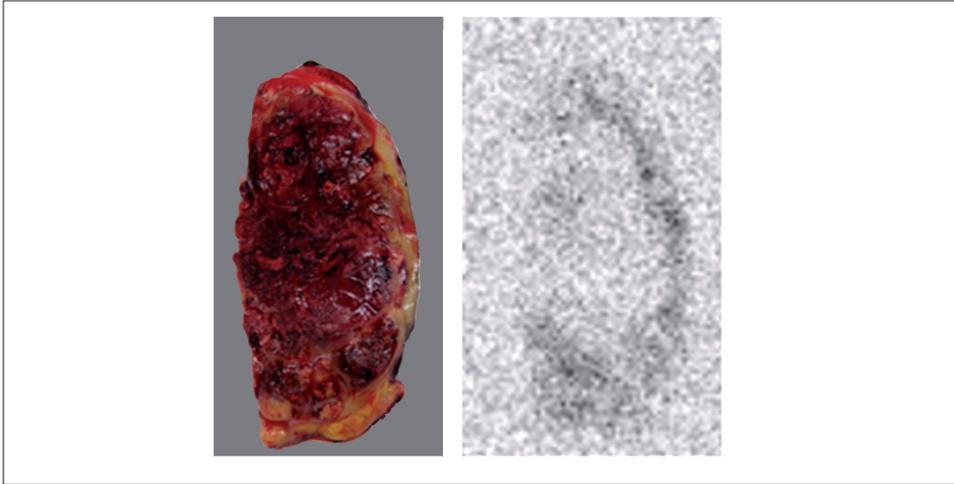


Figure 4. Image of the surgical specimen of patient 7, showing extensive necrosis in almost the whole tumor, except for the more vital borders in which VEGF-A targeting of ^{111}In -bevacizumab is preserved.

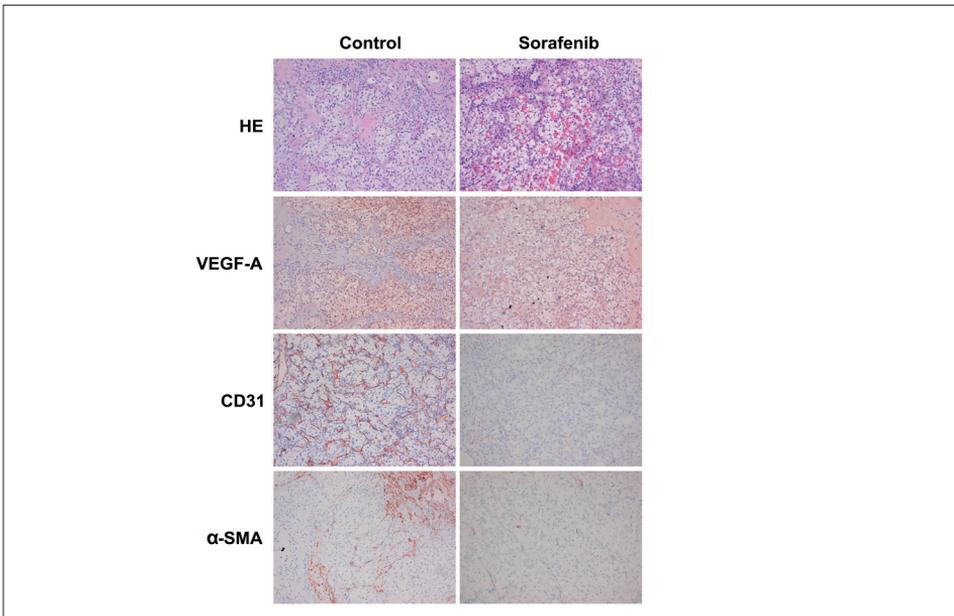


Figure 5. Immunohistochemical analyses. Neoadjuvant treatment with sorafenib results in enhanced necrosis (HE), decreased vessel density (CD31) with excessive loss of young immature vasculature (alpha-SMA). No changes in VEGF-A expression were observed. HE; Haematoxylin and Eosin, alpha-SMA: α -smooth muscle actin, VEGF-A; vascular endothelial growth factor A.

parts showed lower concentrations of the antibody. (**Fig. 2B**) The quantitative values and the measurements of the percentage of the injected dose per gram tumor tissue are summarized in Table 1.

After treatment with sorafenib a significant reduction in ^{111}In -bevacizumab accumulation in the tumors was observed in seven patients with histologically proven ccRCC (mean 0.019 %ID/g vs. 0.007 %ID/g, Table 1, Fig. 3). In one patient only the pretreatment scan was available due to technical problems at the time of the second scan. ^{111}In -bevacizumab targeting did not change in the patient with papillary RCC. In the ccRCC patients, a mean decrease of ^{111}In -bevacizumab uptake of 60.5% was observed (median -46.2%, range +1.5% to -90.1%, $p=0.011$). The pattern of uptake of the ^{111}In -labeled antibody in the tumor slices corresponded well with macroscopic discernable vital and necrotic areas in the tumor, with relatively high uptake in the vital areas and low uptake in the necrotic areas (**Fig. 4**). The overall tumor uptake as derived from the quantitative analysis of the images are shown in Table 1. Tumors resected from sorafenib treated patients contained much larger necrotic areas than tumors of similar size from untreated patients. Only one out of six sorafenib treated patients with metastases had pulmonary metastases larger than 1 cm and was therefore candidate for ^{111}In -bevacizumab uptake evaluation in the metastasis. In this patient the uptake in the metastasis decreased from 0.034 to 0.002 %ID/g tumor (reduction of >95%).

Immunohistochemical analysis

The results of the immunohistochemical analyses of the viable parts of the tumors are presented in Table 1 and Figure 5.

Control group: All ccRCC with enhanced ^{111}In -bevacizumab accumulation stained positive for VEGF-A. The oncocytoma of patient 5, in which no accumulation of ^{111}In -bevacizumab was found, contained minimal amounts of VEGF-A. High expression of VEGF-A was found in viable parts of the tumors, while more necrotic parts and normal kidney tissue only showed limited VEGF-A expression. CAIX expression was high in all viable ccRCC areas. The RCC tumors of patients 2-5 highly expressed CD31 on their vasculature, although not in the sarcomatoid dedifferentiated part of the tumor of patient 4. Low CD31 expression, indicating low vessel density, was observed in the tumor of patient 1.

Sorafenib treated group: All treated tumors expressed VEGF-A. Notably, VEGF-A was also found in necrotic tumor parts. In general, the vessel density was low, as evidenced by low CD31 staining (**Fig. 5**) with a relatively large fraction of the remaining vessels lined with α -SMA positive cells (=mature vessels). The majority of these vessels showed an abnormal aspect with apoptotic cells. All ccRCC were CAIX positive, the papillary RCC was CAIX-negative. Cell proliferation, as judged by Ki67 staining, was low. (**Table 1**)

VEGF analysis

Besides the VEGF staining, we also measured the concentration of VEGF-A in samples of the kidney slices from non-treated patients. The concentration of VEGF-A in these specimens ranged from 0.08-21.10 ng/mg protein (mean 3.67 ng/mg protein). In extracts containing at least 50% vital RCC as estimated on the H&E stained sections of each tumor sample, the mean VEGF-A concentration was 3.24 ng/mg protein (n=40, range 0.12-13.24 ng/mg protein) and in those extracts containing at least 75% vital tumor, the mean VEGF-A concentration was 3.12 ng/mg protein (n=20, range 0.24-7.27 ng/mg protein). Interestingly, in extracts containing a maximum of 20% vital tumor, and thus with a high fraction of necrotic material (>80%), the mean VEGF-A concentration was higher: 5.11 ng/mg protein (n=47, range 0.12-21.10 ng/mg protein). Surprisingly, a negative correlation between the VEGF-A concentration in the tissue extract and the ¹¹¹In-bevacizumab uptake in the tissue cubicles was found (n=89, Spearman ρ r -0.274, p=0.010). This negative correlation was even more significant in a subgroup-analysis when only extracts containing at least 75% viable tumor were analyzed (n=20, r=-0.565, p=0.009). In the samples containing a maximum of 20% viable tumor no correlation between VEGF concentration and ¹¹¹In-bevacizumab uptake was found (n=47, r=-0.231, p=0.119). Accumulation of ¹¹¹In-bevacizumab in within tumors was very heterogeneous and did not correlate with VEGF-A concentration of the same samples (r=0.185, p=0.095). In patients 1 and 4, a negative correlation was found, while patient 2 and 5 showed a positive correlation between VEGF-A concentration and ¹¹¹In-bevacizumab concentration/accumulation.

The mean VEGF plasma level in the control patients was 1.49 ng/ml (range 0.78-2.71 ng/ml). A significant increase in VEGF plasma levels was found after four weeks of treatment with sorafenib (mean 1.55 ng/ml vs. 2.02 ng/ml, p=0.026). There was no correlation between tumor and plasma VEGF-A levels.

DISCUSSION

In the present study, we show that ¹¹¹In-bevacizumab preferentially accumulated in primary RCC and its metastases and that treatment with sorafenib resulted in a dramatic decrease in ¹¹¹In-bevacizumab accumulation, suggesting that sorafenib-induced (vascular) changes are reflected in the reduced accumulation of the radiolabeled antibody.

The reduced uptake of ¹¹¹In-bevacizumab was not the consequence of reduced VEGF-A expression since VEGF-A expression in the RCC lesions was comparable (irrespective of treatment) as evidenced by the immunohistochemical analyses. It is likely that the destruction of the tumor vasculature resulted in decreased ¹¹¹In-bevacizumab delivery and consequently decre-

ased accumulation. We observed extensive necrosis in the tumors after treatment with sorafenib, which was more extensive than observed in untreated RCC tumors of similar size. The macroscopic pattern of viable and necrotic tissue regions corresponded with the intratumoral distribution of ^{111}In -bevacizumab. Immunohistochemical analysis corroborated that the tumor vasculature was greatly altered after sorafenib treatment: a minimal presence of immature vessels was observed, as judged by CD31/ α -SMA staining, and the remaining mature vessels were lined with apoptotic cells. In most tumors, the necrosis was located in the central part of the tumors, while the more vital tumor areas were located at the tumor periphery. The uptake of ^{111}In -bevacizumab in these vital parts of the tumor was not enhanced. There was a three day interval between the ending of sorafenib and the tumor nephrectomy. Therefore, the observed immunohistochemical changes might be not a true reflection of the treatment induced features during sorafenib. However, this interval is short and major changes within this interval are unlikely.

It is important to realize that vascular changes due to treatment with sorafenib are most likely quite dynamic. A time dependent change in tumor vascularization during treatment with anti-angiogenic drugs, starting with normalization of the vasculature and ending with loss of vasculature and necrosis, has been described.⁽²¹⁾ Tumor perfusion would increase temporarily with concomitant enhancement of ^{111}In -bevacizumab uptake. However, at later stages, when necrosis prevails, perfusion is decreased and ^{111}In -bevacizumab uptake will be reduced. Our results strongly suggest that after 4 weeks sorafenib treatment the latter scenario prevails, which was also the case with ^{125}I -cG250 accumulation in a RCC mice model treated with several TKIs, including sorafenib.⁽²²⁾ Multityrosine kinase inhibitors can be given in two approaches: 1) as an anti-angiogenic drug and 2) as a signal transducer inhibitor, focused on optimization of the tumor microenvironment with sustained tumor vasculature normalization and reduced hypoxia in order to enhance combination therapy with for example chemotherapy or radiotherapy.⁽²³⁾ The present study indicates that further investigations focusing on dosing and timing of (combined) treatment and imaging are warranted.

It is interesting to speculate on the observed vascular changes resulting from sorafenib treatment. Sorafenib treatment caused less effects on the more mature and larger tumor vessels. One could hypothesize that these remnant vessels play an important role in acquiring resistance against sorafenib and other angiogenesis inhibitors. Furthermore, this might support sorafenib treatment at an earlier stage of disease, when more immature vessels are present. This is currently under investigation in large adjuvant trials such as the SORCE trial.⁽²⁴⁾

We found a negative correlation between VEGF-A expression and the ^{111}In -bevacizumab concentration in tissue. For ^{111}In -bevacizumab VEGF-A expression, circulating VEGF-A levels, bevacizumab concentrations and tumor delivery of bevacizumab are important parameters that also affect will determine the extent of tumor accumulation. The relatively low VEGF-A

concentrations in samples with at least 75% vital tumor, combined with the high ¹¹¹In-bevacizumab uptake in these samples, suggest that antigen expression is not the major parameter determining bevacizumab accumulation. Other factors, such as tumor vessel characteristics appear to be more important. In earlier studies we have shown that high antigen expression is a prerequisite for high antibody uptake, but that fulfillment of other conditions is equally pivotal to establish high antibody uptake.⁽²⁵⁾ The intratumoral heterogeneity, inpatient differences and the lack of bevacizumab uptake in a benign VEGF-expressing oncocyoma support this notion. Vessel characteristics can influence ¹¹¹In-bevacizumab uptake in two ways: nonspecific accumulation of antibodies due to enhanced vascular permeability, or insufficient delivery of antibodies due to poor vascularization. Studies in nude mice with human tumors did not demonstrate any accumulation when an antigen blocking dose of antibody was co-administered, suggesting that accumulation of bevacizumab in the tumor was antigen-specific.^{(13), (12)} Obviously, it is difficult to extrapolate results obtained in xenografted mice to patients with RCC.

Two other explanations for the negative correlation between VEGF-A levels and uptake of ¹¹¹In-bevacizumab can be considered. First, one could hypothesize that the relatively low bevacizumab dose used in this study (1 mg) could be saturated by circulating VEGF-A (1.49 ng/ml). However, this low antibody protein dose is still more than a 100-fold molar excess as compared to the VEGF concentration in plasma. This molar excess remains after sorafenib induced increases of plasma VEGF-A (mean baseline 1.55 ng/ml vs. mean after sorafenib 2.02 ng/ml). Only 1% of the administered bevacizumab activity could be complexed with plasma VEGF-A. We therefore did not examine immune complex formation. Second, RCC is known to preferentially express VEGF189, VEGF165 and VEGF121.^{(26), (27)} Bevacizumab binds all VEGF isoforms, but tumor accumulation of ¹¹¹In-bevacizumab is mediated by the cell and matrix-bound VEGF-A isoforms; such as VEGF165 and VEGF189.^{(10), (11)} In contrast, the ELISA used to determine VEGF content in the tumor tissue detects all isoforms of VEGF-A, since no isoform specific ELISA was available. Therefore, the freely diffusible VEGF121 can be a disturbing factor. If vital RCC produce relatively high levels of VEGF121 while the VEGF165 and VEGF189 amounts are similar, then this would explain the negative correlation since wash out of immune complexes of bevacizumab and VEGF121 will occur. In the same way, when tumors have lower amounts of VEGF but with relatively high levels of VEGF165 and VEGF189, ¹¹¹In-bevacizumab uptake can be enhanced. The expression patterns of VEGF isoforms within RCC do differ and a relation with tumor histology, tumor growth or stage has been suggested.^{(26), (27), (28), (29)}

The implementation of therapeutics targeting the VEGF pathway with their effects on tumor physiology, and the need for patient stratification, warrants imaging techniques that are able to determine VEGF expression in vivo and that provide functional information. ¹¹¹In-be-

vacizumab scintigraphy could provide functional information about the effect of neoadjuvant treatment with sorafenib in RCC. The next step will be the comparison of ^{111}In -bevacizumab scintigraphy not only to conventional CT scans defining response with the RECIST criteria, but also to new approaches, for example incorporation of (modified) Choi criteria in RCC evaluations ⁽³⁰⁾ or dynamic contrast enhanced MRI (DCE-MRI).⁽³¹⁾

CONCLUSION

In conclusion, ^{111}In -bevacizumab scintigraphy is able to depict RCC lesions. Furthermore, neoadjuvant treatment with sorafenib significantly reduces accumulation of ^{111}In -bevacizumab in RCC lesions. ^{111}In -bevacizumab is an attractive biomarker for clinical response and needs further study.

ACKNOWLEDGEMENTS

The authors would like to thank Gerben Franssen, Lieke Joosten, Mirjam de Weijert and Anneke Geurts-Moespot for their help on the VEGF tumor extracts and Cathy Maass and Gursah Kats for their help on the immunohistochemical stainings.

REFERENCES

- (1) Therasse P, Arbuuck SG, Eisenhauer EA et al. New guidelines to evaluate the response to treatment in solid tumors. European Organization for Research and Treatment of Cancer, National Cancer Institute of the United States, National Cancer Institute of Canada. *J Natl Cancer Inst.* 2000;92(3):205-216.
- (2) Eisenhauer EA, Therasse P, Bogaerts J et al. New response evaluation criteria in solid tumours: revised RECIST guideline (version 1.1). *Eur J Cancer.* 2009;45(2):228-247.
- (3) Desar IM, van Herpen CM, van Laarhoven HW, Barentsz JO, Oyen WJ, van der Graaf WT. Beyond RECIST: Molecular and functional imaging techniques for evaluation of response to targeted therapy. *Cancer Treat Rev.* 2009;35:309-321.
- (4) Takahashi A, Sasaki H, Kim SJ et al. Markedly increased amounts of messenger RNAs for vascular endothelial growth factor and placenta growth factor in renal cell carcinoma associated with angiogenesis. *Cancer Res.* 1994;54(15):4233-4237.
- (5) Turner KJ, Moore JW, Jones A et al. Expression of hypoxia-inducible factors in human renal cancer: relationship to angiogenesis and to the von Hippel-Lindau gene mutation. *Cancer Res.* 2002;62(10):2957-2961.
- (6) Raica M, Cimpean AM, Anghel A. Immunohistochemical expression of vascular endothelial growth factor (VEGF) does not correlate with microvessel density in renal cell carcinoma. *Neoplasma.* 2007;54(4):278-284.
- (7) Ferrara N, Carver-Moore K, Chen H et al. Heterozygous embryonic lethality induced by targeted inactivation of the VEGF gene. *Nature.* 1996;380(6573):439-442.
- (8) Kusters B, de Waal RM, Wesseling P et al. Differential effects of vascular endothelial growth factor A isoforms in a mouse brain metastasis model of human melanoma. *Cancer Res.* 2003;63(17):5408-5413.
- (9) Roodink I, van der LJ, Kusters B et al. Development of the tumor vascular bed in response to hypoxia-induced VEGF-A differs from that in tumors with constitutive VEGF-A expression. *Int J Cancer.* 2006;119(9):2054-2062.
- (10) Hoeben A, Landuyt B, Highley MS, Wildiers H, van Oosterom AT, de Bruijn EA. Vascular endothelial growth factor and angiogenesis. *Pharmacol Rev.* 2004;56(4):549-580.
- (11) Park JE, Keller GA, Ferrara N. The vascular endothelial growth factor (VEGF) isoforms: differential deposition into the subepithelial extracellular matrix and bioactivity of extracellular matrix-bound VEGF. *Mol Biol Cell.* 1993;4(12):1317-1326.
- (12) Nagengast WB, de Vries EG, Hospers GA et al. In vivo VEGF imaging with radiolabeled bevacizumab in a human ovarian tumor xenograft. *J Nucl Med.* 2007;48(8):1313-1319.
- (13) Stollman TH, Scheer MG, Leenders WP et al. Specific imaging of VEGF-A expression with radiolabeled anti-VEGF monoclonal antibody. *Int J Cancer.* 2008;122(10):2310-2314.
- (14) Scheer MG, Stollman TH, Boerman OC et al. Imaging liver metastases of colorectal cancer patients with radiolabelled bevacizumab: Lack of correlation with VEGF-A expression. *Eur J Cancer.* 2008;44(13):1835-1840.
- (15) Brouwers AH, van Eerd JE, Frielink C et al. Optimization of radioimmunotherapy of renal cell carcinoma: labeling of monoclonal antibody cG250 with ¹³¹I, ⁹⁰Y, ¹⁷⁷Lu, or ¹⁸⁶Re. *J Nucl Med.* 2004;45(2):327-337.
- (16) Collingridge DR, Carroll VA, Glaser M et al. The development of [(124)I]iodinated-VG76e: a novel tracer for imaging vascular endothelial growth factor in vivo using positron emission tomography. *Cancer Res.* 2002;62(20):5912-5919.
- (17) Brouwers AH, Buijs WC, Oosterwijk E et al. Targeting of metastatic renal cell carcinoma with the chimeric monoclonal antibody G250 labeled with (¹³¹)I or (¹¹¹)In: an inpatient comparison. *Clin Cancer Res.* 2003;9(10 Pt 2):3953S-3960S.
- (18) Scheer MGW, Stollman TH, Boerman OC et al. Radiolabeled bevacizumab as a tracer of VEGF-expression in patients with colorectal liver metastasis. *Eur J Cancer.* In press.

- (19) Visser E, Postema E, Boerman O, Visschers J, Oyen W, Corstens F. Software package for integrated data processing for internal dose assessment in nuclear medicine (SPRIND). *Eur J Nucl Med Mol Imaging*. 2007;34(3):413-421.
- (20) Span PN, Grebenchtchikov N, Geurts-Moespot J, Westphal JR, Lucassen AM, Sweep CG. EORTC Receptor and Biomarker Study Group Report: a sandwich enzyme-linked immunosorbent assay for vascular endothelial growth factor in blood and tumor tissue extracts. *Int J Biol Markers*. 2000;15(2):184-191.
- (21) Jain RK. Normalization of tumor vasculature: an emerging concept in antiangiogenic therapy. *Science*. 2005;307(5706):58-62.
- (22) Oosterwijk-Wakka JC, Kats-Ugurlu G, Leenders WP et al. Effect of tyrosine kinase inhibitor treatment of renal cell carcinoma on the accumulation of carbonic anhydrase IX-specific chimeric monoclonal antibody cG250. *BJU Int*. 2010.
- (23) Maity A, Bernhard EJ. Modulating Tumor Vasculature through Signaling Inhibition to Improve Cytotoxic Therapy. *Cancer Res*. 2010;70:2141-2145.
- (24) Kapoor A, Gharajeh A, Sheikh A, Pinthus J. Adjuvant and neoadjuvant small-molecule targeted therapy in high-risk renal cell carcinoma. *Curr Oncol*. 2009;16 Suppl 1:S60-S66.
- (25) Steffens MG, Oosterwijk E, Zegwaart-Hagemeier NE et al. Immunohistochemical analysis of intratumoral heterogeneity of [¹³¹I]cG250 antibody uptake in primary renal cell carcinomas. *Br J Cancer*. 1998;78(9):1208-1213.
- (26) Nicol D, Hii SI, Walsh M et al. Vascular endothelial growth factor expression is increased in renal cell carcinoma. *J Urol*. 1997;157(4):1482-1486.
- (27) Tomisawa M, Tokunaga T, Oshika Y et al. Expression pattern of vascular endothelial growth factor isoform is closely correlated with tumour stage and vascularisation in renal cell carcinoma. *Eur J Cancer*. 1999;35(1):133-137.
- (28) Jacobsen J, Grankvist K, Rasmuson T, Ljungberg B. Different isoform patterns for vascular endothelial growth factor between clear cell and papillary renal cell carcinoma. *BJU Int*. 2006;97(5):1102-1108.
- (29) Rivet J, Mourah S, Murata H et al. VEGF and VEGFR-1 are coexpressed by epithelial and stromal cells of renal cell carcinoma. *Cancer*. 2008;112(2):433-442.
- (30) Smith AD, Lieber ML, Shah SN. Assessing tumor response and detecting recurrence in metastatic renal cell carcinoma on targeted therapy: importance of size and attenuation on contrast-enhanced CT. *AJR Am J Roentgenol*. 2010;194(1):157-165.
- (31) Hahn OM, Yang C, Medved M et al. Dynamic contrast-enhanced magnetic resonance imaging pharmacodynamic biomarker study of sorafenib in metastatic renal carcinoma. *J Clin Oncol*. 2008;26(28):4572-4578.

CHAPTER 6

ImmunoPET imaging of renal cell carcinoma with ^{124}I - and ^{89}Zr -labeled anti-CAIX monoclonal antibody cG250 in mice

Alexander B. Stillebroer^{1,2} MD, Gerben M. Franssen¹ BSc, Peter F.A. Mulders² MD PhD, Wim J.G. Oyen¹ MD PhD, Guus A.M.S. van Dongen³ MD PhD, Peter Laverman¹ PhD, Egbert Oosterwijk² PhD, Otto C. Boerman¹ PhD

Departments of Nuclear Medicine¹ and Urology², Radboud University Nijmegen Medical Center, Nijmegen, The Netherlands.

Department of Otolaryngology/Head and Neck Surgery³, VU University Medical Center, Amsterdam, The Netherlands.

Published Cancer Biother Radiopharm. 2013 Sep;28(7):510-5



ABSTRACT

Introduction

Monoclonal antibody (mAb) cG250 recognizes carbonic anhydrase IX (CAIX), overexpressed on clear cell renal cell carcinoma (ccRCC). ^{124}I -cG250 is currently under clinical investigation for the detection of ccRCC. However, the ^{124}I label is rapidly excreted from the tumour cells after internalization of the radiolabeled mAb. We hypothesized that labeling cG250 with the residualizing positron emitter ^{89}Zr would lead to higher tumour uptake and more sensitive detection of ccRCC lesions.

Materials and methods

Nude mice with CAIX-expressing ccRCC xenografts (SK-RC-52 or NU-12) were i.v. injected with ^{89}Zr -cG250 or ^{124}I -cG250. To determine specificity of ^{89}Zr -cG250 uptake in ccRCC, one control group was i.v. injected with ^{89}Zr -MOPC21 (irrelevant mAb). PET images were acquired using a small animal PET camera and the biodistribution of the radiolabeled mAb was determined.

Results

The ccRCC xenografts were clearly visualized after injection of ^{89}Zr -cG250 and ^{124}I -cG250. Tumour uptake of ^{89}Zr -cG250 was significantly higher than that of ^{124}I -cG250 in the NU-12 tumour model (114.7 ± 25.2 % injected dose per gram (%ID/g) vs. 38.2 ± 18.3 %ID/g, $p=0.029$), but in the SK-RC-52 the difference in tumor uptake was not significant (48.7 ± 15.2 %ID/g vs. 32.0 ± 22.9 %ID/g, $p=0.26$). SK-RC-52 tumours were not visualized with ^{89}Zr -MOPC21 (tumour uptake 3.0 %ID/g). Intraperitoneal SK-RC-52 lesions as small as 7 mm³ were visualized with ^{89}Zr -cG250 PET.

Conclusion

ImmunoPET imaging with cG250 visualized s.c. and i.p. ccRCC lesions in murine models. This confirms the potential of cG250 immunoPET in the diagnosis and (re)staging of ccRCC. PET imaging of ccRCC tumours with ^{89}Zr -cG250 could be more sensitive than ^{124}I -cG250-PET.

INTRODUCTION

Renal cell carcinoma (RCC) accounts for 2% of all malignancies and the current treatment for localized disease is tumour nephrectomy. When metastasized, prognosis is bleak with a median survival of 12 months ⁽¹⁾. With the advent of targeted agents (e.g. sunitinib, sorafenib and temsirolimus), it is crucial to adequately diagnose and (re)stage RCC. Considering that a number of patients have long-lasting stable disease without treatment, adequate timing of when to start these treatments is crucial, because considerable toxicities are associated with the use of these targeted agents ⁽²⁾. The preoperative characterization of renal lesions suspect for RCC is difficult with the current radiological techniques. Moreover, since conventional radiological follow-up may not be adequate for response assessment of targeted agents ⁽³⁾, new techniques are warranted to assess biological tumour changes and hence predict the response to treatment.

The diagnosis and (re)staging of RCC is currently performed with conventional radiological techniques, such as computed tomography (CT) or ultrasound. The diagnosis of primary RCC by FDG PET is hampered by the low FDG-avidity of RCC and the physiologic uptake in the normal kidneys due to the renal clearance of the tracer ⁽⁴⁾. FDG PET has been studied in a small number of patients for the detection and follow-up of RCC metastases. Although a high specificity was reported, sensitivity was relatively low and FDG PET is now considered unsuited for staging of patients with RCC ⁽⁴⁾.

Monoclonal antibody (mAb) cG250 has a high affinity for carbonic anhydrase IX (CAIX), a tumour-associated antigen ubiquitously expressed on clear cell RCC (ccRCC) ⁽⁵⁾. The use of cG250 in radioimmunoscinigraphy (RIS) and radioimmunotherapy (RIT) to detect or treat ccRCC has been investigated extensively ⁽⁶⁻¹⁰⁾. A few investigations have studied the capabilities of cG250-based immunoPET, i.e. combining the favorable characteristics of PET (high spatial resolution, three-dimensional (3D) imaging and accurate quantification of tumour uptake) with the high and specific targeting of cG250 to CAIX-expressing cells ⁽¹¹⁻¹³⁾. The relatively slow pharmacokinetics of i.v. injected radiolabeled mAbs (optimal tumour uptake after several days) prevents the use of the most commonly used positron emitters (¹¹C and ¹⁸F) because their half-lives (20 and 110 min, respectively) are too short to be used in immunoPET. The half-lives of the positron emitters ⁸⁹Zr ($T_{1/2} = 78$ h, mean β^+ 397 keV (23% yield), γ 909 keV), and ¹²⁴I ($T_{1/2} = 100$ h, mean β^+ 824 keV (23% yield), γ 603 (63% yield) and 722/1691 keV (10% yield) do match the relatively slow kinetics of antibodies. In a prospective study by Divgi et al. 25 patients with suspect renal lesions scheduled for nephrectomy were studied with ¹²⁴I-cG250. Of sixteen patients with pathologically confirmed ccRCC after surgery, 15 had a positive scan (tumour-to-normal kidney ratio \geq 3:1). The failure in one patient was attributed

to technical problems with the labeled material. The study showed that ^{124}I -cG250 could aid in the preoperative characterization of suspect renal masses and might guide crucial aspects of surgical RCC management ⁽¹¹⁾. A large multicenter trial comparing conventional diagnostic CT to ^{124}I -cG250 immunoPET/CT for the detection of ccRCC in 226 patients scheduled for nephrectomy showed a significantly higher rate of ccRCC detection with ^{124}I -cG250 immunoPET/CT over conventional CT ($p=0.016$) ⁽¹⁴⁾.

We hypothesized that, due to its residualizing characteristics and favourable lower beta-emission, labeling cG250 with ^{89}Zr instead of ^{124}I will lead to higher tumour uptake, higher tumour-to-background (T/B) ratios and higher PET resolution and hence more accurate detection of ccRCC lesions.

Here, we studied the biodistribution of ^{89}Zr -Df-cG250 and ^{124}I -cG250 in nude mice with subcutaneous (s.c.) ccRCC xenografts. FDG PET was used as a reference in this study. The specific targeting of cG250 to ccRCC was assessed by comparing tumour uptake of ^{89}Zr -Df-cG250 and an irrelevant control mAb. The feasibility of ^{89}Zr -immuno-PET with ^{89}Zr -Df-cG250 was studied in mice with intraperitoneally growing ccRCC tumours.

Materials and methods

Chimeric monoclonal antibody G250. The isolation and immunohistochemical reactivity of mAb G250 have been described elsewhere ⁽¹⁵⁾. To reduce the immunogenicity of the murine form of G250, a chimeric version (cG250) has been developed ⁽¹⁰⁾. MAb cG250 IgG1 is reactive with the transmembrane glycoprotein carbonic anhydrase isoenzyme IX ($K_a = 4 \times 10^9 \text{ M}^{-1}$). Expression on the cell surface of ccRCC cells is ubiquitous (>95%), whereas expression on normal tissues is restricted to the epithelial structures of the upper gastrointestinal tract and larger bile ducts ⁽¹⁶⁾.

Murine monoclonal antibody MOPC21. MOPC21 is a myeloma-produced murine IgG1 mAb (Sigma-Aldrich, Zwijndrecht, The Netherlands) which is not directed against any known antigen and was used as an isotype control mAb to investigate the specificity of uptake of mAb cG250 in CAIX-positive ccRCC xenografts.

Conjugation, radiolabeling and quality control. For ^{89}Zr labeling, cG250 and MOPC21 were conjugated with desferal (Df) essentially as described previously ⁽¹⁷⁾. Briefly, desferal (Novartis Pharma AG, Bern, Switzerland) was succinylated, temporarily filled with Fe^{3+} and coupled to the mAb via the tetrafluorophenolester of Df. After the conjugation of Df to the mAb and removal of the Fe^{3+} , the Df-conjugated mAb was labeled with ^{89}Zr (IBA Pharma, Leuven, Belgium) during 30 minutes in 0.25 M HEPES buffer, at pH 7.3 at 37 °C. The ^{89}Zr -Df-cG250 and ^{89}Zr -Df-MOPC21 were purified on a PD10 column (Amersham Pharmacia Biotech, Uppsala, Sweden), that was eluted with 0.9% NaCl, 5 mg/mL gentisic acid, pH 5.0. The specific activity of ^{89}Zr -Df-cG250 was 0.41 MBq/ μg or 0.54 MBq/ μg .

Radioiodination of cG250 with ^{124}I (IBA Pharma, Leuven, Belgium) was performed according to the Iodogen method ⁽¹⁰⁾. The ^{124}I -cG250 was purified on a PD-10 column that was eluted with 0.5 M PBS. Specific activity of ^{124}I -cG250 was 0.24 MBq/ μg or 1.7 MBq/ μg . Labeling efficiency was between 55 and 70% (^{89}Zr -Df-cG250/MOPC21) and between 73 and 82% (^{124}I -cG250). After purification, at the time of i.v. injection, instant thin layer chromatography showed a radiochemical purity of > 95% of all preparations used in the studies. The immunoreactive fraction at infinite antigen excess of all radiolabeled cG250 preparations was determined on freshly trypsinized SK-RC-52 RCC cells essentially as described by Lindmo et al. ⁽¹⁸⁾. The immunoreactive fraction of ^{89}Zr -Df-cG250 was between 75% and 89% and the immunoreactive fractions of all ^{124}I -cG250 preparations exceeded 83%.

RCC tumours in nude mice. The ccRCC cell lines SK-RC-52 (CAIX-positive) and SK-RC-59 (CAIX-negative) were derived from metastases of primary ccRCC patients as described by Ebert et al ⁽¹⁹⁾. To induce s.c. tumours, $2\text{-}3 \cdot 10^6$ cells were injected subcutaneously in the flank of 6-8 weeks old male BALB/c nu/nu mice and tumours were established after 2-3 weeks. To obtain intraperitoneally growing SK-RC-52 lesions, $2\text{-}3 \cdot 10^6$ SK-RC-52 cells were injected intraperitoneally and after 3 weeks multiple tumour nodules were found in the abdominal cavity. The ccRCC cell line NU-12 (CAIX-positive) was derived from a primary ccRCC ⁽²⁰⁾ and tumours were noted 6-8 weeks after serial s.c. transplantation. Animals were housed and fed according to the Dutch animal welfare regulations. Experiments were approved by the Institutional Animal Care and Use Committee of the Radboud University Nijmegen Medical Center, and were performed in accordance with their guidelines.

MicroPET imaging. Mice with s.c. SK-RC-52 tumours were i.v. injected with 12.3 MBq ^{89}Zr -Df-cG250/MOPC21 (30 μg) or 7.2 MBq ^{124}I -cG250 (30 μg) ⁽²¹⁾. Mice with s.c. NU-12 tumours were i.v. injected with 1.5 MBq ^{89}Zr -Df-cG250 (3 μg) or 5.1 MBq ^{124}I -cG250 (3 μg) ⁽²¹⁾. Mice injected with FDG (IBA, Amsterdam, The Netherlands) received 10 MBq. PET images were acquired with a dedicated animal PET/CT scanner (Inveon, Siemens Preclinical Solutions, Knoxville, TN) with an intrinsic spatial resolution of 1.5 mm. Mice were placed in a prone (experiments 1 and 2) or supine (experiment 3) position in the scanner and body temperature was maintained at 37 °C using a warmed mattress (M2M imaging Inc, Cleveland, OH). Scans were reconstructed using Inveon Acquisition Workplace software version 1.2 (Siemens Preclinical Solutions, Knoxville, TN). PET reconstruction was performed using an ordered subset expectation maximization-3D/maximum a posteriori (OSEM3D/MAP) algorithm ⁽²²⁾. All animals were gas-anesthetized with a mixture of nitrous oxide/oxygen/isoflurane. Before intravenous injection of FDG, mice were fasted 6 hours. Emission images after injection of FDG were acquired 1 h p.i. CT images were ac-

quired with the same Inveon animal PET/CT scanner (80 kV, 500 μ A, exposure time 300 msec, 360° rotation in 180 steps, 0.5 mm aluminum filter). Scans were reconstructed using COBRA software version 6 (Exxim Computing Corporation, Pleasanton, USA). CT acquisition was performed 7 days after injection of ^{89}Zr -Df-cG250, ^{89}Zr -Df-MOPC21 and ^{124}I -cG250, or 1 h after injection of [^{18}F]FDG.

At the end of the experiments (1 h p.i. of FDG or 7 days p.i. of ^{89}Zr -Df-cG250, ^{89}Zr -Df-MOPC21 and ^{124}I -cG250) mice were euthanized and the biodistribution of the radiolabel was determined. Tumour and samples of normal tissues (blood, muscle, lung, spleen, kidney, liver, small intestine, stomach and thyroid) were dissected, weighed and counted in a γ -counter (1480 Wizard 3", LKB/Wallace, Perkin-Elmer, Boston, MA). Injection standards were counted simultaneously to correct for radioactive decay.

Biodistribution studies. Biodistribution of ^{89}Zr -Df-cG250 and ^{124}I -cG250 was studied in mice with either a s.c. SK-RC-52 or NU-12 tumour using FDG as reference. Six groups of mice were studied, with 3 groups bearing a s.c. SK-RC-52 tumour and 3 groups bearing a s.c. NU-12 tumour. Groups consisted of 6 mice and were injected with ^{89}Zr -Df-cG250, ^{124}I -cG250 or FDG (1.5 – 12.3 MBq/mouse).

The specificity of cG250-targeting to CAIX-expressing ccRCC tumours was evaluated in two groups of mice with a s.c. SK-RC-52 tumour (CAIX-positive) in the left flank and a s.c. SK-RC-59 tumour (CAIX-negative) in the right flank. One group of mice received ^{89}Zr -Df-cG250 (12.3 MBq/mouse), the other group received ^{89}Zr -Df-MOPC21 (12.3 MBq/mouse). To determine immunoPET imaging of intraperitoneally growing ccRCC lesions 6 mice with i.p. SK-RC-52 tumours were injected with ^{89}Zr -Df-cG250 (16.2 MBq/mouse).

Statistical analysis. Statistical analysis was performed using the non-parametric repeated measures one-way analysis of variance (ANOVA). Differences were considered significant when $p < 0.05$, two-sided. All values are expressed as mean \pm standard deviation (s.d.).

Results

The biodistribution of ^{89}Zr -Df-cG250 and ^{124}I -cG250 7 days after injection in mice with CAIX-expressing ccRCC tumours is summarized in **Figure 1**. In the NU-12 tumour model tumour uptake of ^{89}Zr -Df-cG250 was significantly higher than that of ^{124}I -cG250 (114.7 ± 25.2 %ID/g vs. 38.2 ± 18.3 %ID/g, respectively, $p=0.029$) (Figure 1a), whereas in the SK-RC-52 tumour model uptake of ^{89}Zr -Df-cG250 and ^{124}I -cG250 was similar (48.7 ± 15.2 %ID/g vs. 32.0 ± 22.9 %ID/g, respectively, $p=0.257$) (**Figure 1b**). When comparing the biodistribution of ^{89}Zr -Df-cG250 with that of ^{124}I -cG250, uptake of ^{89}Zr -Df-cG250 was higher in liver ($p<0.001$) and spleen ($p<0.001$) and uptake of ^{124}I was higher in the thyroid ($p<0.001$) in both models. Uptake of the two cG250 preparations in other organs did

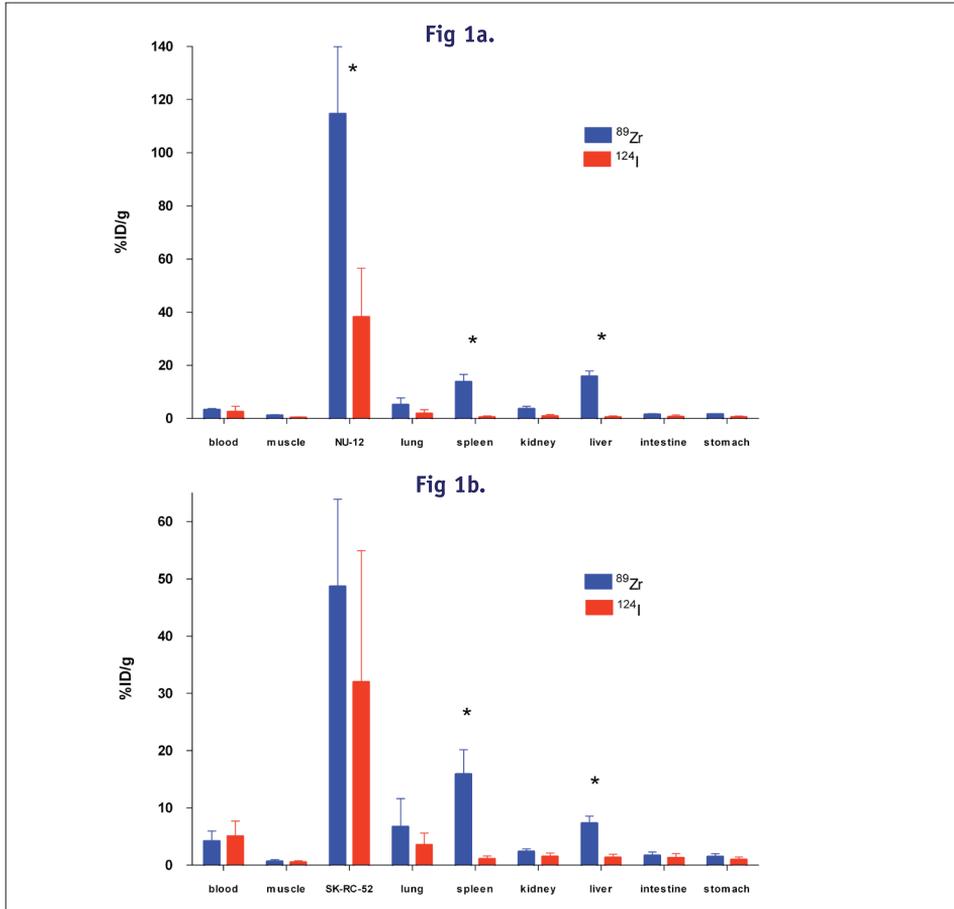


Figure 1. Biodistribution of ^{89}Zr -Df-cG250 and ^{124}I -cG250 in mice with a s.c. NU-12 tumour (**Figure 1a.**) or a s.c. SK-RC-52 tumour (**Figure 1b.**), 7 days p.i. Values are expressed as mean \pm s.d. Antibody dosing was $3\mu\text{g}$ cG250/mouse in NU-12 and $30\mu\text{g}$ cG250/mouse in SK-RC-52 tumours. Significant differences ($p < 0.05$) in uptake between ^{89}Zr -Df-cG250 and ^{124}I -cG250 are marked with an asterisk*.

not differ significantly. PET images of mice injected with ^{89}Zr -Df-cG250 and ^{124}I -cG250 is shown in **Figure 2**. Tumours were visualized from day 1 onwards with both radiolabeled antibody preparations and optimal image contrast was seen day 7 p.i. The physical characteristics of ^{124}I caused more noisy and lower contrast images. Uptake of FDG in the NU-12 and SK-RC-52 tumours was relatively low (2.7 ± 0.5 %ID/g vs. 5.7 ± 3.9 %ID/g) and both tumours were not visualized on PET images since uptake in the tumour was similar to that in surrounding tissues (results not shown).

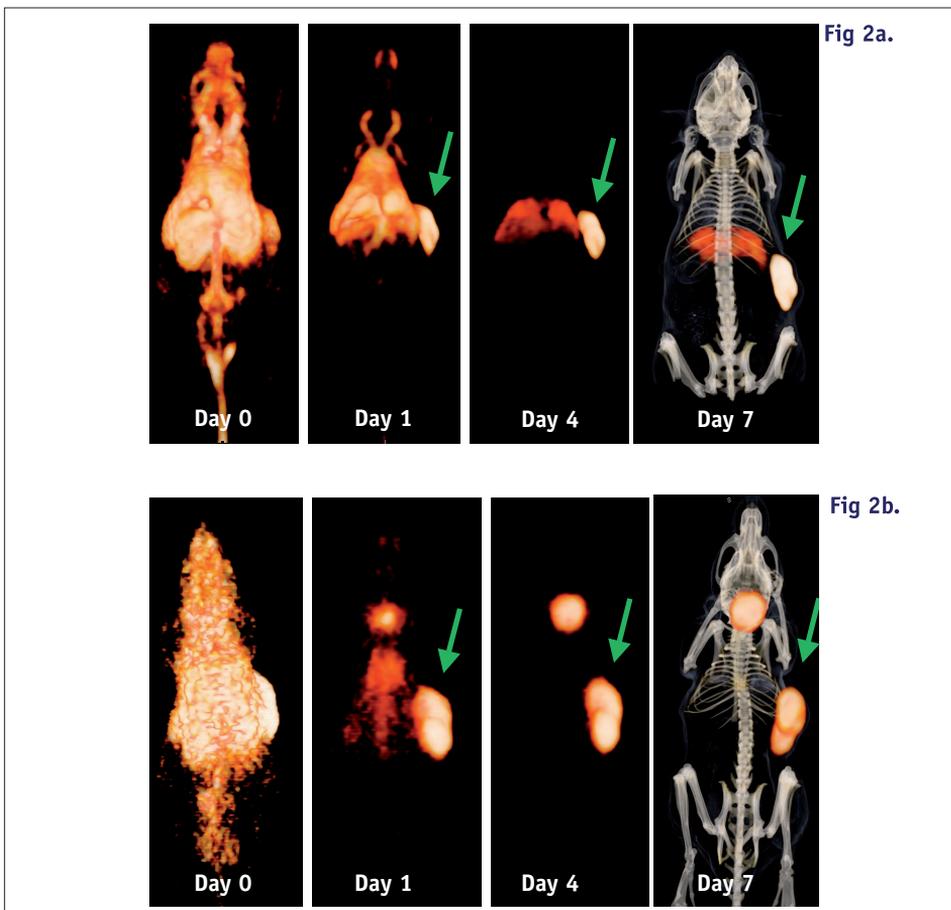


Figure 2. 3D reconstructed PET images of representative mice with a s.c. NU-12 tumour on the right flank 0, 1 and 4 days after injection and fused PET/CT images after 7 days of ^{89}Zr -Df-cG250 (**Figure 2a.**) or ^{124}I -cG250 (**Figure 2b.**). Antibody dosing was $3\mu\text{g}$ cG250/mouse. Note the clear visualization of the s.c. tumour (green arrows) from day 1 p.i. onwards with both radio-labeled mAbs.

The biodistribution of ^{89}Zr -Df-cG250 and ^{89}Zr -Df-MOPC21 7 days p.i. were compared to determine the specificity of cG250 localization in CAIX-positive tumours (**Figure 3a**). Uptake of ^{89}Zr -Df-cG250 in the CAIX-positive SK-RC-52 tumour was high (36.5 ± 6.2 %ID/g), whereas the uptake was significantly lower in the CAIX-negative SK-RC-59 tumour (6.7 ± 1.4 %ID/g, $p=0.029$). Uptake of ^{89}Zr -Df-cG250 and ^{89}Zr -Df-MOPC21 differed significantly in the CAIX-positive SK-RC-52 tumour (36.5 ± 6.2 %ID/g vs. 6.8 ± 2.3 %ID/g, $p=0.010$), indicating that the uptake of ^{89}Zr -Df-cG250 in the CAIX-positive tumour was due to the affinity of the cG250

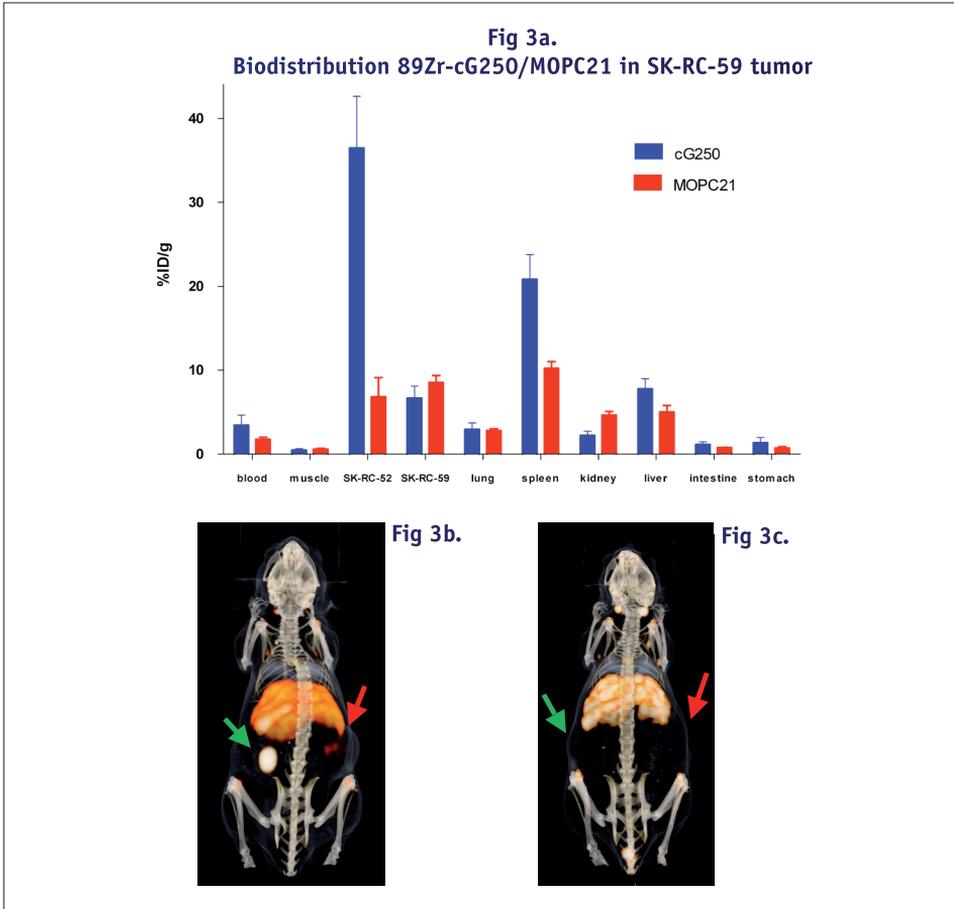


Figure 3. Biodistribution 7 days after injection of ^{89}Zr -Df-cG250 or ^{89}Zr -Df-MOPC21 in mice with a s.c. SK-RC-52 tumour and a s.c. SK-RC-59 tumour (**Figure 3a.**). Values are expressed as mean \pm s.d. Antibody dosing was $30\mu\text{g}$ cG250/mouse ^{89}Zr -Df-cG250 (**Figure 3b.**) or ^{89}Zr -Df-MOPC21 (**Figure 3c.**) in representative mice with a s.c. SK-RC-52 tumour on the left flank and a s.c. SK-RC-59 tumour on the right flank. Note the high uptake of ^{89}Zr -Df-cG250 in the SK-RC-52 tumour (green arrow), which is not seen in the SK-RC-59 tumour (red arrow). No specific uptake in both tumours is noted after injection with ^{89}Zr -Df-MOPC21.

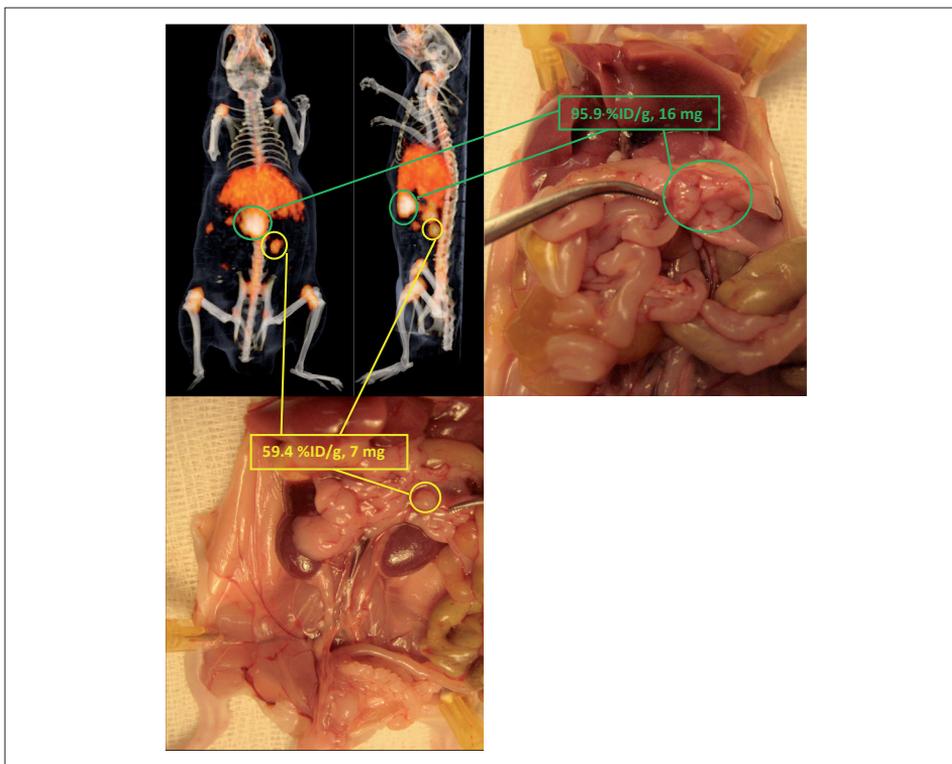


Figure 4. Upper panels: coronal and sagittal sections of a 3D reconstructed PET/CT image 7 days after injection of ^{89}Zr -Df-cG250 (left) and anatomical localization of an SK-Rc-52 lesion (green circles) upon dissection with an uptake of 95.9 %ID/g, weight 16 mg (right). Lower image: localization of another SK-Rc-52 lesion (yellow circles) with 59.4 %ID/g uptake, weight 7 mg. Antibody dosing was $30\mu\text{g}$ cG250/mouse.

antibody for CAIX. PET images of mice with s.c. SK-Rc-52 and SK-Rc-59 tumours injected with ^{89}Zr -Df-MOPC21 or ^{89}Zr -Df-cG250 are shown in Figure 3b. The CAIX-positive SK-Rc-52 tumour was clearly visualized with ^{89}Zr -Df-cG250 on day 7 p.i. The CAIX-negative SK-Rc-59 tumour was not visualized with ^{89}Zr -Df-cG250. None of the s.c. tumours was visualized with the irrelevant mAb ^{89}Zr -Df-MOPC21. These results demonstrate the specific localization of ^{89}Zr -Df-cG250 in CAIX-positive tumours.

Intraperitoneally growing SK-Rc-52 tumours were clearly visualized 7 days after injection of ^{89}Zr -Df-cG250 as shown in **Figure 4**. Tumour lesions as small as 7 mg in the vicinity of the liver and spleen were clearly visualized and uptake in individual lesions was as high as up to 95.9 %ID/g. All tumour lesions that were identified with PET were identified during dissection.

DISCUSSION

The biodistribution profiles of ^{89}Zr -Df-cG250 and ^{124}I -cG250 in nude mice with s.c. ccRCC xenografts were compared to determine the optimal radionuclide for immunoPET with cG250. In both CAIX-positive ccRCC xenografts uptake of ^{89}Zr -Df-cG250 was higher than uptake of ^{124}I -cG250 7 days after injection of the radiolabeled mAbs, albeit this difference was only statistically significant in the NU-12 tumour model. In this study, mice were not stratified to groups according to size of the tumour xenograft. The group bearing a SK-RC-52 xenograft injected with ^{124}I -cG250 consisted of mice with large differences in tumour size (results not shown), evidenced by the large standard deviation in tumour uptake of this group. This could explain why uptake of ^{89}Zr -Df-cG250 was not significantly higher than ^{124}I -cG250 in the SK-RC-52 tumour model. PET images acquired with a dedicated small animal PET camera showed preferential tumour uptake of both radiolabeled mAbs from day 1 p.i. onwards and image contrast improved with time. The images obtained with ^{89}Zr -Df-cG250 had less noise and higher contrast, allowing for more specific detection of ccRCC lesions with ^{89}Zr -Df-cG250 as compared to ^{124}I -cG250. The brightness and contrast settings of the ^{89}Zr -Df-cG250-images in Figure 2 have been chosen specifically to show the uptake in the liver for anatomical reference. Moreover, since uptake of ^{89}Zr -Df-cG250 in ccRCC lesions was higher than that of ^{124}I -cG250, immunoPET imaging of ccRCC with ^{89}Zr -Df-cG250 in these models was superior to immunoPET with ^{124}I -cG250.

The enhanced uptake of ^{89}Zr -Df-cG250 as compared to ^{124}I -cG250 in the NU-12 ccRCC tumour model is most likely due to the residualizing properties of the ^{89}Zr radiolabel. Internalized radiolabeled antibody is metabolized in the tumor cell lysosomes and the ^{124}I -labeled metabolite (^{124}I -tyrosine) is rapidly excreted from the tumor cell, whereas the metabolite labeled with metallic radionuclides, such as ^{111}In , ^{89}Zr and ^{177}Lu , is trapped in the lysosomes (23-25). This phenomenon has also been described in a clinical inpatient comparison study examining the differences between ^{131}I -cG250 and ^{111}In -cG250. Five mRCC patients were injected with ^{131}I -cG250 and ^{111}In -cG250 one week apart. Uptake of ^{111}In -cG250 in ccRCC tumour lesions was higher than that of ^{131}I -cG250, which was attributed to the intracellular entrapment of internalized ^{111}In -cG250 metabolites (7). This could also explain the higher liver and spleen uptake of ^{89}Zr -Df-cG250 as compared to that of ^{124}I -cG250 (26;27).

FDG PET has a poor sensitivity for detecting RCC lesions mainly due to the fact that many RCC lesions are not FDG-avid (4). This was also observed in the present study: none of the CAIX-positive ccRCC xenografts were visualized by FDG PET, since uptake of FDG was similar to that in surrounding tissues. In an earlier study, FDG failed to visualize ccRCC xenografts in nude rats (12). ImmunoPET with cG250 could therefore be of value as a functional imaging technique to detect ccRCC lesions.

The high tumour uptake of ^{89}Zr -Df-cG250 and ^{124}I -cG250 was the result of specific uptake of

cG250 in the CAIX-positive tumours. The irrelevant mAb ^{89}Zr -Df-MOPC21 did not accumulate in the CAIX-positive tumour SK-RC-52, demonstrating that accretion was not the consequence of aberrant tumour perfusion, but antigen-driven. ^{89}Zr -Df-cG250 accumulated in the CAIX-positive tumour, but not in the CAIX-negative tumour, further demonstrating that accretion was antigen-driven.

ImmunoPET with cG250 is well suited for imaging ccRCC in patients since PET has the advantage of producing 3D images with a much higher resolution than planar scintigraphy or single photon emission computed tomography (SPECT). This is illustrated by the very sensitive detection of ccRCC lesions with a dedicated small animal PET camera. Intraperitoneal lesions as small as 7 mm^3 were visualized with ^{89}Zr -Df-cG250 and could easily be discriminated from the liver and spleen. Preoperative characterization of renal masses with cG250 immuno-PET might be useful in the clinical management of RCC patients ⁽¹¹⁾. The results from this study suggest that immunoPET in RCC patients may be improved by using ^{89}Zr -Df-cG250 instead of ^{124}I -cG250.

CONCLUSIONS

Our results indicate that uptake of ^{89}Zr -Df-cG250 in ccRCC xenografts was higher than uptake of ^{124}I -cG250. The higher specific uptake of ^{89}Zr -Df-cG250 produced higher PET image contrast, despite higher uptake in various normal tissues, such as the liver and spleen. PET imaging of ccRCC tumours with ^{89}Zr -cG250 could be more sensitive than ^{124}I -cG250-PET. Small intraperitoneal ccRCC lesions could be visualized and easily discriminated from the liver and the spleen with cG250-based immunoPET.

Acknowledgements

MAB cG250 was a kind donation of Dr. P. Bevan (Wilex AG, München, Germany). The authors wish to thank B. Lemmers-van de Weem and K. Lemmens-Hermans for their assistance in the animal experiments. This work was supported by a grant of the Dutch Cancer Foundation (KWF grant KUN 2005-3339).

REFERENCES

- (1) Jemal A, Siegel R, Ward E, Hao Y, Xu J, Thun MJ. Cancer statistics, 2009. *CA Cancer J Clin* 2009 July;59(4):225-49.
- (2) Hartmann JT, Haap M, Kopp HG, Lipp HP. Tyrosine kinase inhibitors - a review on pharmacology, metabolism and side effects. *Curr Drug Metab* 2009 August;10(5):470-81.
- (3) Griffin N, Gore ME, Sohaib SA. Imaging in metastatic renal cell carcinoma. *AJR Am J Roentgenol* 2007 August;189(2):360-70.
- (4) Powles T, Murray I, Brock C, Oliver T, Avril N. Molecular positron emission tomography and PET/CT imaging in urological malignancies. *Eur Urol* 2007 June;51(6):1511-20.
- (5) Grabmaier K, Vissers JL, De Weijert MC, Oosterwijk-Wakka JC, Van BA, Brakenhoff RH, Noessner E, Mulders PA, Merckx G, Figdor CG, Adema GJ, Oosterwijk E. Molecular cloning and immunogenicity of renal cell carcinoma-associated antigen G250. *Int J Cancer* 2000 March 15;85(6):865-70.
- (6) Brouwers AH, van Eerd JE, Frielink C, Oosterwijk E, Oyen WJ, Corstens FH, Boerman OC. Optimization of radioimmunotherapy of renal cell carcinoma: labeling of monoclonal antibody cG250 with ¹³¹I, ⁹⁰Y, ¹⁷⁷Lu, or ¹⁸⁶Re. *J Nucl Med* 2004 February;45(2):327-37.
- (7) Brouwers AH, Buijs WC, Oosterwijk E, Boerman OC, Mala C, De Mulder PH, Corstens FH, Mulders PF, Oyen WJ. Targeting of metastatic renal cell carcinoma with the chimeric monoclonal antibody G250 labeled with (¹³¹I or (¹¹¹In): an inpatient comparison. *Clin Cancer Res* 2003 September 1;9(10 Pt 2):3953S-60S.
- (8) Brouwers AH, Mulders PF, De Mulder PH, van den Broek WJ, Buijs WC, Mala C, Joosten FB, Oosterwijk E, Boerman OC, Corstens FH, Oyen WJ. Lack of efficacy of two consecutive treatments of radioimmunotherapy with ¹³¹I-cG250 in patients with metastasized clear cell renal cell carcinoma. *J Clin Oncol* 2005 September 20;23(27):6540-8.
- (9) Steffens MG, Boerman OC, De Mulder PH, Oyen WJ, Buijs WC, Witjes JA, van den Broek WJ, Oosterwijk-Wakka JC, Debruyne FM, Corstens FH, Oosterwijk E. Phase I radioimmunotherapy of metastatic renal cell carcinoma with ¹³¹I-labeled chimeric monoclonal antibody G250. *Clin Cancer Res* 1999 October;5(10 Suppl):3268s-74s.
- (10) Steffens MG, Boerman OC, Oosterwijk-Wakka JC, Oosterhof GO, Witjes JA, Koenders EB, Oyen WJ, Buijs WC, Debruyne FM, Corstens FH, Oosterwijk E. Targeting of renal cell carcinoma with iodine-131-labeled chimeric monoclonal antibody G250. *J Clin Oncol* 1997 April;15(4):1529-37.
- (11) Divgi CR, Pandit-Taskar N, Jungbluth AA, Reuter VE, Gonen M, Ruan S, Pierre C, Nagel A, Pryma DA, Humm J, Larson SM, Old LJ, Russo P. Preoperative characterisation of clear-cell renal carcinoma using iodine-124-labelled antibody chimeric G250 (¹²⁴I-cG250) and PET in patients with renal masses: a phase I trial. *Lancet Oncol* 2007 April;8(4):304-10.
- (12) Brouwers A, Verel I, Van EJ, Visser G, Steffens M, Oosterwijk E, Corstens F, Oyen W, Van DG, Boerman O. PET radioimmunoscintigraphy of renal cell cancer using ⁸⁹Zr-labeled cG250 monoclonal antibody in nude rats. *Cancer Biother Radiopharm* 2004 April;19(2):155-63.
- (13) Lawrentschuk N, Lee FT, Jones G, Rigopoulos A, Mountain A, O'Keefe G, Papenfuss AT, Bolton DM, Davis ID, Scott AM. Investigation of hypoxia and carbonic anhydrase IX expression in a renal cell carcinoma xenograft model with oxygen tension measurements and (¹²⁴I)-cG250 PET/CT. *Urol Oncol* 2009 June 11.
- (14) Divgi CR, Uzzo RG, Gatsonis C, Bartz R, Treutner S, Yu JQ, Chen D, Carrasquillo JA, Larson S, Bevan P, Russo P. Positron emission tomography/computed tomography identification of clear cell renal cell carcinoma: results from the REDECT trial. *J Clin Oncol*. 2013 Jan 10; 31(2).
- (15) Oosterwijk E, Ruiter DJ, Hoedemaeker PJ, Pauwels EK, Jonas U, Zwartendijk J, Warnaar SO. Monoclonal antibody G 250 recognizes a determinant present in renal-cell carcinoma and absent from normal kidney. *Int J Cancer* 1986 October 15;38(4):489-94.
- (16) Thiry A, Dogne JM, Masereel B, Supuran CT. Targeting tumor-associated carbonic anhydrase IX in cancer

- therapy. *Trends Pharmacol Sci* 2006 November;27(11):566-73.
- (17) Verel I, Visser GW, Boellaard R, Stigter-van WM, Snow GB, van Dongen GA. 89Zr immuno-PET: comprehensive procedures for the production of 89Zr-labeled monoclonal antibodies. *J Nucl Med* 2003 August;44(8):1271-81.
 - (18) Lindmo T, Boven E, Cuttitta F, Fedorko J, Bunn PA, Jr. Determination of the immunoreactive fraction of radiolabeled monoclonal antibodies by linear extrapolation to binding at infinite antigen excess. *J Immunol Methods* 1984 August 3;72(1):77-89.
 - (19) Ebert T, Bander NH, Finstad CL, Ramsawak RD, Old LJ. Establishment and characterization of human renal cancer and normal kidney cell lines. *Cancer Res* 1990 September 1;50(17):5531-6.
 - (20) Beniers AJ, Peelen WP, Schaafsma HE, Beck JL, Ramaekers FC, Debruyne FM, Schalken JA. Establishment and characterization of five new human renal tumor xenografts. *Am J Pathol* 1992 February;140(2):483-95.
 - (21) Kranenborg MH, Boerman OC, De Weijert MC, Oosterwijk-Wakka JC, Corstens FH, Oosterwijk E. The effect of antibody protein dose of anti-renal cell carcinoma monoclonal antibodies in nude mice with renal cell carcinoma xenografts. *Cancer* 1997 December 15;80(12 Suppl):2390-7.
 - (22) Visser EP, Disselhorst JA, Brom M, Laverman P, Gotthardt M, Oyen WJ, Boerman OC. Spatial resolution and sensitivity of the Inveon small-animal PET scanner. *J Nucl Med* 2009 January;50(1):139-47.
 - (23) Sharkey RM, Behr TM, Mattes MJ, Stein R, Griffiths GL, Shih LB, Hansen HJ, Blumenthal RD, Dunn RM, Juweid ME, Goldenberg DM. Advantage of residualizing radiolabels for an internalizing antibody against the B-cell lymphoma antigen, CD22. *Cancer Immunol Immunother* 1997 May;44(3):179-88.
 - (24) Shih LB, Thorpe SR, Griffiths GL, Diril H, Ong GL, Hansen HJ, Goldenberg DM, Mattes MJ. The processing and fate of antibodies and their radiolabels bound to the surface of tumor cells in vitro: a comparison of nine radiolabels. *J Nucl Med* 1994 May;35(5):899-908.
 - (25) Press OW, Shan D, Howell-Clark J, Eary J, Appelbaum FR, Matthews D, King DJ, Haines AM, Hamann P, Hinman L, Shochat D, Bernstein ID. Comparative metabolism and retention of iodine-125, yttrium-90, and indium-111 radioimmunoconjugates by cancer cells. *Cancer Res* 1996 May 1;56(9):2123-9.
 - (26) Perk LR, Vosjan MJ, Visser GW, Budde M, Jurek P, Kiefer GE, van Dongen GA. p-Isothiocyanatobenzyl-desferrioxamine: a new bifunctional chelate for facile radiolabeling of monoclonal antibodies with zirconium-89 for immuno-PET imaging. *Eur J Nucl Med Mol Imaging* 2009 September 18.
 - (27) Verel I, Visser GW, Boellaard R, Boerman OC, Van EJ, Snow GB, Lammertsma AA, van Dongen GA. Quantitative 89Zr immuno-PET for in vivo scouting of ⁹⁰Y-labeled monoclonal antibodies in xenograft-bearing nude mice. *J Nucl Med* 2003 October;44(10):1663-70.

CHAPTER 7

Optical imaging of Renal Cell Carcinoma using the anti-CAIX monoclonal antibody girentuximab

Alexander B. Stillebroer^{1,2} MD, Constantijn H.J. Muselaers^{1,2} MD, Mark Rijpkema² PhD,
Gerben M. Franssen² BSc, Egbert Oosterwijk¹ PhD, Peter F.A. Mulders¹ MD PhD,
Wim J.G. Oyen² MD PhD, Otto C. Boerman² PhD

Departments of Urology¹ and Nuclear Medicine²,
Radboud University Nijmegen Medical Centre, Nijmegen, The Netherlands

Submitted for publication



ABSTRACT

Background

Near-infrared dye tagged antibodies can be used for sensitive detection of tumor tissue in vivo. Surgery for clear cell renal cell carcinoma (ccRCC) could potentially benefit from optical imaging by facilitating intra-operative detection of Carbonic Anhydrase IX (CAIX) expressing tumor lesions with chimeric monoclonal antibody (mAb) girentuximab that has shown excellent imaging capabilities for ccRCC. Here we studied the potential to detect ccRCC tumors with fluorescence imaging in nude mice with RCC xenografts using mAb girentuximab conjugated with IRDye800CW, using SPECT imaging as a reference.

Methods

Groups of athymic BALB/c mice with s.c. CAIX-positive SK-RC-52 RCC tumors were i.v. injected with ^{125}I -labeled girentuximab-IRDye800CW or ^{125}I -labeled girentuximab. To determine the specificity of the accumulation of the anti-CAIX antibody conjugate in ccRCC, a separate group of mice bearing a CAIX-positive SK-RC-52 and CAIX-negative tumor (SK-RC-59) received ^{125}I -girentuximab-IRDye800CW or ^{125}I -labeled MOPC21-IRDye800CW (control mAb).

Optical images and microSPECT images were acquired until 3 days p.i. Mice were euthanized after the last imaging session and the biodistribution of the radiolabeled antibodies preparations was determined.

Results

Optical and SPECT imaging one day after injection of ^{125}I -girentuximab-IRDye800CW showed clear delineation of the CAIX-expressing ccRCC xenografts and image contrast improved with time. Fluorescence imaging and biodistribution studies showed high and specific uptake of ^{125}I -girentuximab-IRDye800CW in CAIX-positive ccRCC xenografts (SK-RC-52: 31.5 ± 9.6 %ID/g at 72 hours p.i.). Tumor uptake was specific, since very low uptake of ^{125}I -girentuximab-IRDye800CW was noted in the CAIX-negative SK-RC-59 tumor (4.1 ± 1.5 %ID/g) and no uptake of the control mAb ^{125}I -MOPC21-IRDye800CW was noted in the CAIX-positive SK-RC-52 tumor (1.2 ± 0.1 %ID/g).

Conclusion

Subcutaneous CAIX-expressing ccRCC xenografts can be visualized with optical imaging using ^{125}I -girentuximab-IRDye800CW. Optical images showed good concordance with the microSPECT images. The accumulation of ^{125}I -girentuximab-IRDye800CW in ccRCC tumors was high and specific. Potentially, girentuximab-IRDye800CW could be used for intraoperative detection CAIX-expressing tumors, assessment of residual tumor in the resection margins and/or metastatic lymph nodes in ccRCC patients.

INTRODUCTION

Renal cell carcinoma (RCC) accounts for approximately 2% of all malignancies¹. Surgical resection is usually the first choice for localized disease, but when metastasized, prognosis is bleak. Due to the increased use of conventional radiological modalities like computed tomography (CT) and ultrasound (US), RCCs are found more frequently and at earlier stages of the disease². The recommended treatment for localized RCC depends on tumor size. Nephron-sparing surgery is performed in case of smaller RCCs (especially ≤ 4 cm diameter)³, as overall survival data of T1-T3 tumors are comparable for partial and radical nephrectomy⁴. Negative surgical resection margins are crucial for the clinical outcome, preventing additional surgical interventions⁵. Adequate characterization and resection of the renal tumor and metastatic lymph nodes is therefore of utmost importance.

The use of near-infrared (NIR) imaging probes for improved tumor characterization and delineation during surgery is increasing, although clinical application has been limited so far. Potentially, the sensitivity of NIR imaging is extremely high, and because of the low tissue autofluorescence in this part of the light spectrum, the use of NIR imaging probes could yield optimal visualization of tissues of interest. Unfortunately, the penetration depth of the emitted light of these agents is limited, hampering whole body applications⁶.

Fluorescent agent IRDye800CW is a typical example of a NIR dye and emits near infrared 789 nm photons when excited at 774 nm. IRDye800CW can be coupled to targeting molecules, such as peptides or monoclonal antibodies (mAbs) and can be detected with a NIR imaging camera.

For clear cell renal cell carcinoma (ccRCC), the most common subtype of RCC which is present in approximately 85 percent of the patients presenting with a malignant renal tumor, chimeric mAb girentuximab (also known as cG250) could serve as a such a targeting molecule. Girentuximab specifically recognizes carbonic anhydrase IX (CAIX), a tumor-associated antigen ubiquitously expressed in ccRCC. The use of girentuximab in radioimmunosciintigraphy (RIS) and radioimmunotherapy (RIT) to detect or treat ccRCC has been investigated extensively (for review see^{7, 8}). Because of the high and specific targeting and accumulation of girentuximab in ccRCC tumors, we hypothesized that this antibody could also act as a carrier for the delivery of IRDye800CW in these tumors. When girentuximab-IRDye800CW is administered intravenously before (partial) nephrectomy, sensitive, *in vivo*, intra-operative detection of positive resection margins, metastatic lymph nodes or distant ccRCC metastases might be feasible.

Here, we characterized girentuximab-IRDye800CW in a subcutaneous (s.c.) mouse model.

The antibody-IRDye800CW conjugate was radiolabeled to quantitatively determine the bio-distribution. Studies were conducted to demonstrate tumor-specific and antigen-mediated uptake of the girentuximab-IRDye800CW conjugate. In addition, tumor targeting and bio-distribution of the conjugate was compared with that of unconjugated radiolabeled girentuximab. This NIR-imaging system could potentially be used intraoperatively to enhance tumor visualization and resection in the near future.

MATERIALS AND METHODS

RCC tumors in nude mice

Cell lines

The ccRCC cell lines SK-RC-52 (CAIX-positive) and SK-RC-59 (CAIX-negative) were derived from metastases of primary ccRCC patients as described by Ebert et al.⁹. Cells were cultured and washed as described previously¹⁰.

Animal model

The animal experiments were approved by the internal review board of the Radboud University Nijmegen Medical Center, and were performed in accordance with their guidelines. Animals were housed and fed according to the Dutch animal welfare regulations. To obtain s.c. tumors, $2-3 \times 10^6$ cells were injected s.c. into the flank of 6-8 weeks old male BALB/c nu/nu mice (Janvier, Cedex, FR) and tumors grew to a size of 50-200 mm³ within 2-3 weeks.

Imaging agents and labeling

Monoclonal antibody girentuximab

The isolation and immunohistochemical reactivity of mAb G250 have been described elsewhere¹¹. To reduce the immunogenicity of murine G250 in humans, a chimeric version (girentuximab) has been developed¹². mAb girentuximab is reactive with the transmembraneous glycoprotein CAIX ($K_a = 4 \times 10^9$ M⁻¹). Expression of CAIX on the cell surface of ccRCC cells is ubiquitous (>95%), whereas expression on normal tissues is restricted to the epithelial structures of the upper gastrointestinal tract and larger bile ducts^{13, 14}.

Monoclonal antibody MOPC21

MOPC21 is a murine IgG1 mAb (Sigma-Aldrich, Zwijndrecht, The Netherlands) which is not directed against any known antigen and was used as a nonspecific control mAb in these studies.

Conjugation, radiolabeling and quality control

Conjugation of mAb girentuximab and MOPC21 with IRDye800CW-NHS (LICOR biosciences, Lincoln, NE) was performed according to the supplier's protocol. One mg mAb was incubated with 0.03 mg IRDye800CW for 2 h at room temperature in 1 ml 10 mM phosphate buffer at pH 8.5. The reaction mixture was transferred into a Slide-A-Lyzer cassette (molecular weight cut-off: 10,000 Da, Pierce, Rockford, IL) and extensively dialysed against PBS for three days to remove the unconjugated IRDye800CW. On average 1.6 IRDye800CW molecules were conjugated per mAb molecule as determined spectrophotometrically. The concentration of the conjugate was adjusted to 1 mg/ml and aliquots were stored in the dark at -20 °C until use. Girentuximab and girentuximab-IRDye800CW were radioiodinated with ¹²⁵I (Perkin Elmer, Groningen, The Netherlands) according to the Iodogen method ¹². The ¹²⁵I-girentuximab was purified by gel filtration on a PD10 column eluted with PBS containing 0.5% BSA. Specific activity of ¹²⁵I-girentuximab and ¹²⁵I-girentuximab-IRDye800CW was 4.0 and 7.8 MBq/μg, respectively.

The radiochemical purity of the radiolabeled mAb preparations was determined by instant thin layer chromatography (ITLC), using ITLC silica gel strips (Biodex Medical Systems, Shirley, NY), and 0.1 M of citrate buffer pH 5.0 as the mobile phase. Labeling efficiency exceeded 90% for all antibody preparations. After purification by gel filtration on a PD10 column, the radiochemical purity of all preparations used in the studies exceeded 95%. The immunoreactive fraction of all radiolabeled girentuximab preparations, as determined on freshly trypsinized SK-RC-52 ccRCC cells essentially as described by Lindmo et al. ¹⁵, was ≥ 79% for ¹²⁵I-girentuximab and ≥ 67% for ¹²⁵I-girentuximab-IRDye800CW .

Optical imaging and microSPECT imaging

Images were recorded at 1 h, 1 day, and 3 days after i.v. mAb injection. Optical images were acquired with the IVIS Lumina imaging system (recording time 1-3 min; binning factor 4; emission filter ICG; FOV 12.5; excitation filter 745 nm) (Caliper life sciences, Hopkinton, MA). Mice were placed in a prone position in the scanner and body temperature was maintained at 37 °C with a heated imaging stage. All animals were gas-anesthetized with a mixture of oxygen, N₂O, and isoflurane. MicroSPECT images were acquired with a U-SPECT II (MILabs, Utrecht, The Netherlands) microSPECT scanner using the GP-RM 1.0 mm diameter pinhole collimator tube. SPECT images were reconstructed

with OSEM (6 iterations, 16 subsets, voxel size 0.1875 mm) using the U-SPECT-Rec software (MILabs, Utrecht, The Netherlands).

Study design

To study changes in girentuximab biodistribution as a result of the conjugation of the mAb to IRDye800CW was assessed in two groups of five mice. Mice with a s.c. SK-RC-52 tumor were injected with either ^{125}I labeled girentuximab-IRDye800CW or unconjugated ^{125}I -girentuximab. Both groups were studied with microSPECT imaging, and the ^{125}I -girentuximab-IRDye800CW group was also studied with optical imaging. Biodistribution studies were performed in both groups.

To determine if tumor targeting of the girentuximab constructs was CAIX-antigen mediated, two groups of six mice with a s.c. CAIX-positive tumor (SK-RC-52) in the left flank and a s.c. CAIX-negative tumor (SK-RC-59) in the right flank were used. One group of mice received ^{125}I -girentuximab-IRDye800CW and the other group received the nonspecific ^{125}I -MOPC21-IRDye800CW. Both groups were studied with optical imaging as well as microSPECT imaging and biodistribution studies were performed.

To evaluate the specificity of girentuximab targeting to CAIX-expressing ccRCC tumors was studied in an additional group of five SK-RC-52 bearing mice. These mice were co-injected with ^{125}I -girentuximab-IRDye800CW and an excess (500 μg) of unlabeled girentuximab. Again, optical imaging as well as microSPECT imaging and biodistribution studies were performed.

Biodistribution studies

After the last images were acquired (three days p.i.), mice were euthanized, and the biodistribution of the radiolabel was determined. Tumors and samples of normal tissues (blood, muscle, lung, spleen, kidney, liver, small intestine, and stomach) were dissected, weighed and counted in a γ -counter (1480 Wizard 3", LKB/Wallace, Perkin-Elmer, Boston, MA). Results of the biodistribution are given as percentage of the injected dose per gram tissue (%ID/g). The thyroid was also dissected and counted, and results of this organ were expressed as percentage of the injected dose (%ID). Injection standards were counted simultaneously to correct for radioactive decay.

Statistical analysis

Statistical analysis was performed using t-tests. Differences were considered significant at $p < 0.05$, two-sided. All values are expressed as mean \pm standard deviation (SD).

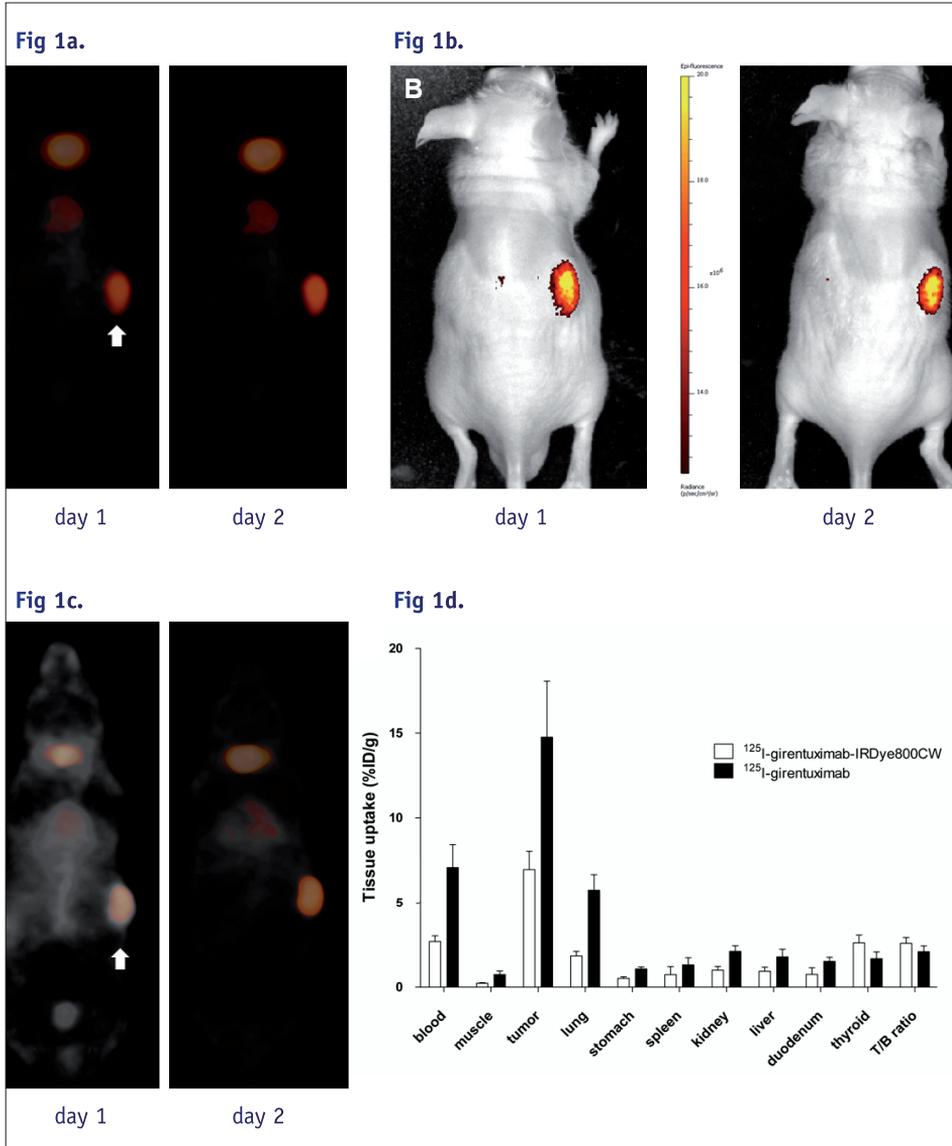


Figure 1a. MicroSPECT images of a mouse bearing a SK-RC-52 tumor on the right flank (indicated by the arrow) injected with ^{125}I -girentuximab-IRDye800CW, 1 day and 3 days p.i. In addition to tumor uptake, minimal uptake in the heart and thyroid can also be observed.

Figure 1b. Optical images of the same mouse 1 day and 3 days p.i. (same image settings used for day 1 and 3). Some reflectance-induced image artifacts on the back of the mice can also be observed.

Figure 1c. MicroSPECT images of a mouse bearing a SK-RC-52 tumor on the right flank (indicated by the arrow) injected with ^{125}I -girentuximab, 1 day and 3 days p.i.

Figure 1d. Biodistribution of ^{125}I -girentuximab-IRDye800CW and ^{125}I -girentuximab in mice with a s.c. SK-RC-52 tumor, 3 days p.i. Values are expressed as mean + SD. T/B ratio: tumor-to-blood ratio.

Results

The optical images of mice bearing a s.c. CAIX-positive SK-RC-52 tumor injected with ^{125}I -girentuximab-IRDye800CW showed targeting of the tumor by the IRDye800CW-conjugated antibody preparation at 1 day and at 3 days p.i. (**Figure 1a**). No tumor uptake was detected at 1 h p.i. (data not shown). MicroSPECT images of the same animals confirmed accumulation of ^{125}I -girentuximab-IRDye800CW in the CAIX-expressing tumors (**Figure 1b**). The biodistribution of the radiolabel in these mice is summarized in Figure 1d. These data (SK-RC-52 uptake 6.9 ± 1.1 %ID/g) confirm the preferential uptake of ^{125}I -girentuximab-IRDye800CW in the tumors as visualized in the optical images and the SPECT images. MicroSPECT images of SK-RC-52 tumor bearing mice injected with ^{125}I -girentuximab show tumor uptake at 1 day and at 3 days p.i. (**Figure 1c**). No tumor uptake was detected at 1 h p.i. (data not shown). The biodistribution data of ^{125}I -girentuximab confirm the preferential tumor accumulation observed in the microSPECT images (14.8 ± 3.3 %ID/g, Figure 1d). Three days p.i., the blood levels of ^{125}I -girentuximab-IRDye800CW were significantly lower than those of ^{125}I -girentuximab (2.7 ± 0.35 vs. 7.1 ± 1.3 %ID/g respectively, $p=0.001$), suggesting faster clearance of the IRDye800CW-conjugated antibody preparation from the blood. However, tumor-to-blood ratios did not differ significantly between the IRDye800CW-conjugated antibody and the unconjugated antibody (2.6 ± 0.34 vs. 2.1 ± 0.34 %ID/g respectively, $p=0.053$).

In the second experiment we investigated the specificity of the CAIX-mediated targeting of girentuximab by administering ^{125}I -girentuximab-IRDye800CW or ^{125}I -MOPC21-IRDye800CW to mice with both a CAIX-positive tumor and a CAIX-negative tumor. Optical images and biodistribution data are shown in **Figure 2**. Three days p.i. the uptake of ^{125}I -girentuximab-IRDye800CW was high in the CAIX-positive tumors (31.5 ± 9.6 %ID/g, tumor-to-blood ratio 3.2 ± 2.0), whereas low uptake was observed in the CAIX-negative tumors (4.1 ± 1.5 %ID/g, tumor-to-blood ratio 0.4 ± 0.2). Both tumor uptake and tumor-to-blood ratios were significantly different between these tumors ($p=0.003$ and $p=0.018$, respectively). No tumor uptake was detected at 1 h p.i. (data not shown). Mice injected with the nonspecific control ^{125}I -MOPC21-IRDye800CW conjugate demonstrated significantly lower tumor uptake (CAIX-positive SK-RC-52: 1.2 ± 0.1 %ID/g, tumor-to-blood ratio 0.4 ± 0.1 ; CAIX-negative SK-RC-59: 2.0 ± 0.5 %ID/g, tumor-to-blood ratio 0.5 ± 0.4) compared to mice that received ^{125}I -girentuximab-IRDye800CW ($p=0.002$ and $p=0.027$ respectively).

In the third experiment the nonspecific uptake of girentuximab-IRDye800CW in the tumors was assessed, by injecting a group of three mice bearing SK-RC-52 tumors with ^{125}I -girentuximab-IRDye800CW and an excess unlabeled girentuximab. MicroSPECT images acquired 1 h, 1 day, and 3 days p.i. did not show any uptake of the radiola-

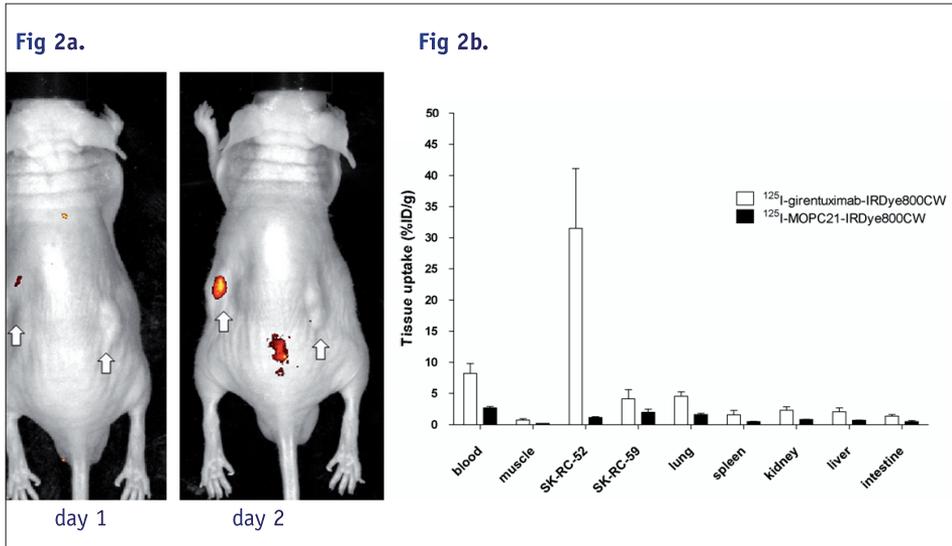


Figure 2a. Optical images of a mouse bearing a CAIX-positive SK-RC-52 tumor on the left flank and a CAIX-negative SK-RC-59 tumor on the right flank (indicated by the arrows), injected with ^{125}I -girentuximab-IRDye800CW 1 day and 3 days p.i. (same image settings used for day 1 and 3). Some reflectance-induced image artifacts on the back of the mice can also be observed.

Figure 2b. Biodistribution 3 days after injection of ^{125}I -girentuximab-IRDye800CW or ^{125}I -MOPC21-IRDye800CW in mice with a s.c. SK-RC-52 tumor and a s.c. SK-RC-59 tumor. Values are expressed as mean \pm SD.

beled mAb in the CAIX-expressing tumors (data not shown). Biodistribution studies confirmed that the nonspecific uptake of the IRDye800CW-conjugated antibody in these tumors was very low (0.91 ± 0.25 %ID/g, tumor-to-blood ratio 0.31 ± 0.06). Taken together, these results show that ^{125}I -girentuximab-IRDye800CW can target CAIX-expressing tumors with high specificity and can be assessed by microSPECT and NIR fluorescence imaging.

DISCUSSION

Both imaging and ex vivo biodistribution studies demonstrated high and specific targeting and high tumor-to-blood ratios of girentuximab-IRDye800CW in a s.c. xenograft model of CAIX-expressing ccRCC tumors. The preferential accumulation of the dual-labeled girentuximab in CAIX-expressing tumors was confirmed with both optical and microSPECT imaging. In both imaging modalities, the radiolabeled girentuximab-IRDye800CW conjugate accumulated specifically in the CAIX-positive tumors, whereas the non-specific mAb MOPC21-IRDye800CW did not. Moreover, girentuximab-IRDye800CW accumulated in CAIX-positive tumors, but not in CAIX-negative tumors. These results clearly demonstrate that the accumulation of the girentuximab-IRDye800CW conjugate is antigen-mediated. The feasibility of optical imaging of CAIX-expressing tumors using girentuximab-IRDye800CW suggests a potential role for this tracer in intraoperative detection of positive surgical margins and/or tumor-infiltrated lymph nodes.

The results of our study are in line with other preclinical and clinical studies on dual-label imaging. Terwisscha van Scheltinga et al. reported specific and sensitive detection of tumor lesions in vivo using fluorescence-labeled antibodies targeting VEGF or HER2 in a breast cancer xenograft mouse model ¹⁶. The animals in this study received a second injection with the same antibodies labeled with a positron-emitting radionuclide, ⁸⁹Zirconium, to enable a comparison between fluorescence and with PET imaging. The addition of a radioactive tracer seems to be indispensable for intraoperative tumor detection because of the limited penetration depth of the optical signal. However, it is yet to be determined whether co-injection of both an optical and radiotracer will give the same results as administration of a dual-label tracer. With co-injection, the biodistribution of the optical tracer could differ from that of the radiolabeled tracer, in contrast to a dual-label tracer, where both signals originate from the same molecule. Clinically, non-targeted dual-label tracers have been applied for sentinel lymph node biopsy and resection after intratumoral injection of nanocolloid ¹⁷. Results clearly demonstrate improved lymph node detection, especially when positive nodes are located in lymph node rich regions, for example in the case of prostate cancer or head and neck cancer ^{18, 19}. Another study in ovarian cancer patients already showed the feasibility and potential of this approach for intraoperative fluorescence imaging in a clinical setting ²⁰. Currently, another clinical trial is underway using fluorescently labeled bevacizumab to enable image-guided surgery in breast cancer patients (NCT01508572). These preclinical and clinical studies demonstrate the feasibility of dual-modality imaging for image-guided surgery.

Although the present study demonstrates optical imaging of CAIX-expressing tumors is feasible, there are some limitations for direct clinical translation of targeted fluorescence imaging in ccRCC patients. In this study, we used ¹²⁵I for small animal imaging

and ex vivo biodistribution studies. Because of its long half life (59.4 days) and less favorable gamma characteristics ($E_{\gamma} = 35 \text{ keV}$), ^{125}I is not suitable for SPECT imaging in the clinical setting. Labeling girentuximab-IRDye800CW with ^{124}I or with the residualizing radiometal $^{111}\text{Indium}$ using the chelator DTPA, could enable preoperative molecular imaging in ccRCC patients, and thus enabling both pre- and peroperative imaging in ccRCC ²¹⁻²⁴. Recently, Divgi et al. assessed the accuracy of ^{124}I -girentuximab PET/CT in a large cohort of patients with a primary renal mass scheduled for surgery ²³. The authors found a high sensitivity and specificity of ^{124}I -girentuximab PET/CT for detecting ccRCC lesions (86.2 and 85.9 percent, respectively), which is in concordance with prior experience with this tracer and indicative that this imaging modality can improve patient care in the pre-operative setting ²¹. Our results also endorse the tumor specific targeting of girentuximab and indicate that a whole new application for girentuximab-based imaging, namely the intraoperative detection of ccRCC tumors with optical imaging, might be feasible.

CONCLUSIONS

Girentuximab-based fluorescence imaging may support accurate intraoperative tumor detection. Clinical studies are warranted to assess safety, feasibility, and validity of this fluorescent imaging approach in ccRCC patients.

REFERENCES

1. Chow WH, Dong LM, Devesa SS. Epidemiology and risk factors for kidney cancer. *Nat Rev Urol.* May 2010;7(5):245-257.
2. Patard JJ. Incidental renal tumours. *Current opinion in urology.* Sep 2009;19(5):454-458.
3. Ljungberg B, Cowan NC, Hanbury DC, et al. EAU guidelines on renal cell carcinoma: the 2010 update. *European urology.* Sep 2010;58(3):398-406.
4. Weight CJ, Lythgoe C, Unnikrishnan R, Lane BR, Campbell SC, Fergany AF. Partial nephrectomy does not compromise survival in patients with pathologic upstaging to pT2/pT3 or high-grade renal tumors compared with radical nephrectomy. *Urology.* May 2011;77(5):1142-1146.
5. Sutherland SE, Resnick MI, MacLennan GT, Goldman HB. Does the size of the surgical margin in partial nephrectomy for renal cell cancer really matter? *The Journal of urology.* Jan 2002;167(1):61-64.
6. Kovar JL, Simpson MA, Schutz-Geschwender A, Olive DM. A systematic approach to the development of fluorescent contrast agents for optical imaging of mouse cancer models. *Analytical biochemistry.* Aug 1 2007;367(1):1-12.
7. Stillebroer AB, Mulders PF, Boerman OC, Oyen WJ, Oosterwijk E. Carbonic anhydrase IX in renal cell carcinoma: implications for prognosis, diagnosis, and therapy. *European urology.* Jul 2010;58(1):75-83.
8. Muselaers S, Mulders P, Oosterwijk E, Oyen W, Boerman O. Molecular imaging and carbonic anhydrase IX-targeted radioimmunotherapy in clear cell renal cell carcinoma. *Immunotherapy.* May 2013;5(5):489-495.
9. Ebert T, Bander NH, Finstad CL, Ramsawak RD, Old LJ. Establishment and characterization of human renal cancer and normal kidney cell lines. *Cancer Res.* Sep 1 1990;50(17):5531-5536.
10. Brouwers A, Verel I, Van Eerd J, et al. PET radioimmunosintigraphy of renal cell cancer using ⁸⁹Zr-labeled cG250 monoclonal antibody in nude rats. *Cancer Biother Radiopharm.* Apr 2004;19(2):155-163.
11. Oosterwijk E, Ruiter DJ, Hoedemaeker PJ, et al. Monoclonal antibody G 250 recognizes a determinant present in renal-cell carcinoma and absent from normal kidney. *International journal of cancer. Journal international du cancer.* Oct 15 1986;38(4):489-494.
12. Steffens MG, Boerman OC, Oosterwijk-Wakka JC, et al. Targeting of renal cell carcinoma with iodine-131-labeled chimeric monoclonal antibody G250. *J Clin Oncol.* Apr 1997;15(4):1529-1537.
13. Leibovich BC, Sheinin Y, Lohse CM, et al. Carbonic anhydrase IX is not an independent predictor of outcome for patients with clear cell renal cell carcinoma. *J Clin Oncol.* Oct 20 2007;25(30):4757-4764.
14. Thiry A, Dogne JM, Masereel B, Supuran CT. Targeting tumor-associated carbonic anhydrase IX in cancer therapy. *Trends in pharmacological sciences.* Nov 2006;27(11):566-573.
15. Lindmo T, Boven E, Cuttitta F, Fedorko J, Bunn PA, Jr. Determination of the immunoreactive fraction of radiolabeled monoclonal antibodies by linear extrapolation to binding at infinite antigen excess. *J Immunol Methods.* Aug 3 1984;72(1):77-89.
16. Terwisscha van Scheltinga AG, van Dam GM, Nagengast WB, et al. Intraoperative near-infrared fluorescence tumor imaging with vascular endothelial growth factor and human epidermal growth factor receptor 2 targeting antibodies. *Journal of nuclear medicine : official publication, Society of Nuclear Medicine.* Nov 2011;52(11):1778-1785.
17. van der Poel HG, Buckle T, Brouwer OR, Valdes Olmos RA, van Leeuwen FW. Intraoperative laparoscopic fluorescence guidance to the sentinel lymph node in prostate cancer patients: clinical proof of concept of an integrated functional imaging approach using a multimodal tracer. *European urology.* Oct 2011;60(4):826-833.
18. van den Berg NS, Valdes-Olmos RA, van der Poel HG, van Leeuwen FW. Sentinel lymph node biopsy for prostate cancer: a hybrid approach. *Journal of nuclear medicine : official publication, Society of Nuclear Medicine.* Apr 2013;54(4):493-496.
19. Brouwer OR, Buckle T, Vermeeren L, et al. Comparing the hybrid fluorescent-radioactive tracer indocyanine green-^{99m}Tc-nanocolloid with ^{99m}Tc-nanocolloid for sentinel node identification: a validation study using lymphoscintigraphy and SPECT/CT. *Journal of nuclear medicine : official publication, Society of Nuclear Medicine.* Jul 2012;53(7):1034-1040.
20. van Dam GM, Themelis G, Crane LM, et al. Intraoperative tumor-specific fluorescence imaging in ovarian cancer by folate receptor-alpha targeting: first in-human results. *Nature medicine.* Oct 2011;17(10):1315-

1319.

21. Divgi CR, Pandit-Taskar N, Jungbluth AA, et al. Preoperative characterisation of clear-cell renal carcinoma using iodine-124-labelled antibody chimeric G250 (¹²⁴I-cG250) and PET in patients with renal masses: a phase I trial. *Lancet Oncol.* Apr 2007;8(4):304-310.
22. Stillebroer AB, Boerman OC, Desar IM, et al. Phase 1 Radioimmunotherapy Study with Lutetium 177-labeled Anti-Carbonic Anhydrase IX Monoclonal Antibody Girentuximab in Patients with Advanced Renal Cell Carcinoma. *European urology.* Aug 21 2012.
23. Divgi CR, Uzzo RG, Gatsonis C, et al. Positron emission tomography/computed tomography identification of clear cell renal cell carcinoma: results from the REDECT trial. *J Clin Oncol.* Jan 10 2013;31(2):187-194.
24. Muselaers CH, Boerman OC, Oosterwijk E, Langenhuijsen JF, Oyen WJ, Mulders PF. Indium-111-labeled Girentuximab ImmunoSPECT as a Diagnostic Tool in Clear Cell Renal Cell Carcinoma. *European urology.* Jun 2013;63(6):1101-1106.

SUMMARY

The aim of the studies described in this thesis was to investigate the potential of diagnostic and therapeutic applications of radiolabeled anti-CAIX monoclonal antibody (mAb) cG250 in clear cell Renal Cell Carcinoma (ccRCC).

In **Chapter 1** a review of the literature on the use of mAbs in solid malignancies is presented, with particular attention to the use of the anti-CAIX mAb cG250 in ccRCC. MAb cG250 is directed against the carbonic anhydrase isoform IX (CAIX) antigen, an epitope ubiquitously expressed on ccRCC cells. Although progress has been made, radioimmunotherapy in solid malignancies is not as successful as in hematological malignancies. There are several factors that limit the accumulation of mAbs in solid malignancies: slow extravasation of antibodies, poor tumor perfusion, heterogeneity in target antigen expression and the high interstitial fluid pressure. These factors hamper the adequate delivery of mAbs to the tumor cells.

The mechanism of CAIX expression and the use of CAIX and antibodies against CAIX in the prognosis, diagnosis and therapy of RCC were reviewed in **Chapter 2**. CAIX expression is mainly regulated by the Von-Hippel Lindau (VHL) protein. Through mutational loss of VHL in ccRCC, expression of the hypoxia inducible factor (HIF) 1 α is upregulated and as a result CAIX is ubiquitously expressed in ccRCC. High CAIX expression is correlated with an increased mortality, and thus CAIX is an independent prognostic marker in ccRCC patients. Incorporation of CAIX expression improves the prognostic accuracy of RCC nomograms. Targeting CAIX with radiolabeled cG250 in ccRCC patients showed excellent visualization of CAIX-expressing ccRCC primary tumors and metastases with single photon emission tomography (SPECT) and positron emission tomography (PET). Imaging CAIX with cG250 could therefore be an attractive diagnostic modality for (re)staging and might prevent unnecessary surgery in patients with renal masses of unknown etiology. Radioimmunotherapy with cG250 labeled with high activity doses of ^{131}I was investigated in multiple treatment regimens (single high-dose, multiple high-dose and fractionated), but results were discouraging with limited therapeutic efficacy.

Brouwers et. al. observed that radioimmunoscintigraphy in patients using cG250 in ccRCC tumors with the residualizing radionuclide ^{111}In gave higher uptake of the radiolabel in the tumor as compared to the non-residualizing ^{131}I . Moreover, cG250 radioimmunotherapy in mice with human RCC xenografts using cG250 labeled with the residualizing radionuclide ^{177}Lu markedly better prolonged survival than when labeled with ^{131}I . These findings led to a phase I study in which progressive metastatic ccRCC patients were treated with escalating activity doses of ^{177}Lu -cG250. The goals of this study were to determine the maximum tolerated dose (MTD) and

assess preliminary therapeutic efficacy of maximally three doses of ^{177}Lu -cG250 radioimmunotherapy. The results of this trial are described in **Chapter 3**. The MTD of ^{177}Lu -cG250 radioimmunotherapy was determined to be 2405 MBq/m^2 , with hematological toxicity being the dose limiting factor. Of the 23 patients treated, 17 had stabilization of their previously progressive disease after the first cycle (74%) and one patient had a partial remission. Four patients completed all three radioimmunotherapy administrations, of which two had stabilisation of disease lasting for almost two and six years. Growth of the longest diameter of all target lesions of all patients was reduced from 40.4% before treatment to 5.5% after the first treatment cycle ($p < 0.001$), which indicates that ^{177}Lu -cG250 radioimmunotherapy could stabilize previously progressive metastatic ccRCC. Administrations of ^{111}In -cG250 and ^{177}Lu -cG250 were safe and well tolerated. The results of this trial have led to the initiation of a phase II trial, in which progressive metastatic ccRCC patients are treated with ^{177}Lu -cG250 radioimmunotherapy at the MTD of 2405 MBq/m^2 , with a maximum of three treatment cycles.

In **Chapter 4**, the ^{111}In -cG250 and ^{177}Lu -cG250 scans from the study described in chapter 3 were analyzed dosimetrically to estimate the radiation absorbed doses after ^{177}Lu -cG250 radioimmunotherapy. Diagnostic ^{111}In -cG250 imaging data were used to estimate the residence times of ^{177}Lu -cG250 and ^{90}Y -cG250 in the relevant tissues. Radiation absorbed doses were calculated for the whole body, red marrow, normal tissues and tumor metastases for the therapeutic ^{177}Lu -cG250, simulated ^{177}Lu -cG250 and simulated ^{90}Y -cG250 data. The red marrow dose was calculated using two methods: a blood-based method using radioactivity measurements of blood samples drawn at various time points after administration of the radiolabeled antibody and an image-based method by using the uptake in the cranium region on the scintigraphic images as a surrogate for the uptake in the red marrow. A strong correlation was found between thrombocyte and leukocyte toxicity and the red marrow dose based on the activity measurements in the blood samples. A correlation was also found between thrombocyte toxicity and the image-based red marrow dose, but not between leukocyte toxicity and image-based red marrow dose. Thus, the ^{111}In -cG250 uptake data could be used to predict the myelotoxicity as caused by treatment with ^{177}Lu -cG250. This might lead to patient specific dosing based on a toxicity risk assessment based on ^{111}In -cG250 pharmacokinetics or scintigraphy prior to radioimmunotherapy. An inverse relationship was found between tumor size and radiation absorbed dose. Tumor-sterilizing doses ($> 50 \text{ Gy}$) were found in 2 of the 40 tumors, but 12 of 40 tumors reached dose levels of $> 25\text{Gy}$ in the first treatment cycle, indicating that with subsequent treatments tumor-sterilizing doses might be achieved. A comparison between the ^{177}Lu -cG250 and ^{90}Y -cG250 dosimetry showed a higher tumor-to-red-marrow ratio for ^{177}Lu -cG250 as compared to ^{90}Y -cG250 (15.7 vs. 12.0) when the blood-based method was used for red marrow dose calculations. The longer half-life of ^{177}Lu as compared to ^{90}Y (6.7 vs. 2.7 days) is more compatible

with the slow pharmacokinetics of cG250 accretion in ccRCC, favoring ^{177}Lu as the more suitable radionuclide for radioimmunotherapy in ccRCC patients.

Delivery of mAbs to solid tumors is, among other factors, hampered by an aberrant intratumoral vasculature. The vascular endothelial growth factor (VEGF) is highly expressed in ccRCC, also due to the aforementioned upregulation of HIF-1 α . Bevacizumab is a mAb directed against VEGF-A. In previous studies ^{111}In -labeled bevacizumab has shown to depict VEGF-A expression in colorectal carcinoma. Neo-angiogenesis inhibitors such as sorafenib or sunitinib are registered for treatment of metastatic ccRCC. However, traditional measurements of response to treatment (conventional CT imaging) might not be adequate for neo-angiogenesis treatment, since responses are usually not tumor shrinkage, but central tumor necrosis. This study investigated the potential of ^{111}In -bevacizumab imaging of ccRCC and the effect of sorafenib treatment on imaging of ccRCC lesions with ^{111}In -bevacizumab. In **Chapter 5**, 9 RCC patients scheduled for tumor nephrectomy were analyzed. Patients were imaged after administration of ^{111}In -bevacizumab and subsequently treated with sorafenib 2dd400mg for four weeks. In the last week of treatment, again ^{111}In -bevacizumab was administered and images were acquired. In the control group of 5 patients only ^{111}In -bevacizumab imaging was performed a week before tumor nephrectomy. Patients underwent tumor nephrectomy and the change in ^{111}In -bevacizumab uptake in the tumor before and after sorafenib treatment was correlated with immunohistochemical analyses of expression of VEGF-A and vascular markers of the surgical specimen. The ^{111}In -labeled bevacizumab clearly depicted ccRCC primary tumors and metastases. Neo-adjuvant treatment with sorafenib resulted in a significant decrease of ^{111}In -bevacizumab uptake in the tumor (mean decrease 60,5%, $p=0.011$). Immunohistochemistry revealed an unchanged VEGF-A expression after sorafenib treatment and a destruction of tumour vasculature. These results could indicate that the effect of sorafenib on the tumor vasculature caused the reduced uptake of the radiolabeled antibody in the tumor.

In **Chapter 6**, the most suitable radionuclide for immuno-PET imaging of ccRCC was determined in a mouse model. Immuno-PET imaging in patients pre-operatively with ^{124}I -cG250 is well characterized. Since ^{124}I is a non-residualizing radionuclide while the positron emitter ^{89}Zr is residualizing, the hypothesis of this study was that ^{89}Zr -cG250 would be more suitable than ^{124}I -cG250 for immuno-PET of ccRCC. Mice with CAIX-positive SK-RC-52 or NU-12 xenografts were injected with either ^{89}Zr -cG250 or ^{124}I -cG250 and microPET imaging and biodistribution studies were performed to assess tumor uptake and image contrast of both radiolabeled mAbs. The results of this study show that both radiolabeled mAbs visualized the CAIX-expressing xenografts, but that tumor uptake and tumor-nontumor ratios of ^{89}Zr -cG250 were higher in both tumor models (NU-12: 114.7 vs. 38.2, $p=0.029$; SK-RC-52 48.7 vs. 32.0, $p=0.26$), indicating

that ^{89}Zr -cG250 immuno-PET could be more sensitive than ^{124}I -cG250.

In **Chapter 7**, the use of cG250-based fluorescent imaging was studied in nude mice with ccRCC xenografts. In vivo fluorescent imaging was performed with fluorophors, which emit light of a defined wavelength when excited. Fluorescent imaging is a potentially extremely sensitive imaging modality, but its clinical applications are limited due to the relatively low penetration depth (< 2 cm) of the emitted light in tissue. Potentially, sensitive intra-operative detection of tumor tissue might be feasible. In this study, mice with ccRCC xenografts were injected with cG250 conjugated with the fluorescent dye IRdye-800CW and fluorescent images were acquired to assess tumor uptake and feasibility of optical imaging in ccRCC. The cG250-IRdye-800CW conjugate was labeled with ^{125}I . The biodistribution of the cG250-IRdye-800CW was determined and micro-single photon emission computed tomography (SPECT) scans were acquired. The IRdye-800CW-conjugated mAb clearly visualized the CAIX-expressing tumors and there was a clear correlation between fluorescence and micro-SPECT imaging. Moreover, the biodistribution studies showed specific uptake of the cG250-IRdye-800CW conjugate in the tumor xenografts (SK-RC-52: 31.5 ± 9.6 %ID/g). This study provided proof of principle that fluorescence imaging of ccRCC lesions with cG250-IRdye-800CW is feasible. Fluorescent imaging in ccRCC could be applied to intra-operatively detect positive surgical margins during (partial) tumor nephrectomy, tumor affected lymph nodes or occult metastases.

The studies described in this thesis have added to the knowledge of the use of mAb cG250 in the imaging and therapy of ccRCC lesions. In the current clinical practice there is not yet a role for mAb cG250 in the diagnosis or treatment of ccRCC. Further elucidation of the role of cG250 might eventually offer a clinical benefit for the patients who have to bear this disease with its often dismal prognosis.

SAMENVATTING

Het doel van de studies zoals beschreven in dit proefschrift was om de diagnostische en therapeutische toepassingen van radioactief gelabeld anti-CAIX monoklonaal antilichaam (mAb) cG250 bij heldercellig niercelcarcinoom (ccRCC) te onderzoeken.

In **Hoofdstuk 1** is een overzicht van de literatuur gegeven over het gebruik van mAbs in solide maligniteiten, met speciale aandacht voor het gebruik van anti-CAIX mAb cG250 in ccRCC. MAb cG250 is gericht tegen het carbonische anhydrase isoform IX (CAIX) antigeen, een epitoom welke alomtegenwoordig tot expressie komt op ccRCC cellen. Howel vooruitgang is geboekt, is radioimmunotherapie in solide maligniteiten niet zo succesvol als in hematologische maligniteiten. Er zijn verschillende factoren die de opname van mAbs in solide maligniteiten bemoeilijken: trage extravasatie van antilichamen, slechte perfusie van tumoren, heterogeniteit in antigeen expressie waar het mAb tegen gericht is en de hoge interstitiële vloeistofdruk in tumorweefsel. Al deze factoren bemoeilijken de adequate opname van mAbs in tumor cellen.

Het mechanisme van CAIX expressie en het gebruik van CAIX en antilichamen gericht tegen CAIX in de prognose, diagnose en therapie van ccRCC werden uitgediept in **Hoofdstuk 2**. Expressie van CAIX wordt voornamelijk gereguleerd door het Von-Hippel Lindau (VHL) eiwit. Wanneer VHL door mutaties niet meer wordt geproduceerd in ccRCC, zal meer Hypoxia inducible factor (HIF) 1 α geproduceerd worden, waardoor als gevolg CAIX alomtegenwoordig tot expressie komt in ccRCC. Hoge CAIX expressie is gecorreleerd met een toegenomen mortaliteit, wat CAIX een onafhankelijke prognostische marker maakt in patiënten met ccRCC. Toevoegen van CAIX expressie aan RCC nomogrammen laat de prognostische nauwkeurigheid toenemen. Targeten van CAIX met radioactief gelabeld cG250 in patiënten met ccRCC liet uitstekende visualisatie zien van ccRCC primaire tumoren en metastasen die CAIX tot expressie brengen met single photon emission tomography (SPECT) en positron emission tomography (PET). Afbeelden van CAIX met cG250 zou daarmee een interessante diagnostische modaliteit kunnen zijn voor (her) stagen van ccRCC en zou onnodige operaties kunnen voorkomen in patiënten met massa's in de nier met onbekende etiologie. Radioimmunotherapie met hoge doses radioactief ¹³¹I gelabeld cG250 is onderzocht in verschillende behandelingschema's (eenmalig hoge dosis, multi-pele hoge doses en gefractioneerd), maar de resultaten van deze studies waren ontmoedigend met beperkte therapeutische werkzaamheid.

Brouwers et. al. ontdekten dat wanneer radioimmunoscintigrafie met cG250 in patiënten met ccRCC met het residualiserende radioactieve label ¹¹¹In werd verricht er een hogere tumor opname bleek dan wanneer het niet-residualiserende radioactieve label ¹³¹I werd gebruikt. Daarbij,

cG250 radioimmunotherapie in muizen met humane ccRCC xenograften met cG250 gelabeld met het residualiserende radionuclide ^{177}Lu verbeterde de overleving significant ten opzichte van het niet-residualiserende ^{131}I . Deze bevindingen hebben geleid tot een fase 1 studie waarin progressieve gemetastaseerde ccRCC patiënten behandeld werden met oplopende activiteitsdoses ^{177}Lu -cG250. De doelen van deze studie waren de maximaal toelaatbare dosering (MTD) en de therapeutische effectiviteit te bepalen van maximaal drie doses ^{177}Lu -cG250 radioimmunotherapie. De resultaten van deze studie zijn beschreven in **Hoofdstuk 3**. De MTD van ^{177}Lu -cG250 radioimmunotherapie bleek 2405 MBq/m^2 te zijn, waarbij de hematologische toxiciteit de limiterende factor bleek. Bij 17 van de 23 patiënten die behandeld werden trad stabilisatie op van voorheen progressieve ziekte na de eerste behandelcyclus (74%) en één patiënt had een partiële remissie. Vier patiënten kregen alle drie radioimmunotherapie toedieningen, waarbij twee patiënten stabilisatie van de ziekte hadden die bijna twee en zes jaar duurde. Groei van de langste diameter van alle evalueerbare lesies van alle patiënten was verminderd van 40,4% voor behandeling naar 5,5% na de eerste behandelcyclus ($p < 0,001$), wat aangeeft dat ^{177}Lu -cG250 radioimmunotherapie voorheen progressief gemetastaseerd ccRCC kon stabiliseren. Toedieningen van ^{177}Lu -cG250 radioimmunotherapie waren veilig en werden goed verdragen. De resultaten van deze studie hebben geleid tot de start van een fase 2 trial, waarin patiënten met progressief gemetastaseerd ccRCC behandeld worden met ^{177}Lu -cG250 radioimmunotherapie met de MTD van 2405 MBq/m^2 , met een maximum van drie behandelcycli.

In **Hoofdstuk 4** werden de ^{111}In -cG250 en ^{177}Lu -cG250 scans van de studie beschreven in hoofdstuk 3 dosimetrisch geanalyseerd om de opgenomen dosis straling te bepalen na ^{177}Lu -cG250 radioimmunotherapie. Data van diagnostische ^{111}In -cG250 scans werd gebruikt om de verblijfstijden van ^{177}Lu -cG250 en ^{90}Y -cG250 in relevante weefsels te schatten. Opgenomen doses straling werden berekend voor het hele lichaam, rode beenmerg, normale weefsels en tumor metastasen op de therapeutische ^{177}Lu -cG250 scans en op de gesimuleerde ^{177}Lu -cG250 en gesimuleerde ^{90}Y -cG250 data. De dosis op het rode beenmerg werd berekend middels twee methoden: een bloed-gebaseerde methode waarbij radioactiviteitsmetingen op bloed afnames die op vaste tijdstippen na injectie werden afgenomen werd verricht en een scan-gebaseerde methode waarbij de opname in de schedel regio op de scintigrafische afbeeldingen als surrogaat voor de opname in het rode beenmerg werd berekend. Een sterke correlatie werd gevonden tussen trombocyten- en leucocyten toxiciteit en de rode beenmerg dosis die berekend was met de radioactiviteitsmetingen in de bloed afnames. Een correlatie werd ook gevonden tussen trombocyten toxiciteit en de scan-gebaseerde rode beenmerg dosis, maar niet tussen de leucocyten toxiciteit en de scan-gebaseerde rode beenmerg dosis. Dus, de berekende doses van opname van ^{111}In -cG250 konden worden gebruikt om de myelotoxiciteit te voorspellen zoals veroorzaakt door behandeling met ^{177}Lu -cG250. Dit zou kunnen leiden tot patiënt specifieke doseringen gebaseerd op een toxiciteitsrisico analyse van ^{111}In -cG250 farmacokinetiek of scin-

tigrafie voorafgaand aan radioimmunotherapie. Een omgekeerde relatie werd gevonden tussen tumor grootte en opgenomen doses straling. Tumor-steriliserende doseringen (>50 Gy) werden gevonden in 2 van 40 tumoren, maar 12 van de 40 tumoren bleken >25 Gy opgenomen doses te hebben in de eerste behandelcyclus, wat aangeeft dat met opeenvolgende behandelingen tumor-steriliserende doses haalbaar zouden kunnen zijn. Een vergelijking tussen ¹⁷⁷Lu-cG250 en ⁹⁰Y-cG250 dosimetrie toonde een hogere tumor-rode beenmerg ratio voor ¹⁷⁷Lu-cG250 in vergelijking met ⁹⁰Y-cG250 (15,7 vs. 12,0) wanneer de bloed-gebaseerde methode werd gebruikt voor berekening van de rode beenmerg dosis. De langere halfwaardetijd van ¹⁷⁷Lu in vergelijking met ⁹⁰Y (6,7 vs. 2,7 dagen) is beter verenigbaar met de trage farmacokinetiek van cG250 accumulatie in ccRCC, waardoor ¹⁷⁷Lu het te verkiezen radionuclide zou zijn voor cG250 radioimmunotherapie in ccRCC patiënten.

Opname van mAbs in solide tumoren wordt, onder andere, verhinderd door een aberrante tumor vasculatuur. De vascular endothelial growth factor (VEGF) komt sterk tot expressie in ccRCC, ook onder invloed van de voornoemde toegenomen productie van HIF-1 α . Bevacizumab is een mAb gericht tegen VEGF-A. In eerdere studies is gebleken dat ¹¹¹In-gelabeld bevacizumab VEGF-A expressie in colorectaal carcinoom kon afbeelden. Neo-angiogenese remmers zoals sorafenib en sunitinib zijn geregistreerd voor de behandeling van gemetastaseerd ccRCC. Echter, traditionele response metingen van behandeling (conventionele CT scans) zijn mogelijk niet geschikt voor neo-angiogenese behandeling, aangezien responses meestal niet tumor-krimp zijn, maar centrale tumor necrose. Deze studie onderzocht het potentieel van ¹¹¹In-bevacizumab om ccRCC af te beelden en het effect van sorafenib behandeling op het afbeelden van ccRCC tumoren met ¹¹¹In-bevacizumab. In **Hoofdstuk 5** werden 9 RCC patiënten die gepland stonden voor tumor nefrectomie geanalyseerd. Patiënten werden gescand na toediening van ¹¹¹In-bevacizumab en daaropvolgend behandeld met sorafenib 2dd400mg voor 4 weken. In de laatste week van de behandeling werden opnieuw scans gemaakt na toediening van ¹¹¹In-bevacizumab. In de controle groep van 5 patiënten werden alleen scans gemaakt na toediening van ¹¹¹In-bevacizumab een week voor de tumor nefrectomie. Alle patiënten ondergingen de tumor nefrectomie en de veranderingen in opname van ¹¹¹In-bevacizumab voor en na sorafenib behandeling werden gecorreleerd met de immunohistochemische analyse van VEGF-A expressie en vasculaire markers van het chirurgische preparaat. ¹¹¹In-bevacizumab kon duidelijk ccRCC primaire tumoren en metastasen afbeelden. Neo-adjuvante behandeling met sorafenib resulteerde in een significante vermindering van opname van ¹¹¹In-bevacizumab in de tumor (gemiddelde afname 60,5%, p=0,011). Immunohistochemie toonde een onveranderde VEGF-A expressie na sorafenib behandeling en een verwoeste tumor vasculatuur. Deze resultaten laten zien dat het effect van sorafenib op de tumor vasculatuur zorgt voor de verminderde opname van radiogelabeld mAb in de tumor.

In **Hoofdstuk 6** is het meest geschikte radionuclide bepaald voor immuno-PET scans van ccRCC in een muizenmodel. Immuno-PET scans in pre-operatieve RCC patiënten met ^{124}I -cG250 is goed onderzocht. Omdat ^{124}I een niet-residualiserend radionuclide is, waar de positron emitter ^{89}Zr wel residualiserend is, was de hypothese van deze studie dat ^{89}Zr -cG250 beter geschikt zou zijn dan ^{124}I -cG250 voor immuno-PET van ccRCC. Muizen met CAIX-positieve SK-RC-52 of NU-12 xenograften werden geïnjecteerd met of ^{89}Zr -cG250 of ^{124}I -cG250. Micro-PET scans en biodistributie studies werden verricht om de tumoropname en contrast van de scans te vergelijken van beide radiogelabelde mAbs. De resultaten van deze studies laten zien dat beide radiogelabelde mAbs de CAIX-positieve tumoren konden visualiseren, maar dat de tumor opname en tumor-niet tumor ratios van ^{89}Zr -cG250 hoger waren in beide tumor modellen (NU-12: 114,7 vs. 38,2, $p=0,029$; SK-RC-52: 48,7 vs. 32,0, $p=0,26$), wat aangeeft dat immuno-PET met ^{89}Zr -cG250 meer sensitief zou kunnen zijn dan met ^{124}I -cG250.

In **Hoofdstuk 7** werd het gebruik van fluorescent gelabelde cG250 scans bestudeerd in naakte muizen met ccRCC xenografts. In vivo fluorescerende scans werd verricht met fluorophors, welke licht op een bepaalde golflengte uitzenden wanneer ze aangeslagen worden. Fluorescent scan-nen is een potentieel extreem gevoelige modaliteit, maar de klinische toepasbaarheid wordt beperkt door de relatief lage penetratie diepte (<2 cm) van het uitgezonden licht in weefsel. Potentieel zou ultrasensitieve detectie van tumor weefsel mogelijk zijn. In deze studie werden muizen met ccRCC xenograften geïnjecteerd met cG250 geconjugeerd met de fluorescente dye IRdye-800CW en fluorescente scans werden gemaakt om de tumor opname en haalbaarheid van optical imaging in ccRCC te bepalen. Het cG250-IRdye-800CW conjugaat was gelabeld met ^{125}I . De biodistributie van het cG250-IRdye-800CW werd bepaald en micro-single photon emission computed tomography (SPECT) scans werden vervaardigd. Het cG250-IRdye-800CW conjugaat kon duidelijk de xenograften die CAIX tot expressie brengen visualiseren op de scans en er was een sterke correlatie tussen fluorescentie en de micro-SPECT scans. Daarbij lieten de biodistributie studies zien dat er specifieke opname was van het cG250-IRdye-800CW conjugaat in de tumor xenografts (SK-RC-52: $31,5 \pm 9,6$ %ID/g). Deze studie geeft het bewijs dat fluorescente imaging van ccRCC lesies mogelijk is met gebruik van cG250-IRdye-800CW. Fluorescente imaging zou kunnen worden toegepast om intra-operatief positieve resectievlakken te diagnosticeren tijdens (partiële) tumor nefrectomie, door tumor aangetaste lymfeklieren te onderscheiden of voor het ontdekken van occulte metastasen.

De studies beschreven in dit proefschrift dragen bij aan de kennis van het gebruik van mAb cG250 in de diagnostiek en therapie van ccRCC lesies. In de huidige klinische praktijk is er nog geen rol voor mAb cG250 in de diagnose of behandeling van ccRCC. Het verder onderzoeken van de functie en significantie van cG250 zou uiteindelijk een voordeel op kunnen leveren voor de patiënten die deze ziekte moeten dragen met een vaak sombere prognose.

GENERAL DISCUSSION AND FUTURE PROSPECTS

In this thesis, results of preclinical and clinical trials are described which aimed to further investigate the potential of monoclonal antibody (mAb) cG250 in the diagnosis and treatment of renal cell carcinoma (RCC).

Radioimmunotherapy prospects

Although great progress has been made in the treatment of metastatic RCC patients in the past years with tyrosine kinase inhibitors (TKI) such as sunitinib and sorafenib, the disease still is lethal for all patients. Progression-free and overall survival rates have increased significantly, but at the cost of side-effects that are high in frequency as well as in severity ^{1,2}. This leads to a decrease in quality of life in many patients. The results of the activity dose escalation study in 23 RCC patients indicated that the maximum tolerated dose of radiolabeled ¹⁷⁷Lu-cG250 radioimmunotherapy in metastatic RCC patients was 65 mCi/m² (chapter 3), with hematologic toxicity being dose-limiting. Moreover, clinical efficacy of the radioimmunotherapy was noted as it halted disease progression in most patients that received a therapeutic dose. This result is in contrast with previous radioimmunotherapy trials in metastatic RCC using cG250 labeled with the non-residualising radiolabel ¹³¹I in which no substantial antitumoral activity was noted ³. The observation that radioimmunotherapy with ¹⁷⁷Lu-cG250 might stop or decrease metastatic RCC growth is promising, albeit this was seen in a small cohort of patients treated with various doses of ¹⁷⁷Lu-cG250 and needs verification. In a phase 2 study currently metastatic RCC patients are treated with a maximum of three cycles of ¹⁷⁷Lu-cG250 radioimmunotherapy to determine antitumoral activity. Severe (grade 3 or 4 CTC) side effects of ¹⁷⁷Lu-cG250 radioimmunotherapy were only hematological. Patients did not suffer from severe clinical side effects: only mild and passing nausea and fatigue were observed the first weeks after ¹⁷⁷Lu-cG250 injection. Residence times of the scout ¹¹¹In-cG250 dose were similar to those of the therapeutic ¹⁷⁷Lu-cG250 dose. Therefore the absorbed doses and toxicity of the red bone marrow, the dose limiting factor in radioimmunotherapy, could be predicted using the images acquired after injection of ¹¹¹In-cG250. ¹¹¹In-cG250 scans were used to predict tumor absorbed doses of ¹⁷⁷Lu-cG250 and ⁹⁰Y-cG250 radioimmunotherapy and ¹⁷⁷Lu-cG250 revealed higher tumor-to-red-marrow dose ratios than ⁹⁰Y-cG250, making ¹⁷⁷Lu the more suitable radionuclide for radioimmunotherapy in RCC (chapter 4). Our observation that higher radiation doses were guided to smaller tumor lesions is in line with the observations of Brouwers et. al. ⁴. This provides a rationale to treat RCC patients with radioimmunotherapy in the early stages of metastatic disease, possibly even before TKI treatment is started which is accompanied by many side effects and a possible decrease in quality of life. Further studies will, however, have to show that ¹⁷⁷Lu-cG250 radioimmunotherapy does not prevent TKI treatment in patients due to sustained hematotoxicity. One could consider

to treat patients with radioimmunotherapy at a lower activity dose, since antitumoral effects were also seen at doses < 65 mCi/m².

One future strategy to improve radioimmunotherapy efficacy and reduce hematotoxicity could be pretargeting. In pretargeted radioimmunotherapy (PRIT), administration of the mAb is separated from the injection of the radionuclide. The unlabeled mAb is first injected and binds to the tumor and clears from circulation and normal organs. The radionuclide is administered in a second injection as a rapidly clearing agent with high affinity for the previously administered mAb. Affinity of the rapidly clearing radioactive agent binding to the mAb may be achieved through avidin-biotin interaction or with bispecific mAbs (bsmAbs). This has been evaluated in colorectal cancer (CRC) bearing mice using a peptide targeting the carcinoembryonic antigen which is ubiquitously expressed in CRC⁵. This study showed that PRIT using ¹⁷⁷Lu-labeled peptides potentially is an effective anti-tumor treatment modality with limited (hemato)toxicity. Moreover, in 47 progressive metastatic medullary thyroid carcinoma patients PRIT showed high response rates with manageable hematologic toxicity⁶. For cG250, a bsmAb (cG250 X DTIn-1) was produced and pretargeting experiments in nude mice with RCC xenografts targeted with ¹¹¹In-labeled bivalent peptide showed excellent tumor targeting⁷.

The use of alpha particle emitting radionuclides has the advantage of high cytotoxic potency, combined with a low range, which might reduce radiation effects to normal tissues that are not targeted by the antibody. However, most alpha-emitters have a half-life of less than one hour, which is not compatible with mAbs targeting tumors. Combining the high cytotoxicity of the alpha emitting radionuclides with pretargeting could overcome the slow accrual of intact mAb in tumors and deliver high radiation doses to tumor lesions. Radioimmunotherapy with tumor targeting peptides labeled with the alpha-emitter Bi-213 (t_{1/2} = 45 min) has been studied in mice with intraperitoneal melanoma metastases, showing increased survival and mild renal toxicity⁸.

Positron emission tomography (PET) is a technique which is increasingly used due to the high spatial resolution and accurate quantitative analysis of the images. PET imaging of RCC lesions with ¹²⁴I-cG250 is well characterized in patients scheduled for nephrectomy⁹. In immuno-PET using mAb cG250, higher tumor uptake and more sensitive imaging can be achieved when cG250 is labeled with ⁸⁹Zr instead of ¹²⁴I (chapter 6). Therefore, (pre-operative) characterization of RCC lesions using cG250-PET might best be done with ⁸⁹Zr-cG250 instead of ¹²⁴I-cG250. A clinical comparative study is warranted to test this hypothesis.

Bone marrow toxicity following ¹⁷⁷Lu-cG250 radioimmunotherapy could be predicted from the ¹¹¹In-cG250 images, but also based on activity measurements in blood samples after injection of ¹¹¹In-cG250. This could allow for individualized dosing in radioimmunotherapy, and subsequently a possible reduction of hematologic toxicity. Arguably, more specific dosimetric analyses can be performed on ¹¹¹In-cG250 imaging with single photon emission computed tomo-

graphy (SPECT) ¹⁰. Since ⁸⁹Zr is a residualising radionuclide, dosimetric analyses on ⁸⁹Zr-cG250 scout PET imaging preceding ¹⁷⁷Lu-cG250 radioimmunotherapy might yield even more accurate bone marrow toxicity predictions than ¹¹¹In-cG250 SPECT. Consequently, this might even further improve the individualized ¹⁷⁷Lu-cG250 radioimmunotherapy dosing schedule.

Antibody accumulation in tumors

One of the major limitations of radioimmunotherapy is inefficient delivery of the radiolabeled mAb to the tumor. Jain et. al. ^{11, 12} have described the barriers that limit accumulation of antibodies in tumors in detail. To enhance the uptake of the radiolabeled mAb in the tumor, barriers within the tumor (vasculature) could be altered. We explored whether ¹¹¹In-labeled mAb bevacizumab would target the VEGF expressed in RCC lesions. Furthermore, we investigated whether treatment of RCC with TKI sorafenib would alter RCC vasculature in a way that it could enhance tumor uptake of ¹¹¹In-bevacizumab. A significant decrease in tumor uptake of ¹¹¹In-bevacizumab uptake 4 weeks after sorafenib treatment of RCC patients was observed. Immunohistochemistry of the surgically removed specimens revealed vessel destruction, and no changes in expression of the target antigens VEGF and CAIX (chapter 5). These results were also observed in patients treated one week with sorafenib who were imaged with ¹¹¹In-cG250. Still, combination treatments of radioimmunotherapy with TKI remains an interesting concept, since TKI treatment does not cause tumor cell death, but merely destruction of tumor blood vessels. Our studies indicate that careful timing of the administration of both treatments is required. Either RIT should precede TKI treatment or the minimum time interval between TKI treatment and optimal antibody tumor uptake should be determined.

Optical imaging

Optical imaging of RCC lesions is feasible with cG250 conjugated with fluorescent IR-Dye800CW as demonstrated in mice with subcutaneous RCC lesions (chapter 7). This provides a rationale for exploring the possibilities of intra-operative detection of RCC masses outside the primary tumor such as tumor-affected lymph nodes or distant metastases. This approach was proven successful in ovarian cancer surgery ¹³. A great advantage of this technique could be the highly sensitive detection of residual tumor lesions without the use of radioactive tracers.

REFERENCES

- (1) Escudier B, Eisen T, Stadler WM et al. Sorafenib in advanced clear-cell renal-cell carcinoma. *N Engl J Med* 2007 January 11;356(2):125-34.
- (2) Motzer RJ, Hutson TE, Tomczak P et al. Sunitinib versus interferon alfa in metastatic renal-cell carcinoma. *N Engl J Med* 2007 January 11;356(2):115-24.
- (3) Brouwers AH, Mulders PF, de Mulder PH et al. Lack of efficacy of two consecutive treatments of radioimmunotherapy with ¹³¹I-cG250 in patients with metastasized clear cell renal cell carcinoma. *J Clin Oncol* 2005 September 20;23(27):6540-8.
- (4) Brouwers AH, Buijs WC, Mulders PF et al. Radioimmunotherapy with [¹³¹I]cG250 in patients with metastasized renal cell cancer: dosimetric analysis and immunologic response. *Clin Cancer Res* 2005 October 1;11(19 Pt 2):7178s-86s.
- (5) Schoffelen R, van der Graaf WT, Franssen G et al. Pretargeted ¹⁷⁷Lu radioimmunotherapy of carcinoembryonic antigen-expressing human colonic tumors in mice. *J Nucl Med*. 2010 Nov;51(11):1780-7
- (6) Salaun PY, Campion L, Bournaud C et al. Phase II trial of anticarcinoembryonic antigen pretargeted radioimmunotherapy in progressive metastatic medullary thyroid carcinoma: biomarker response and survival improvement. *J Nucl Med*. 2012 Aug;53(8):1185-92
- (7) Van Schaijk FG, Oosterwijk E, Molkenboer-Kueneen JD, Soede AC, McBride BJ, Goldenberg DM, Oyen WJ, Corstens FH, Boerman OC. Pretargeting with bispecific anti-renal cell carcinoma x anti-DTPA(In) antibody in 3 RCC models. *J Nucl Med* 2005 March;46(3):495-501.
- (8) Essler M, Gärtner FC, Neff F et al. Therapeutic efficacy and toxicity of ²²⁵Ac-labelled vs. ²¹³Bi-labelled tumour-homing peptides in a preclinical mouse model of peritoneal carcinomatosis. *Eur J Nucl Med Mol Imaging*. 2012 Apr;39(4):602-12.
- (9) Divgi CR, Uzzo RG, Gatsonis C, Bartz R, Treutner S, Yu JQ, Chen D, Carrasquillo JA, Larson S, Bevan P, Russo P. Positron emission tomography/computed tomography identification of clear cell renal cell carcinoma: results from the REDECT trial. *J Clin Oncol*. 2013 Jan 10; 31(2).
- (10) Muselaers CH, Boerman OC, Oosterwijk E, Langenhuijsen JF, Oyen WJ, Mulders PF. Indium-111-labeled Girentuximab ImmunoSPECT as a Diagnostic Tool in Clear Cell Renal Cell Carcinoma. *European urology*. 2013;63:1101-6.
- (11) Jain RK. Delivery of molecular and cellular medicine to solid tumors. *J Control Release* 1998 April 30;53(1-3):49-67.
- (12) Jain M, Venkatraman G, Batra SK. Optimization of radioimmunotherapy of solid tumors: biological impediments and their modulation. *Clin Cancer Res* 2007 March 1;13(5):1374-82.
- (13) Van Dam GM, Themelis G, Crane LM, et al. Intraoperative tumor-specific fluorescence imaging in ovarian cancer by folate receptor-alpha targeting: first in-human results. *Nature medicine*. 2011;17:1315-9.

LIST OF PUBLICATIONS

Radiolabeled antibodies in renal cell carcinoma, *Stillebroer AB*, Oosterwijk E, Oyen WJG, Mulders PFA, Boerman OC; *Cancer Imaging*, 2007 Nov 19;7:179-88

Clinical utility of the PCA3 urine assay in European men scheduled for repeat biopsy, Haese A, de la Taille A, van Poppel H, Marberger M, Stenzl A, Mulders PF, Huland H, Abbou CC, Remzi M, Tinzl M, Feyerabend S, *Stillebroer AB*, van Gils MP, Schalken JA; *Eur Urol*. 2008 Nov;54(5):1081-8

Prostate cancer gene 3 (PCA3): development and internal validation of a novel biopsy nomogram, Chun FK, de la Taille A, van Poppel H, Marberger M, Stenzl A, Mulders PF, Huland H, Abbou CC, *Stillebroer AB*, van Gils MP, Schalken JA, Fradet Y, Marks LS, Ellis W, Partin AW, Haese A; *Eur Urol*. 2009 Oct;56(4):659-67

The reverse side of the victory: flare up of symptoms after discontinuation of sunitinib or sorafenib in renal cell cancer patients. A report of three cases, Desar IM, Mulder SF, *Stillebroer AB*, van Spronsen DJ, van der Graaf WT, Mulders PF, van Herpen CM.; *Acta Oncol*. 2009;48(6):927-31

The prostate cancer gene 3 (PCA3) urine test in men with previous negative biopsies: does free-to-total prostate-specific antigen ratio influence the performance of the PCA3 score in predicting positive biopsies?, Ploussard G, Haese A, Van Poppel H, Marberger M, Stenzl A, Mulders PF, Huland H, Bastien L, Abbou CC, Remzi M, Tinzl M, Feyerabend S, *Stillebroer AB*, Van Gils MP, Schalken JA, de La Taille A.; *BJU Int*. 2010 Oct;106(8):1143-7

Carbonic anhydrase IX in renal cell carcinoma: implications for prognosis, diagnosis, and therapy, *Stillebroer AB*, Mulders PF, Boerman OC, Oyen WJ, Oosterwijk E.; *Eur Urol*. 2010 Jul;58(1):75-83

¹¹¹In-bevacizumab imaging of renal cell cancer and evaluation of neoadjuvant treatment with the vascular endothelial growth factor receptor inhibitor sorafenib, Desar IM*, *Stillebroer AB**, Oosterwijk E, Leenders WP, van Herpen CM, van der Graaf WT, Boerman OC, Mulders PF, Oyen WJ.; *J Nucl Med*. 2010 Nov;51(11):1707-15
(* both authors contributed equally to this manuscript)

Dosimetric analysis of ^{177}Lu -cG250 radioimmunotherapy in renal cell carcinoma patients: correlation with myelotoxicity and pretherapeutic absorbed dose predictions based on ^{111}In -cG250 imaging, *Stillebroer AB, Zegers CM, Boerman OC, Oosterwijk E, Mulders PF, O'Donoghue JA, Visser EP, Oyen WJ.;* J Nucl Med. 2012 Jan;53(1):82-9

Phase 1 Radioimmunotherapy Study with Lutetium 177-labeled Anti-Carbonic Anhydrase IX Monoclonal Antibody Girentuximab in Patients with Advanced Renal Cell Carcinoma, *Stillebroer AB, Boerman OC, Desar IM, Boers-Sonderen MJ, van Herpen CM, Langenhuijsen JF, Smith-Jones PM, Oosterwijk E, Oyen WJ, Mulders PF.;* Eur Urol. 2013 Sep;64(3):478-85

ImmunoPET Imaging of Renal Cell Carcinoma with ^{124}I - and ^{89}Zr -Labeled Anti-CAIX Monoclonal Antibody cG250 in Mice, *Stillebroer AB, Franssen GM, Mulders PF, Oyen WJ, van Dongen GA, Laverman P, Oosterwijk E, Boerman OC.;* Cancer Biother Radiopharm. 2013 Sep;28(7):510-5

BOOK CHAPTER

Renal Cell Carcinoma; Translational Biology, Personalized Medicine, and Novel Therapeutic Targets Editors: Robert A. Figlin, W. Kimryn Rathmell, Brian I. Rini, Springer 2012 pages 253-270

Carbonic Anhydrase IX: Its Role as a Biomarker, Diagnostic, and Therapeutic Target in Renal Cell Carcinoma, E. Oosterwijk, A. B. Stillebroer, P. F. A. Mulders



CURRICULUM VITAE

Alexander Boudewijn Stillebroer werd 15 augustus 1982 geboren te Terheijden, Noord-Brabant. Na enkele jaren verhuisde het gezin naar Waalwijk alwaar in 2000 het Atheneum cum laude werd afgerond aan het Willem van Oranje College. De studie geneeskunde werd aangevangen aan de Universiteit Maastricht datzelfde jaar. Gedurende de studie werd stage gelopen in het Tygerberg Childrens Hospital in Kaapstad, verbonden aan de Stellenbosch Universiteit, Zuid-Afrika.



Tevens werkte Alexander mee als student-assistent aan het onderzoek van dr. C. Henquet, waarbij onderzoek werd gedaan naar het effect van cannabis op psychosen. In deze periode was Alexander lid van het studentenplatform van de KNMG en studentendispuut Spiritus Vitalis te Maastricht. Vanaf 2004 begonnen de co-schappen, welke deels werden gevolgd aan het Sint Maarten Medical Center in Phillipsburg, Sint Maarten en aan het Radboud Universitair Medisch Centrum Nijmegen.

Na het behalen van de artsenbul in 2006 begon Alexander als promovendus te werken aan het resultaat wat voor u ligt aan het Radboud Universitair Medisch Centrum Nijmegen op de afdelingen nucleaire geneeskunde en urologie. In 2008 en 2009 werkte hij ook als ANIOS op de afdeling urologie van het Rijnstate Ziekenhuis te Arnhem (opleider: Dr. P.C. Weijerman). Tijdens zijn promotietijd heeft hij bijgedragen aan het opzetten van de Clinical PhD Council aan de Medische faculteit van de Radboud Universiteit. In 2010 en 2011 werd de vooropleiding algemene chirurgie in het Catharina Ziekenhuis te Eindhoven doorlopen (opleider: Dr. G.A.P. Nieuwenhuijzen). Het perifere deel van de urologische opleiding werd gevolgd in het Atrium Medisch Centrum te Heerlen (opleiders: Dr. K.P.J. Delaere en Drs. W. Strijbos) in 2012 en 2013. Vanaf 2014 zal Alexander werkzaam zijn in het Universitair Medisch Centrum Utrecht voor het academische deel van de urologische opleiding (opleider: Prof. Dr. J.L.H.R. Bosch).

Dit onderzoek heeft Alexander twee keer de Vlietstraprijs opgeleverd, de prijs voor de beste voordracht tijdens de halfjaarlijkse NVU vergadering. Tevens is hij als derde geëindigd in de verkiezing van de 'Marie Curie Award', de prijs voor het beste onderzoek gepresenteerd op de jaarlijkse vergadering van de Europese Vereniging van Nucleaire Geneeskunde.

Alexander woont samen met Karin de Jong in Utrecht en heeft als hobbys reizen, koken en sporten (hockey, hardlopen en wielrennen).



DANKWOORD

Prof. Dr. Boerman, beste Otto, ik wil je bedanken voor je onvoorwaardelijke steun en je rotsvaste vertrouwen in de goede afloop van dit proefschrift. Het preklinische deel van dit proefschrift is grotendeels geïnspireerd op jouw ideeën en ook bij de klinische studies was je nooit ver met raad en daad. Dank voor je inspiratie en het geduld wat je met me hebt gehad.

Prof. Dr. Mulders, beste Peter, dank voor je begeleiding bij de klinische studies en het behouden van het overzicht waar het soms makkelijk is af te dwalen in ogenschijnlijk interessante, maar minder toepasbare ideeën.

Prof. Dr. Oyen, beste Wim, vanuit de achtergrond nooit ver weg. Bij grote vraagstukken of problemen wist je altijd snel en beslissend te handelen. Ook bij het schrijven van de artikelen was jouw snelle en richting gevende commentaar onmisbaar, dank daarvoor.

Dr. Oosterwijk, beste Egbert, dank voor je inzichtelijk commentaar bij de artikelen en je inbeng vanuit het urologisch preklinische perspectief bij het opzetten van de dierstudies.

Na mijn begeleiders wil ik nu eerst en vooral de mensen bedanken zonder wie dit proefschrift nooit tot stand was gekomen: de patiënten die hun vertrouwen aan de klinische studies hebben geschonken. Ondanks de zeer ernstige ziekte waar u allen mee te maken had was u bereid een bijdrage te leveren aan de wetenschappelijke ontwikkeling van diagnostische en therapeutische middelen voor de ziekte waar u mee kampte. Dit in een zeer moeilijke periode van uw leven en dat van uw naasten. Hier wil ik niet alleen mijn dank voor uitspreken, maar ook mijn bewondering.

Graag wil ik de leden van de manuscriptcommissie danken voor het beoordelen van de wetenschappelijke waarde van dit proefschrift; Prof. Dr. Kaanders, Prof. Dr. Gerritsen en Dr. Brouwers.

De collega's op de afdeling nucleaire geneeskunde uit het Aquarium: Gerben, Annemarie, Peter, Huub, Annemieke, Cathelijne en Maichel. Dank jullie allen voor de labelingen, celculturen, hulp bij de dierstudies en alle andere zaken waardoor dit proefschrift een succes is geworden. Ook de collega's van het laboratorium urologie Dorien, Mirjam en Jeanette wil ik bedanken voor de hulp met de celculturen en de dierstudies.

Alle medewerkers van de afdeling nucleaire geneeskunde: dank voor de gezelligheid op de weekendjes weg, afdelingsuitjes en natuurlijk alle scans die ingepland en gemaakt moesten worden. Heerlijk dat jullie zo flexibel waren, heb het altijd fijn samenwerken gevonden.

Bianca en Kitty van het dierenlab: ondanks de minder prettige werkzaamheden die soms moesten gebeuren maakten jullie het altijd leuk om naar het CDL te komen. Dank voor het verzor-

gen van de proefdieren en jullie kundige blik bij het praktisch inplannen van de experimenten. Anita en José van de polikliniek urologie, dank voor jullie hulp bij de klinische studies en de inzet voor de werving van patiënten.

Ingrid Desar, van alle co-auteurs wil ik jou toch even persoonlijk bedanken voor de samenwerking. Gedurende de periode dat ik in Arnhem heb gewerkt, heb jij de klinische studie draaiende gehouden. Verder heb je veel werk verzet voor de neo-adjuvante studie, waar we nu gedeeld 1e auteur zijn. Ik wil je danken voor je collegialiteit en je heel veel succes wensen met je verdere carrière in de medische oncologie.

Natuurlijk moeten de promovendi op de afdelingen nucleaire geneeskunde, pathologie en medische oncologie genoemd worden: Gabie, Maarten, Johnny, Rafke, Annemarije, Gursah, Frits en Sandra. De samenwerking in het aquarium zal ik nooit vergeten, een letterlijke kweek'vijver' waar prachtig onderzoek gedaan wordt, afgewisseld met flauwe grappen en grollen. Ik wil jullie allemaal bedanken voor de gezelligheid en inspiratie en succes wensen in jullie carrières.

De urologie-promovendi in de NCMLS: Harm, Martine, Jos, Kees, Luc, Frank, Dick en Minya. Congressen, uitjes, vrijdagmiddagborrels in de Aesculaaf, polimiddagen, uroski... Het was een mooie tijd!

Ook wil ik alle co-auteurs bedanken. In het bijzonder wil ik van de afdeling medische oncologie Dr. Carla van Herpen bedanken voor de inspirerende overlegmomenten. Helaas is in het begin van mijn promotietraject Prof. Dr. De Mulder overleden, ondanks de korte samenwerking heeft hij een blijvende indruk op mij achter gelaten door zijn doorzettingsvermogen en scherpe analyses. William Leenders van de afdeling pathologie wil ik danken voor het bekijken van de coupes van de neo-adjuvante studie en de mogelijkheden die je op het lab hebt geschapen voor zowel de neo-adjuvante studie als het optical imaging project.

Stijn Muselaers, jij hebt het stokje van mij overgenomen op het G250-project. Heel veel succes met de studies en de opleiding urologie.

De studenten die mee hebben gewerkt aan delen van het onderzoek. Karin, jij hebt me ontzettend geholpen met de dosimetrische analyse en het vervolmaken van het manuscript. Door jouw inbreng heeft het artikel meer diepte gekregen, dank voor je bijzondere inzet! Duby, de eerste stappen in de optical imaging op onze afdeling heb jij samen met Huub gezet.

In het Catharina ziekenhuis Eindhoven wil ik Dr. Grard Nieuwenhuijzen bedanken voor de mogelijkheden om aan mijn proefschrift te werken in de hectische periode die de vooropleiding algemene chirurgie toch is.

In het Atrium medisch centrum Heerlen wil ik eerst en vooral Dr. Karl Delaere bedanken. In de transitieperiode van de chirurgie naar de urologie heeft u mij aan de hand genomen en opnieuw duidelijk gemaakt wat de urologie zo mooi maakt. Dank voor uw vertrouwen en dat u mij heeft laten zien wat de kracht van de bescheidenheid is. Uiteraard wil ik ook de andere stafleden danken voor hun bereidheid en inzet mij te begeleiden in mijn pad van assistent naar aanstaand collega. Mijn mede-assistenten wil ik bedanken voor een zeer gezellige tijd en prettige werksfeer in het Heerlense: Bart, Floris, Maarten, Jessica, Melanie, Mark, Geert, Leonie, Sam, Rens en Matthijs.

Mijn paranimfen Matthijs en Pieter-Jan. Matthijs, dank voor je onvoorwaardelijke steun bij het schrijven van mijn 'stukjes' en ik ben er trots op dat jij als mijn broer achter mij staat als ik dit werk mag verdedigen. Pieter-Jan, vriendschap kan soms vloeibaar zijn, maar bij ons is dat gelukkig niet gebleken. Door de jaren heen zijn wij voor mijn gevoel alleen maar dichter bij elkaar gekomen, al was de afstand soms groot. Ik ben blij dat je nu weer het geluk gevonden hebt en hoop dat onze vriendschap zich zal blijven verdiepen. Heb in ieder geval nu al zin in de vrijdagmiddagborrels afgewisseld in Utrecht en Den Bosch!

Ik wil mijn familie bedanken; mam, pap, Yvonne, Ernst, Kim, Charlotte, Kendra en Jan-Willem. Dank jullie allemaal voor de continue steun, onverdeelde interesse en de soms zo noodzakelijke ruggensteun om dit project tot een goed einde te brengen. Zoals iedere familie heeft ook de onze donkere dagen gekend, maar gelukkig hebben we altijd steun bij elkaar kunnen vinden.

René en Dricus, onze vakantie vorig jaar in Andalusië samen met Pieter-Jan was in mijn ogen niet alleen om onze 30e verjaardag te vieren, het was vooral een uiting van onze fantastische vriendschap. Ik vind het geweldig dat wij dit soort dingen kunnen blijven doen en ik vrees al voor de reis die we gaan maken als we 60 worden!

Lieve Karin, dank voor je enorme geloof in mij. Als consultant wil je graag orde in de chaos scheppen, maar helaas waren je spreadsheets en timeframes aan mij niet besteed ("I did it my way"). Desalniettemin bleef je me onvoorwaardelijk steunen en op een positieve manier aansporen. Als ik heel eerlijk ben is dat een van de grootste redenen dat dit boekje hier überhaupt voor u ligt.

